Natural Resources Canada | Ressources naturelles Canada

GEOLOGICAL SURVEY OF CANADA
OPEN FILE 9247

Environmental signature of granitic pegmatite-hosted U-Th-REE deposits of the Bancroft region, Ontario: mineralogy, petrography, and autoradiography

J.B. Percival, K.E. Venance, I. Bilot, P.A. Hunt,
A.J. Desbarats, A.B. Laudadio, and M. Beauchamp

2025

Canada

GEOLOGICAL SURVEY OF CANADA
OPEN FILE 9247

Environmental signature of granitic pegmatite-hosted U-Th-REE deposits of the Bancroft region, Ontario: mineralogy, petrography, and autoradiography

J.B. Percival[1], K.E. Venance[1], I. Bilot[1], P.A. Hunt[1], A.J. Desbarats[1], A.B. Laudadio[2,3], and M. Beauchamp[1]

[1]Natural Resources Canada, Geological Survey of Canada, 601 Booth Street, Ottawa, Ontario K1A 0E8
[2]Department of Earth Sciences, Carleton University, 1125 Colonel By Drive, Ottawa, Ontario K1S 5B6
[3]Now at Canadian Wildlife Federation, 350 Michael Cowpland Drive, Kanata, Ontario K2M 2W1

2025

This publication is available for free download through the NRCan Open Science and Technology Repository (https://ostrnrcan-dostrncan.canada.ca/).

Recommended citation
Percival, J.B., Venance, K.E., Bilot, I., Hunt, P.A., Desbarats, A.J., Laudadio, A.B., and Beauchamp, M., 2025. Environmental signature of granitic pegmatite-hosted U-Th-REE deposits of the Bancroft region, Ontario: mineralogy, petrography, and autoradiography; Geological Survey of Canada, Open File 9247, 1 .zip file. https://doi.org/10.4095/pt6fwjf05a

Publications in this series have not been edited; they are released as submitted by the author.

ISSN 2292-7875
ISBN 978-0-660-76585-3
Catalogue No. M183-2/9247E-PDF
https://doi.org/10.4095/pt6fwjf05a

Table of Contents

List of Figures and Tables

ABSTRACT

Uranium-thorium-rare earth element (U-Th-REE)-bearing deposits hosted in granitic pegmatites, skarns and marbles occur throughout the Bancroft region of central Ontario within the Grenville Province of the Canadian Shield. These deposits, mined since the late 1950s, were the focus of a study under the GSC's Environmental Geoscience Program, to develop a geoenvironmental ore deposit model including detailed mineralogical and geochemical characteristics.

Representative samples for mineralogical and petrological analyses were collected from 14 sites. Samples included hand specimens and drill core as well as a few tailings and stream sediments. Mineralogy was determined using X-ray diffraction and petrographic analyses, complemented with scanning electron microscopy to identify trace minerals, and electron microprobe analyses to determine mineral chemistry. Autoradiography of polished thin sections was used to identify radioactivity in samples.

Representative host lithologies include pegmatites, gneisses (quartzo-feldspathic, amphibolite/mafic, metapelite, calc-silicate) and marbles. The gneissic samples contain quartz, feldspar, mafic minerals (clinopyroxene, amphibole) and micas. Calcite is dominant in the calc-silicate gneisses and marbles; fluorite occurs in pegmatites. Accessory minerals include sulphides and oxides as well as a host of other silicate minerals. The main ore minerals were uraninite and uranothorite. Other radioactive minerals include minor to trace thorite, allanite, cyrtolite, pyrochlore, betafite and fergusonite. Monazite and apatite occur in calc-silicate gneisses and quartzo-feldspathic gneisses. These minerals, especially if weathered or metamict, may contribute U, Th and REE into the receiving environment. They are found locally around the mine sites in waste materials (tailings and rocks), in mineralized bedrock, and scattered core samples.

Although these studies are on abandoned mines, they provide sites and samples to develop new methods for analytical, mineralogical and geochemical characterization of ores, mine wastes, and environmental materials. Identifying the factors that control the release of metals and radionuclides will contribute to the development of models for environmental risk assessment and help to guide the development of similar deposits in the future.

RÉSUMÉ

Des gisements d'uranium-thorium-éléments terres rares (U-Th-ETR) encaissés dans des pegmatites granitiques, des skarns et des marbres sont présents dans toute la région de Bancroft, dans le centre de l'Ontario, au sein de la province de Grenville du Bouclier canadien. Ces gisements, exploités depuis la fin des années 1950, ont fait l'objet d'une étude dans le cadre du programme de géosciences environnementales de la CGC, afin de développer un modèle géoenvironnemental pour ce type de gisement comprenant des caractéristiques minéralogiques et géochimiques détaillées.
Des échantillons représentatifs pour analyses minéralogiques et pétrologiques ont été prélevés sur 14 sites. Les échantillons comprenaient des échantillons manuels, des carottes de forage, ainsi que quelques rejets miniers et sédiments de cours d'eau. La minéralogie a été déterminée à l'aide de la diffraction des rayons X et d'analyses pétrographiques, complétées par la microscopie électronique

à balayage pour identifier les minéraux en quantités traces, et par des analyses à la microsonde électronique pour déterminer la chimie des minéraux. L'autoradiographie de lames minces polies a été utilisée pour identifier la radioactivité dans les échantillons. Les lithologies hôtes représentatives comprennent des pegmatites, des gneiss (quartzofeldspathique, amphibolite/mafique, métapélite, calco-silicaté) et des marbres. Les échantillons gneissiques contiennent du quartz, du feldspath, des minéraux mafiques (clinopyroxène, amphibole) et des micas. La calcite est dominante dans les gneiss et les marbres calco-silicatés; la fluorine est présente dans les pegmatites. Les minéraux accessoires comprennent des sulfures et des oxydes ainsi qu'une multitude d'autres silicates. Les principaux minerais sont l'uraninite et l'uranothorite. Les autres minéraux radioactifs comprennent la thorite, l'allanite, la cyrtolite, le pyrochlore, la bétafite et la fergusonite, en quantités traces ou mineures. La monazite
et l'apatite sont présentes dans les gneiss calco-silicatés et les gneiss quartzo-feldspathiques. Ces minéraux, en particulier s'ils sont altérés ou métamorphisés, peuvent apporter de l'U, du Th et des terres rares dans l'environnement récepteur. On les trouve localement autour des sites miniers dans les rejets (résidus de moulin et stériles), dans la roche mère minéralisée et dans des carottes éparses. Bien que ces études portent sur des mines abandonnées, elles fournissent des sites et des échantillons permettant de développer de nouvelles méthodes de caractérisation analytique, minéralogique et géochimique des minerais, des rejets miniers et des matériaux environnementaux. L'identification des facteurs qui contrôlent la libération des métaux et des radionucléides contribuera au développement de modèles pour l'évaluation des risques environnementaux et aidera à orienter le développement de gisements similaires dans le futur.

INTRODUCTION

Exploration, discovery and exploitation of mineral deposits require geoscience knowledge and expertise combined with sophisticated geochemical and geophysical tools. To meet the market demands for key commodities in a sustainable manner also requires geoscience knowledge to predict and assess "downstream" environmental consequences due to resource development. This includes knowledge of geomorphic processes, geohazards, terrain stability, hydrogeology, mineralogy, geochemistry, geophysics, as well as of landscape response to climate change in order to assess and mitigate or minimize significant potential impacts (Burgess *et al.*, 2003). The results obtained from this research help to characterize downstream mineralogical and geochemical signatures, provide knowledge for decision makers, and promote a deeper understanding of mine sites to mitigate risk during future development (Percival *et al.*, 2011, 2015).

Uranium (U), thorium (Th) and rare earth elements (REE) have been mined in the Bancroft region since the late 1950s with sporadic operations until the early 1980s (Desbarats *et al.*, 2016). Non-radioactive commodities such as apatite, calcite, fluorite, feldspar, magnetite, mica, quartz and sodalite have been mined since the 1880s (Satterly, 1957; Sabina, 1986). Demand for U, Th and REE minerals is increasing and there is renewed interest in re-appraising the region for exploration and development. Several old mine sites and occurrences were sampled (rock core, tailings, soils, stream/lake sediments, groundwater, radon) for detailed characterization. This report summarizes the mineralogy and petrology of representative samples collected from 14 U and REE mines and prospective sites in the Bancroft region. The purpose was to determine the mineralogy that influences groundwater chemistry and the mobilization of potential contaminants. Characterization of the mineralogical signature (ore, gangue, alteration) at these sites helps to constrain the mass transfer of uranium and other elements to mine drainage through, for example, geochemical inverse modelling (Desbarats *et al.*, 2016). Identifying the factors that control geological processes such as diagenesis, physical or chemical weathering, will contribute to the development of models for environmental risk assessment.

The main purpose of the field work was to collect rock samples for mineralogical characterization to complement hydrogeochemical investigations. Results of the groundwater part of the study are provided in Desbarats and Percival (2016) and Desbarats *et al.* (2016). The rock, mineral and sediment/tailings samples collected were used to determine what possible minerals occur at each site and the results were used in geochemical modelling of the groundwater. This Open File documents the mineralogical results obtained during this study.

MINERALOGICAL SIGNATURES

To exploit an ore deposit with the least possible environmental impact, it is important to understand how its mineralogy may affect the local environs, both physically and chemically. Characterization of the quantity, texture, grain size, composition, crystallinity, and alteration history of minerals gives insights as to how they will react during processing and potentially impact the environment as waste products. The host rock, ore and gangue minerals behave differently and thus may have detrimental or beneficial effects on the environment (Plumlee and Nash, 1995). For example, it is well known that carbonate gangue minerals associated with sulphide-rich ore bodies

help to minimize impacts from acid rock drainage upon oxidation of the sulphides. Secondary minerals formed in the surficial environment can act as a sink or a source of contaminants such as metal(loids), sulphate, and acidity. With current technologies, minerals can be studied at the macro- to the nano-scale, in the field or in the laboratory, to determine how their surfaces may react to natural (hydrothermal alteration, diagenesis, pedogenesis, weathering) and man-made processes (mineral extraction) over time.

REGIONAL GEOLOGICAL SETTING

The Town of Bancroft is located in southeastern Ontario, approximately 250 km northeast of Toronto and a similar distance southwest of Ottawa (Fig. 1). Bancroft is central to the uranium mining district which straddles Monmouth and Cardiff Townships of Haliburton County and the western part of Faraday Township in Hastings County.

Bancroft lies within the Grenville Province (Fig. 1), the youngest orogenic belt (ca. 1090-980 Ma) of the Canadian Shield (Davidson, 1986; Rivers *et al.*, 2012). This NE-trending belt is about 1600 km long stretching from the Atlantic Ocean to Lake Huron and 400 km wide from the St. Lawrence River to the Grenville Front (Laurin *et al.*, 1972; Wynne-Edwards, 1972). However, more recent reports show the Grenville Orogen may extend from Labrador to Texas, a distance about 5000 km (Rivers *et al.*, 2012) and correlates with the Sveconorwegion orogen (Stephens *et al.*, 2020). In Canada, the Grenville Province is divided into seven major subdivisions based on lithological characteristics: (1) Grenvillian Foreland Belt; (2) Grenville Front Tectonic Zone; (3) Central Gneiss Belt; (4) Central Metasedimentary Belt; (5) Central Granulite Terrain; (6) Baie Comeau Segment; and (7) Eastern Grenville Province (Wynne-Edwards, 1972; Moore and Pride, 1979; Moore, 1982; Easton, 1992; Easton and Davidson, 1994). The Grenville Province has also been subdivided on the basis of tectonic elements that incorporate the polycyclic nature of the orogen, namely: (1) parautochthonous belt; (2) allochthonous polycyclic belt; and (3) allochthonous monocyclic belt (Moore, 1986; Rivers *et al.*, 1989; 2012; Carr *et al.*, 2000). For the purposes of this report, the lithological subdivisions, especially in the Bancroft region, are more appropriate.

In Ontario, trending from northwest to southeast lie the Grenville Front Tectonic Zone (GFTZ), the Central Gneiss Belt (CGB) and the Central Metasedimentary Belt (CMB). Note that, based on work by Carr *et al.* (2000), the CMB is also referred to as the Composite Arc Belt (CAB; Percival and Easton, 2007; Rivers *et al.*, 2012) and the Frontenac Terrane became part of the Frontenac-Adirondack Belt (Fig. 1). The CGB and CMB are separated by a major (crustal-scale) shear zone, several km wide called the Central Metasedimentary Belt Boundary Zone (CMBBZ). This zone is similar to the GFTZ in that it contains NE-trending strongly deformed rocks with local development of mylonites and marble tectonic breccia containing fragments of metasedimentary, plutonic and amphibolite rocks (Easton, 1992).

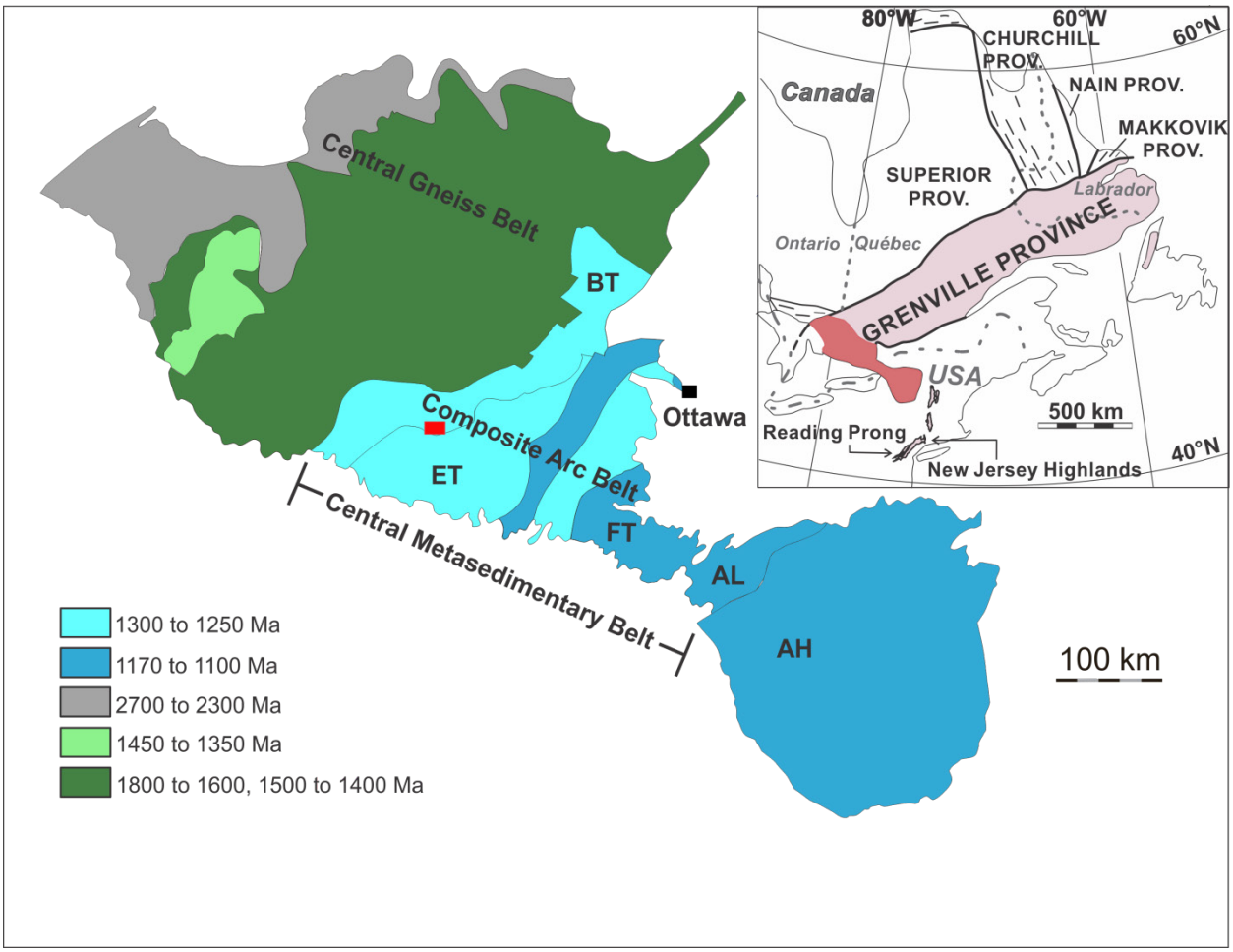

Figure 1. Geological subdivisions of the Grenville Province with age of crust or major period of magmatism in geon time scale (AH: Adirondack Highlands, AL: Adirondack Lowlands, BT: Bancroft Terrane, ET: Elzevir Terrane, FT: Frontenac Terrane). Red square represents detailed location map for mines in Bancroft area (see Fig. 2) Base map is modified after Carr *et al.* (2000) and Corriveau *et al.* (2007).

Progressing from north to south, the GFTZ consists of quartzofeldspathic gneisses, metamorphosed to granulite facies with zones of mylonitization and cataclasis (Wynne-Edwards, 1972) whereas the CGB comprises upper amphibolite facies quartzofeldspathic gneisses with interspersed marble, quartzite and paragneiss (former Grenville Supergroup).

The CMB (CAB) is composed of metamorphic carbonates, calc-silicates, quartzites, paragneisses, amphibolite and metavolcanic rocks (former Grenville Supergroup). These supracrustal rocks were deposited between 1.28 and 1.245 Ga and then intruded by gabbroic and granitic plutons between 1.25 and 1.22 Ga (Percival and Easton, 2007). The study area occurs in the northern part of the Harvey-Cardiff Arch and bordering areas of the Bancroft Terrane (Fig. 2).

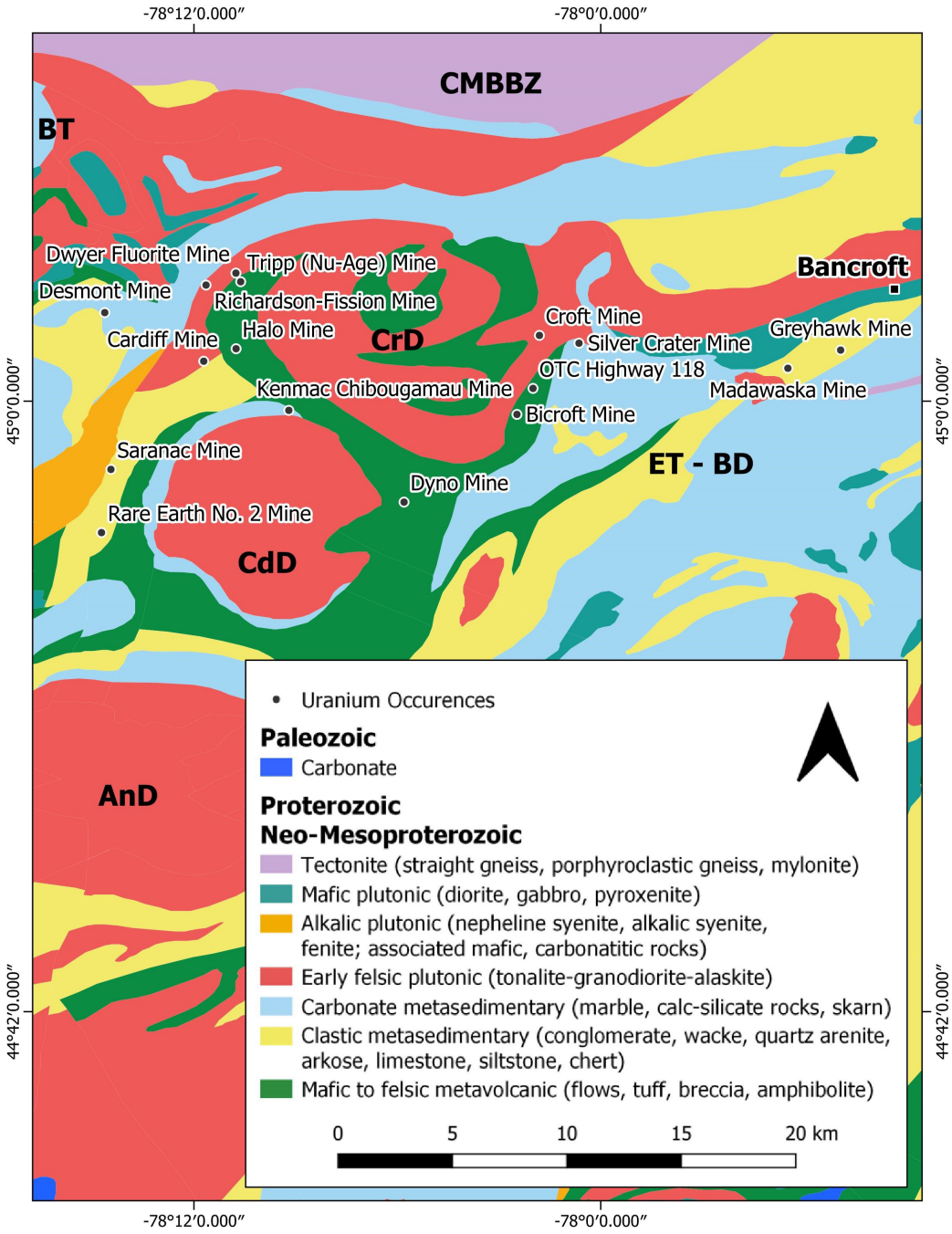

Figure 2. Simplified geological map of the study area showing locations of past producing uranium mines and selected prospects (CMBBZ: Central Metasedimentary Belt Boundary Zone; BT: Bancroft terrane; ET-BD: Belmont Domain of the Elzevir Terrane; ET-HCA:Harvey-Cardiff Arch of the Elzevir Terrane (obscured by legend); AnD: Anstruther Dome; CdD: Cheddar Dome; CrD: Cardiff Dome). Bedrock geology after OGS (1991).

The CMB (or CAB) is subdivided into a series of terranes: Bancroft in the NW, central Elzevir, and the Mazinaw, Sharbot Lake and Frontenac in the SE (Davidson, 1986; Easton, 1992). Carr *et al.* (2000) reported that these terranes have different supracrustal successions and likely developed on different basement substrates (Rivers *et al.*, 2012). The Bancroft and Mazinaw terranes developed on tonalitic basement of the continental margin-arc whereas the Elzevir and Sharbot Lake terranes were considered exotic (Easton, 1992; Carr *et al.*, 2000; Rivers *et al.*, 2012). In addition, Easton (1992) further divided the Elzevir Terrane into the Harvey-Cardiff Arch, Belmont, and Grimsthorpe domains (Fig. 2).

Between 1370 and 1075 Ma the CMB (CAB) was subjected to at least nine periods of plutonism (Easton, 1992). The lithology of these suites and their emplacement ages are summarized in Table 1. The main rock types include tonalite, nepheline syenite, anorthosite, gabbro, diorite and granite and lesser amounts of hornblendite, pyroxenite, monzonite and peridotite. Lumbers *et al.* (1990) reported that the Elzevir tonalite suite is the most abundant plutonic suite in the CMB. In addition to these plutonic suites, there are fenite-carbonatite and granite pegmatite post-tectonic units associated with uranium mineralization. Lumbers *et al.* (1990) suggested that the zones of pegmatite, carbonatite and fenite are metasomatic rocks formed by high-temperature alkaline fluids rising through the crust. In these fluids a variety of alkali, alkaline, transition and rare-earth elements were introduced into the country rocks (Lumbers *et al.*, 1990; Easton, 1992). Lentz (1996) studied the late-tectonic granitic pegmatites in the CGB and the Bancroft Terrane. Based on airborne radiometric surveys (Ford *et al*., 1992), Lentz (1991, 1996) noted a spatial relationship between the gneiss domes (Fig. 2) and these pegmatites. Although Easton (1986) suggests the gneiss domes are protoliths for deep-seated partial melts, Lentz (1996) suggests the structures bounding the gneiss domes acted as conduits and loci for the granitic pegmatite magmas.

Lentz (1991) reported mean U and Th concentrations and U/Th ratios measured in pegmatites, skarns and veins from various areas were positively correlated suggesting a common magmatic-hydrothermal origin. Lentz (1991) noted that hybridization/skarnification along pegmatite margins were key to enrichment in U, Th and REE. The U and REE-bearing deposits of the CMB are the focus of this study. The locations of deposits visited and sampled and their associated major geological structures, including gneiss domes, are shown in Fig. 2 with detailed descriptions in Appendix A.

SAMPLE SELECTION

For this mineralogical study, samples were collected from 14 U and REE mines and prospects including samples from the GSC-drilled geophysical calibration boreholes (Croft “South Zone” prospect) to test new logging systems (see Appendix A; Killeen, 1986). The mine sites and prospects are plotted on Fig. 2 and listed in Table 2. In general, grab samples were collected in an attempt to find a variety of representative rock types for each of the sites (Fig. A1-A in Appendix A). Most of the samples collected were drill core left on site, although a few hand specimens, and sediment/tailings samples were also collected. Samples were collected over several field campaigns between 2010 and 2013 (Table 3 and Table A1 in Appendix A). Each mine or prospect

Table 1. Major plutonic suites in the CMB and study area (after Easton, 1992, from Table 19.16, p. 825).

Location	Rock Suite	Age Range (Ma)	Rock Types
BT (+CMB)	Pegmatite	1050-1030	Pegmatitic granite, granite pegmatite
BT	Fenite-Carbonatite	1070-1040	Fenite-skarn assemblages, calcitic aplite veins, carbonatite
BT, ET, FT	Skootamatta	1090-1075	Monzonite, syenite, diorite, granite, peridotite, lamprophyre
FT	Gananoque	1180-1160	Syenite, monzonite, syenogranite, diorite, gabbro
BT, ET	Methuen	1250-1240	Alaskite, syenite, granite, syenogranite, aplite
ET, FT	Lavant	1250-1240	Diorite, gabbro, tonalite, granodiorite, syenite, granite, pyroxenite
BT, ET	Elzevir	1280-1270	Tonalite, granodiorite, trondhjemite, granite
MT, ET	Killer Creek	1300-1275	Gabbro, hornblendite
BT, ET, SLT	Anorthosite	1280-1250	Anorthosite, gabbro, diorite, tonalite, syenite
BT, ET	Nepheline Syenite	1280-1250	Gneisses, nepheline syenite, urtite, malignite, diorite, gabbro
BT	Dysart	1370-1340	Tonalite, trondhjemite, granodiorite

CMB: Central Metasedimentary Belt; BT: Bancroft Terrane, ET: Elzevir Terrane; FT: Frontenac Terrane; MT: Mazinaw Terrane; SLT: Sharbot Lake Terrane.

Table 2. Commodity, production and ore reserve estimates for past-producing mines and prospects in the Bancroft area. Note reserve estimates are based on historical sources (time of closure) and are not NI 43-101 compliant. For information on minerals found at each of the sites see Table A1 in Appendix A.

Mine Site	Commodity	Production (t)	Reserves (t)	Exploration to Development	Mineralogy	Reference
Bicroft Mine	U, Th	2,333,067	507,117	1956-1963	Uranothorite, uraninite, allanite, thorite ±pyrochlore, betafite	[1]
Canadian Dyno Mine	U, Th	599,523	453,600	1954-1960	Uraninite, uranothorite, allanite, uranophane, cyrtolite, thorite	[2]
Cardiff Mine (prospect)	U, Th, F	–	–	1943; 1947-1951, 1954-1955; 1976	Uraninite, fluorite	[1]
Croft Mine (prospect)	U, Th	–	888,867	1953-1954; 1975; 1977-1978	Uranothorite, secondary uranium minerals	[1]
Desmont Mine	U, Th, Mo	–	–	1942; 1954-1955; 1965; 1976-1977	Uranothorite, uraninite, allanite	[1]
Dwyer Fluorite Mine	F	33.5	–	1918	Fluorite, apatite	[3]
Halo Mine (prospect)	U, Th	–	428,191	1953-1956; 1968; 1973	Uraninite, uranothorite	[1]
Kenmac Chibougamou	U, Th	–	181,436	1955	Uranothorite, allanite	[1]
Millar's Mine	P	–	–	1900	Apatite + (thorite, thorianite, uranophane)	[3]
OTC Highway 118	–	–	–	1979; 1981	Borehole logging calibration site	[4]
Rare Earth Mine 2	U, Th	–	265,305	1954-1956	Allanite, uranothorite, fergusonite, uraninite, uranophane	[1]
Richardson Fission Mine (prospect)	U, Th, F	–	272,155	1922; 1929-1931; 1931-1933; 1946-1948; 1955	Uraninite, uranothorite, allanite, thorite, fluorite	[1]
Silver Crater Mine	U, Th, Mica	426 (mica)	–	1925; 1947-1951; 1953-1954; 1966-1969; 1975-1977	Betafite, pyrochlore	[1]
Tripp (Nu-Age) Mine	U, Th, F	1.8 (fluorite)	–	1924; 1954-1956	Uraninite, uranothorite, allanite, thorite, fluorite	[1]

[1] Gordon *et al.*, 1981; [2] Griffith, 1986; [3] Sabina, 1986; [4] Killeen, 1986

Table 3. Location and list of all rock, mineral and sediment samples collected between 2010 and 2013 field campaigns. Selected samples were further processed for XRD analyses, petrographic study (PTS) and autoradiography (AR).

Sample ID	Sample Site	Easting	Northing	Type	Description	XRD	PTS	AR
July 20-21, 2010		**17T**	**17T**					
PNA-10-01	Bicroft Mine	733889	4986177	Dredge	Composite tailings			
PNA-10-02	Deer Creek	733255	4986409	Dredge	Stream sediment			
PNA-10-02A	Deer Creek	733255	4986409	Dredge	Surface Fe film			
PNA-10-03	Bicroft Mine	773311	4986605	Dredge	Composite tailings			
PNA-10-04	Bicroft Mine	733131	4986574	Dredge	Composite tailings			
PNA-10-05	Croft Mine	733965	4990946	Dredge	Sed., adit entrance	x		
PNA-10-06-A	Dyno Mine	729344	4891523	Hand Sample	Calc-silicate gneiss		x	x
PNA-10-06-B	Dyno Mine	729344	4891523	Hand Sample	Calc-silicate gneiss	x	x	x
PNA-10-06-C	Dyno Mine	729344	4891523	Hand Sample	Calc-silicate gneiss	x	x	x
PNA-10-07	Dyno Mine	729257	4981397	Dredge	Sed., Farrel Lake wetlands	x		
PNA-10-08	Richardson Fission Mine	721100	4993003	Hand Sample	Mineral specimen			
PNA-10-09	Dwyer Flourite Mine	717381	4979090	Hand Sample	Mineral specimen			
PNA-10-10	Cardiff Mine	720858	4988769	Hand Sample	Fluorite in marble	x	x	x
Sept. 27-Oct. 5, 2011								
PNA-11-01-A	Silver Crater Mine	735567	4990495	Hand Sample	Calcite/Marble		x	x
PNA-11-01-B	Silver Crater Mine	735567	4990495	Hand Sample	Pegmatite	x		
PNA-11-01-C	Silver Crater Mine	735567	4990495	Hand Sample	Calc-silicate gneiss	x	x	x
PNA-11-01-D	Silver Crater Mine	735567	4990495	Hand Sample	Calc-silicate gneiss			
PNA-11-02	Silver Crater Mine (adit)	735431	4990545	Dredge	Sediment			
PNA-11-03-A	Rare Earth Mine 2	717266	4979343	Hand Sample	Granite gneiss	x	x	x
PNA-11-03-B	Rare Earth Mine 2	717266	4979343	Hand Sample	Gneiss	x		
PNA-11-03-C	Rare Earth Mine 2	717266	4979343	Hand Sample	Mafic gneiss	x	x	x
PNA-11-03-D	Rare Earth Mine 2	717266	4979343	Hand Sample	Gneiss	x		

Table 3 continued

Sample ID	Sample Site	Easting	Northing	Type	Description	XRD	PTS	AR
PNA-11-04	Richardson-Fission Mine	721092	4993029	Hand Sample	Fluorite	x	x	x
PNA-11-05-A	Halo Mine	722273	4989915	Hand Sample	Calc-silicate gneiss	x	x	x
PNA-11-05-B	Halo Mine	722273	4989915	Hand Sample	Gneiss	x		
PNA-11-05-C	Halo Mine	722273	4989915	Hand Sample	Amphibolite gneiss		x	x
PNA-11-06-A	Halo Mine	722160	4989993	Hand Sample	Feldspar pegmatite	x	x	x
PNA-11-06-B	Halo Mine	722160	4989993	Hand Sample	Massive biotite	x	x	x
PNA-11-07	Halo Mine	722253	4989951	Dredge	Sediment			
PNA-11-08-A	Cardiff Mine	720804	4988747	Hand Sample	Skarn			
PNA-11-08-B	Cardiff Mine	720804	4988747	Hand Sample	Calc-silicate gneiss	x	x	x
PNA11-09-A	Croft Mine	733990	4990918	Core	Mafic gneiss	x	x	x
PNA11-09-B	Croft Mine	733990	4990918	Core	Pegmatite	x	x	x
PNA11-09-C	Croft Mine	733990	4990918	Core	Garnet-sillimanite metapelite	x	x	x
PNA11-09-D	Croft Mine	733990	4990918	Core	Quartz-feldspathic gneiss	x	x	x
PNA11--09E	Croft Mine	733990	4990918	Core	Mafic gneiss	x	x	x
PNA11-09-F	Croft Mine	733990	4990918	Core	Quartz-feldspathic gneiss	x	x	x
Sept. 11-20, 2012								
PNA12-01	Croft Mine	734102	4990609	Dredge	Stream sed., very coarse-grained			
PNA12-02	Croft Mine	734143	4990622	Dredge	Stream sed., very coarse-grained			
PNA12-03-A	Rare Earth Mine 2	717497	4979200	Core	Granite pegmatite			
PNA12-03-B	Rare Earth Mine 2	717497	4979200	Core	Granite pegmatite			
PNA12-03-C	Rare Earth Mine 2	717497	4979200	Core	Amphibolite gneiss	x	x	x
PNA12-03-D	Rare Earth Mine 2	717497	4979200	Core	Amphibolite gneiss	x	x	x
PNA12-03-E	Rare Earth Mine 2	717497	4979200	Core	Amphibolite gneiss	x	x	x
PNA12-03-F	Rare Earth Mine 2	717497	4979200	Core	Amphibolite gneiss			
PNA12-03-G	Rare Earth Mine 2	717497	4979200	Core	Amphibolite gneiss			
PNA12-03-H	Rare Earth Mine 2	717497	4979200	Core	Amphibolite gneiss			

Table 3 continued

Sample ID	Sample Site	Easting	Northing	Type	Description	XRD	PTS	AR
PNA12-04	Rare Earth Mine 2	717452	4979119	Hand Sample	Pegmatite			
PNA12-05	Rare Earth Mine 2	717452	4979119	Hand Sample	Pegmatite			
PNA12-06-A	Rare Earth Mine 2	717619	4982484	Core	Mafic gneiss	x	x	x
PNA12-06-B	Rare Earth Mine 2	717619	4982484	Core	Gneiss			
PNA12-06-C	Rare Earth Mine 2	717619	4982484	Core	Calc-silicate gneiss	x	x	x
PNA12-06-D	Rare Earth Mine 2	717619	4982484	Core	Gneiss			
PNA12-07-A	Cardiff Mine	720804	4988747	Hand Sample	Fluorite-marble			
PNA12-07-B	Cardiff Mine	720804	4988747	Hand Sample	Fluorite-marble			
PNA12-07-C	Cardiff Mine	720804	4988747	Hand Sample	Calcite			
PNA12-07-D	Cardiff Mine	720804	4988747	Hand Sample	Fluorite-bearing calcite			
PNA12-08-A	OTC Highway 118	733788	4987887	Core	Pegmatite			
PNA12-08-B	OTC Highway 118	733788	4987887	Core	Pegmatite			
PNA12-08-C	OTC Highway 118	733788	4987887	Core	Amphibolite gneiss			
PNA12-08-D	OTC Highway 118	733788	4987887	Core	Amphibolite gneiss			
PNA12-08-E	OTC Highway 118	733788	4987887	Core	Amphibolite gneiss			
PNA12-08-F	OTC Highway 118	733788	4987887	Core	Amphibolite gneiss			
PNA12-09	Desmont Mine	717246	4991518	Hand Sample	Pegmatite			
PNA12-10-A	Kenmac Chibougamou	724323	4986472	Core	Pegmatite			
PNA12-10-B	Kenmac Chibougamou	724323	4986472	Core	Pegmatite	x	x	x
PNA12-10-C	Kenmac Chibougamou	724323	4986472	Core	Pegmatite			
PNA12-10-D	Kenmac Chibougamou	724323	4986472	Core	Gneiss	x	x	x
PNA12-10-E	Kenmac Chibougamou	724323	4986472	Core	Gneiss			
PNA12-11-A	Silver Crater Mine	735417	4990635	Hand Sample	Calcite			
PNA12-11-B	Silver Crater Mine	735417	4990635	Hand Sample	Massive biotite			

Table 3 continued

Sample ID	Sample Site	Eastings	Northings	Type	Description	XRD	PTS	AR
PNA12-12-A	Tripp (Nu-Age) Mine	722341	4993489	Core	Pegmatite			
PNA12-12-B	Tripp (Nu-Age) Mine	722341	4993489	Core	Pegmatite			
PNA12-12-C	Tripp (Nu-Age) Mine	722341	4993489	Core	Gneiss	x	x	x
PNA12-12-D	Tripp (Nu-Age) Mine	722341	4993489	Core	Gneiss	x	x	x
PNA12-12-E	Tripp (Nu-Age) Mine	722341	4993489	Core	Pegmatite			
PNA12-12-F	Tripp (Nu-Age) Mine	722341	4993489	Core	Gneiss			
PNA12-12-G	Tripp (Nu-Age) Mine	722341	4993489	Core	Gneiss	x	x	x
PNA12-12-H	Tripp (Nu-Age) Mine	722341	4993489	Core	Gneiss			
PNA12-12-I	Tripp (Nu-Age) Mine	722341	4993489	Hand Sample	Feldspar			
PNA12-12-J	Tripp (Nu-Age) Mine	722341	4993489	Hand Sample	Pegmatite			
Aug. 23-29, 2013								
PNA13-01	Desmont Mine	717551	4991047	Hand Sample	Granite pegmatite			
PNA13-02	Millar's Mine	not taken	not taken	Hand Sample	Granite pegmatite			

is briefly described below based on descriptions in Satterly (1957), Gordon *et al.* (1981), Sabina (1986) and others. A detailed list of minerals associated with each of the sites visited is provided in Table A1 in Appendix A. For a complete review of the showings and prospects in the area, see Satterly (1957); note that only the sampled sites are described in Appendix A.

METHODS

Quantitative Mineralogy

The mineralogy of powdered bulk samples was determined by X-ray powder diffraction (XRD) analysis. The -200 mesh powders were micronized in isopropyl alcohol using a McCrone mill until a grain size of about 5-10 μm was obtained (~ 5 minutes). The samples were dried and then back pressed into an aluminum holder to produce randomly oriented specimens. X-ray patterns were recorded on a Bruker D8 Advance Powder Diffractometer equipped with a Lynx-Eye Detector using Co Kα radiation set at 35 kV and 40 mA. Initial identification of minerals was made using EVA (Bruker AXS Inc.) software with comparison to reference mineral patterns using Powder Diffraction Files (PDF) of the International Centre for Diffraction Data (ICDD) and other available databases. Quantitative analysis was carried out using TOPAS (Bruker AXS Inc.), a PC-based program that performs Rietveld refinement (RR) of XRD spectra using a whole pattern fitting algorithm.

Petrographic Analyses

Polished thin sections were prepared at Vancouver Petrographics. All sections were scanned using a high-resolution Epson flatbed scanner to produce overviews prior to using the SEM.

Scanning Electron Microscopy

Polished thin sections and grain mounts were examined using a Zeiss EVO 50 series Scanning Electron Microscope (SEM) with Extended Pressure capability (up to 3000 Pascals) equipped with a Backscattered Electron Detector (BSD), Everhart-Thornley Secondary Electron Detector (SE), Variable Pressure Secondary Electron Detector (VPSE), and a Cathodoluminescence Detector (CL). The Oxford energy dispersive spectrometry (EDS) system includes the X-MAX 150 Silicon Drift Detector, the INCA Energy 450 software and the latest AZtec microanalysis software. The SEM operating conditions employ a standard working distance of 8.5 mm, high voltage (EHT) set at 20 kV, probe current of 400 pA to 1 nA, and the filament current set to 2^{nd} peak.

Electron Probe Microanalysis

Analyses were acquired at the Geological Survey of Canada on a JEOL JXA-8230 electron probe microanalyzer equipped with five vertical wavelength-dispersive spectrometers running ProbeforEPMA software. Operating conditions used were 20 kV accelerating voltage and 20 nA current; beam size varied with the phase: focussed (approximately 1 micron) for oxides and silicates and up to 40 microns for calcite. Count times were 10 seconds on peak and 5 seconds off-peak. Calibration standards were a mix of well-characterized natural and synthetic minerals. The

correction procedure used was that of Armstrong (1988). As fluorine was not previously analyzed in apatite, a reanalysis of major elements (Ca, P, F, Cl), including fixed compositions determined by average of previous analyses of many minor/trace elements (U, Th, Pb, La, Ce, Nd, Sm, Fe, Y, Zr, Si, Mg, Ti, Nb, Yb, Al) for use in ZAF corrections was undertaken. A 15 keV accelerating voltage, 4 nA probe current, and 10 µm spot size were used.

Autoradiography

Natural radioactivity in thin sections and rock samples can be located with the use of autoradiographs, a technique that has been used for well over 100 years (Goodman and Thompson, 1943; Robinson, 1952; Vandergraaf *et al.*, 1982; Sparkes, 2013). For this study, a more traditional approach used standard X-ray film. Polished thin sections were placed on Agfa Structurix D8 FW industrial X-ray film and set in dark boxes for varying periods of time in order to detect and map weakly to highly radioactive minerals in the samples. The boxes were sealed and left undisturbed for several days (high activity) to several months (very low activity), depending upon the activity measured by a handheld meter (Inovision, Victoreen Survey and Count Rate Meter, Model 190), before developing the film.

RESULTS

Table 3 summarizes the location and types of samples collected for this study. In addition, the samples selected for XRD, petrography and autoradiography are indicated in the right-hand columns. Examples of the hand specimens collected in the field are shown in Figs. 3-5. The examples include fluorite and calcite marbles from the Cardiff and Silver Crater mines (Fig. 3), pegmatites from Rare Earth 2 and Desmont mines (Fig. 4) and gneissic core samples from the Kenmac Chibougamou Mine (Fig. 5).

Mineralogy

Quantitative mineralogical results (wt.%) for selected samples are given in Table 4. The mineral phases reported are those that were XRD-detectable; detection limit is about 3 wt.%. Summary statistics (min, max, mean, standard deviation, median) are provided in Table 5 for all mineral phases and in Table 6 mean concentrations subdivided by lithology. For statistical calculations, a trace amount (tr) was treated as 0.1 wt.%., and non-detectable as 0 wt.%.

In general, most of the samples are dominated by plagioclase feldspar and amphibole, with subordinate quartz, K-feldspar, clinopyroxene and biotite. Minor to trace muscovite and chlorite occur in a few samples. The scapolite-group mineral marialite ($Na_4Al_3Si_9O_{24}Cl$) is found in five samples and silvialite ($(Ca,Na)_4(Al_6Si_6O_{24})(SO_4,CO_3)$) in one sample. Calcite dominates in about five samples but is present in minor to trace amounts in ten others. Fluorapatite, fluorite and garnet occur in a few samples as well, and sillimanite in one. The goodness of fit is moderate (mean = 3.47).

Subdividing the samples by lithology provides a better perspective on the mineralogy. For example, the fluorite-pegmatite is dominated by calcite and minor fluorite yet the other pegmatite samples are dominated by feldspar. The calc-silicate gneisses contain calcite in minor amounts with subequal amounts of plagioclase feldspar, K-feldspar, quartz and amphibole. The mafic gneiss and amphibolite samples are consistent with abundant amphibole and plagioclase feldspar. The metapelite is the only sample containing sillimanite and is dominated by quartz. The sediment/tailings samples are dominated by quartz with subordinate plagioclase feldspar and minor K-feldspar and amphibole. Although only two samples were analysed, their composition reflects the general mineralogy of metapelite and gneissic samples.

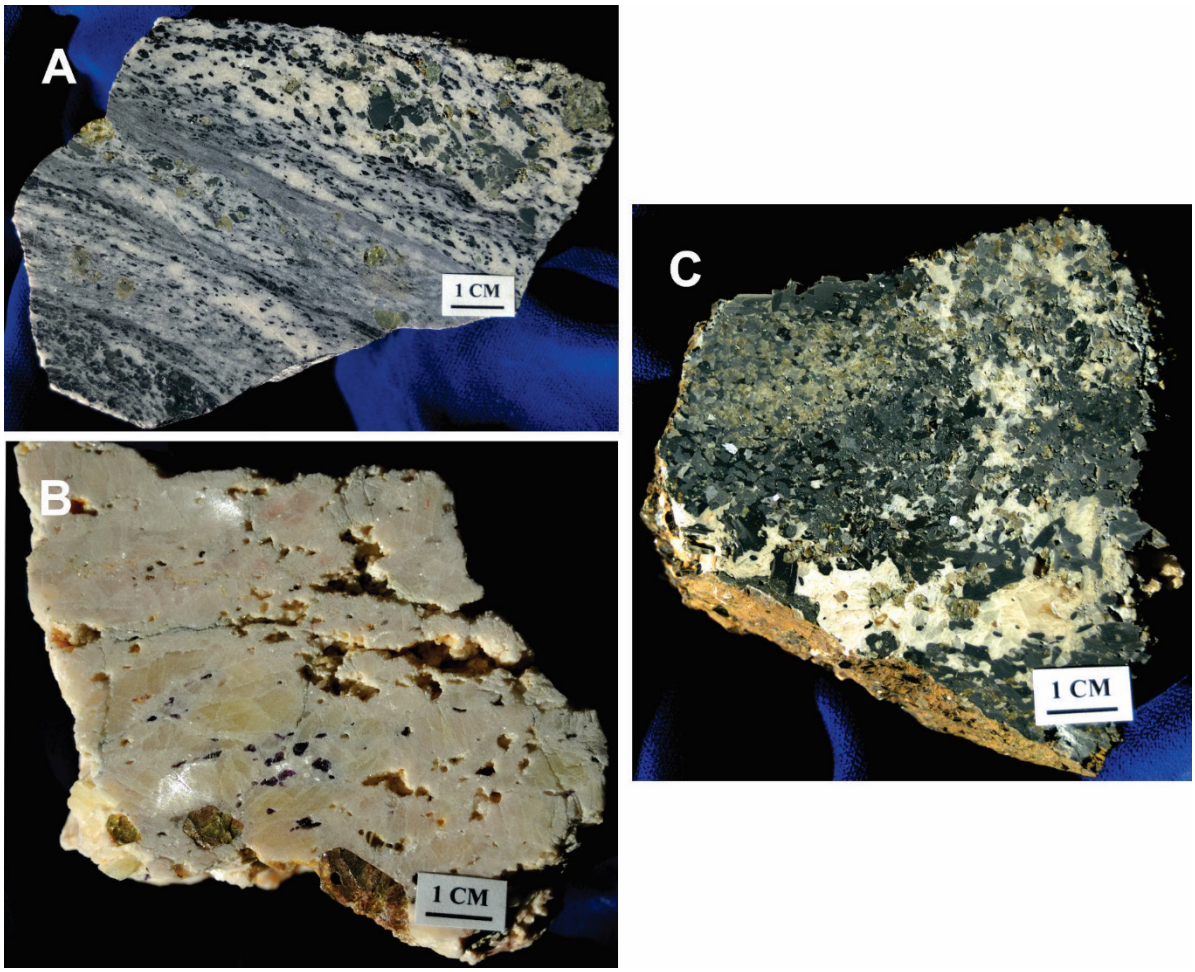

Figure 3. Example of calcite and fluorite found at some deposits in the Bancroft region. A) fluorite in calcite, sample PNA12-07D, Cardiff Mine; B) calcite with small apatite crystals, PNA12-07C, Cardiff Mine; and C) massive biotite in calcite marble, PNA12-11B, Silver Crater Mine.

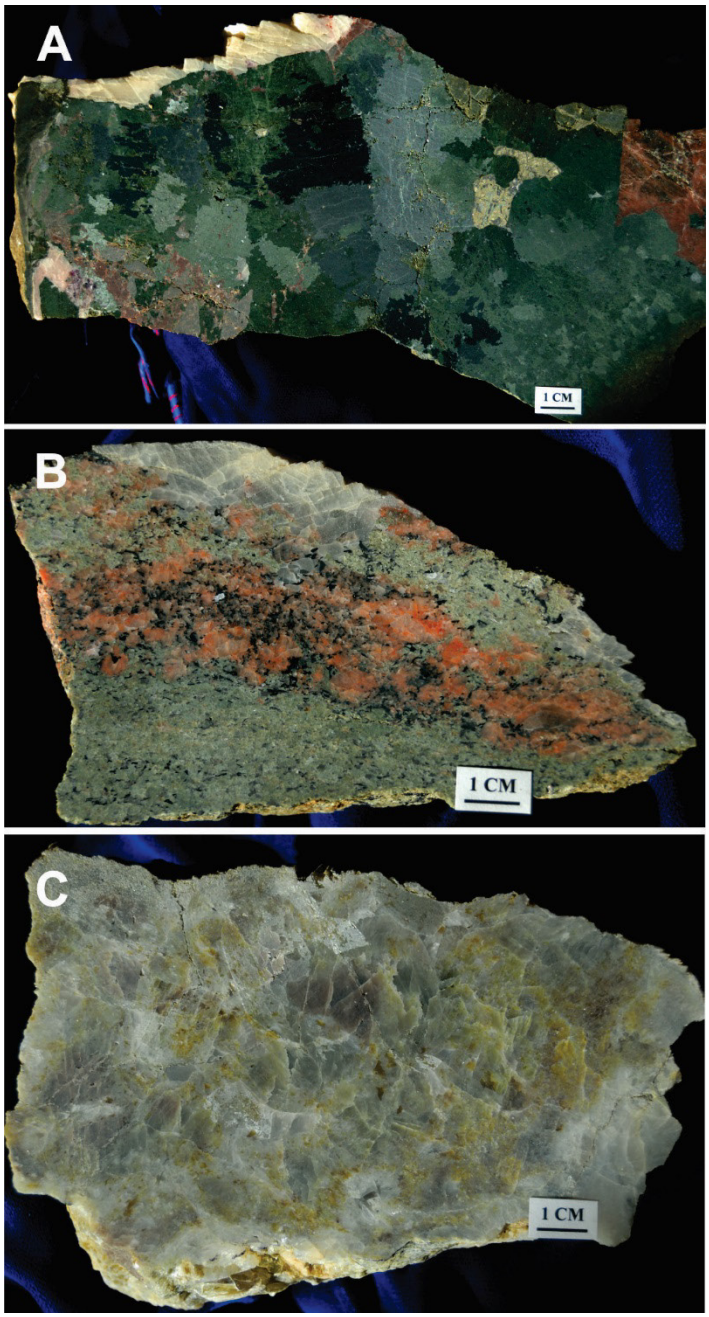

Figure 4. Example of pegmatites found at some deposits in the Bancroft region. A) granitic pegmatite, PNA12-03, Rare Earth Mine 2; B) granitic pegmatite, PNA12-12, Tripp (Nu-Age) Mine; C) calcite marble pegmatite, PNA12-09, Desmont Mine.

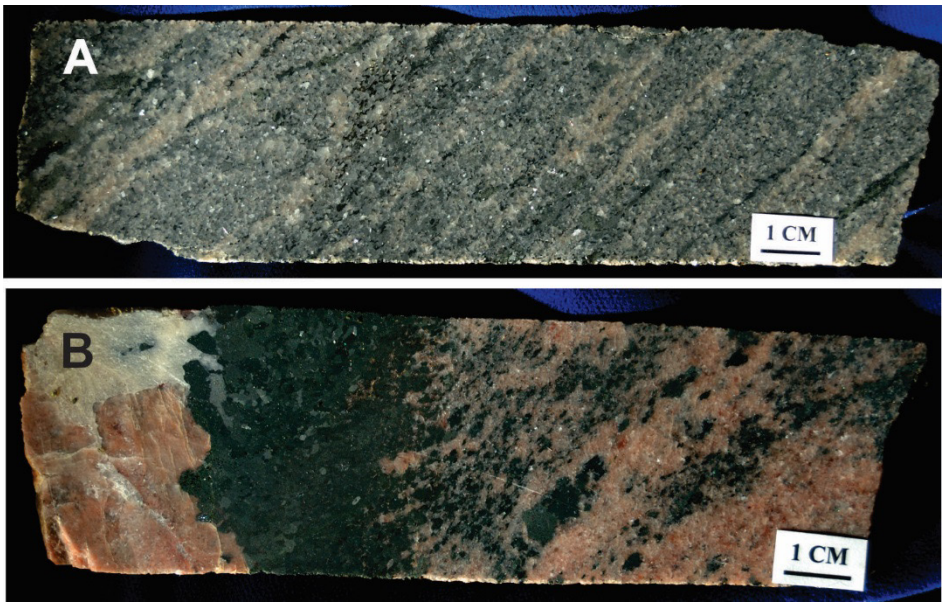

Figure 5. Example of gneissic rocks (drill core) found at some deposits in the Bancroft region. A) amphibolite gneiss, PNA12-10D, Kenmac Chibougamou Mine; B) granitic gneiss/pegmatite, PNA12-10B, Kenmac Chibougamou Mine.

Table 4. Quantitative mineralogy (wt.%) of selected bulk powdered samples by XRD analysis from the Bancroft area.

Sample ID	Qtz	Pl	Kfs	Amp	Cpx	Bt	Ms	Chl	Grt	Mar	Svl	Sil	Cal	Fap	Fl	GoF
PNA10-05	43	32	12	11		2										3.33
PNA10-06B	41	23	35	1		tr										3.26
PNA10-06C	14	46	10			27	3									3.33
PNA10-07	41	28	20	6	3	2										3.43
PNA10-10													86		14	2.56
PNA11-01B													90	10		3.03
PNA11-01C	5	3		60		26							6			3.52
PNA11-03A	26	52	13			8		1								3.49
PNA11-03B	42	51	6					tr					tr			3.54
PNA11-03C	1	37	2	35		25										3.72
PNA11-03D	tr	54		16		30										3.82
PNA11-04													65		35	3.25
PNA11-05A				54		2					20		24			3.51
PNA11-05B		17		87									2			3.39
PNA11-06A	9	41	50													3.21
PNA11-06B		66			17					17						3.61
PNA11-08B	20	18	18	4	31								9			3.58
PNA11-09A	tr	68	8	13		8							3			3.61
PNA11-09B	22	46	9	16		6							1			3.18
PNA11-09C	48	12	6			12			9			13				3.49
PNA11-09D	17	31	41	4		7										3.45
PNA11-09E	10	24	3	60	3											3.71
PNA11-09F	20	tr	54			18		2						6		3.71
PNA12-3C	2	17	tr	68		13		tr					tr			3.59
PNA12-3D	tr	21	5	3	19					52			tr			3.51
PNA12-3E	1	30	2	55		11								1		3.63
PNA12-6A	tr	20	9	56		13			1					1		3.57
PNA12-6C	2	2	15	tr	18	tr				49			14			3.49
PNA12-10B		63	20	1	12								4			3.72
PNA12-10D		62	3	30	1	4							tr			3.41
PNA12-12C		26		40	12					22						3.82
PNA12-12D	1	73	13	13												3.62
PNA12-12G	2	25	1	66	3	3				tr						3.54

Qtz: quartz, Pl: plagioclase feldspar, Kfs: K-feldspar, Amp: amphibole, Cpx: clinopyroxene, Bt: biotite, Ms: muscovite, Chl: chlorite, Grt: garnet, Mar: marialite, Svl: silvialite, Sil: sillimanite, Cal: calcite, Fap: fluorapatite, Fl: fluorite, GoF: goodness of fit

Table 5. Summary statistics for whole rock mineralogy of Bancroft samples. Total number of samples is 33; *n* provided here indicates how many samples have detectable phases (from trace amounts and up).

Parameter	Qtz	Pl	Kfs	Amp	Cpx	Bt	Ms	Chl	Grt	Mar	Svl	Sil	Cal	FAp	Fl	GoF
Min	0.1	0.1	0.1	0.1	1	0.1		0.1	1	0.1			0.1	1	14	2.56
Max	48	73	54	87	31	30		2	9	52			90	10	35	3.82
Mean	15.3	34.1	14.8	30.4	11.9	10.9	3.0	0.8	5.0	28.0	20.0	13.0	20.3	4.5	24.5	3.47
Std. Dev.	16.6	20.6	15.3	27.3	9.6	9.6		0.9	5.7	22.1			32.1	4.4	14.8	0.25
Median	9.5	30.0	9.5	16.0	12.0	8.0		0.6	5.0	22.0			4.0	3.5	24.5	3.51
N	24	29	24	23	10	20	1	4	2	5	1	1	15	4	2	33

Qtz: quartz, Pl: plagioclase feldspar, Kfs: K-feldspar, Amp: amphibole, Cpx: clinopyroxene, Bt: biotite, Ms: muscovite, Chl: chlorite, Grt: garnet, Mar: marialite, Svl: silvialite, Sil: sillimanite, Cal: calcite, Fap: fluorapatite, Fl: fluorite, GoF: goodness of fit

Note trace = 0.1, not-detectable is not included, hence "n" provided for each mineral phase

Table 6. Mean concentrations (wt.%) based on lithology of the Bancroft samples.

Lithology	*n*	Qtz	Pl	Kfs	Amp	Cpx	Mica	Chl	Grt	Scp	Sil	Cal	Fap	Fl	GoF
Fluorite/Pegmatite	3											80	4	16	2.95
Pegmatite	3	10	50	26	6	4	2					2			3.37
Calc-Silicate Gneiss	6	14	15	13	20	8	10			11		9			3.44
Quartz-Feldspathic Gneiss	2	19	16	47	2	12		1					3		3.58
Amphibolite Gneiss	3	1	23	3	42	6	8	tr		17		tr	tr		3.58
Mafic Gneiss	4	3	37	5	41	1	12		tr			1	tr		3.65
Gneiss/Granite Gneiss	8	9	45	4	31	2	6	tr		3		tr			3.58
Metapelite	1	48	12	6			12		9		13				3.49
Sediment/Tailings	2	42	30	16	8	2	2								3.38

Qtz: quartz, Pl: plagioclase feldspar, Kfs: K-feldspar, Amp: amphibole, Cpx: clinopyroxene, Bt: biotite, Ms: muscovite, Chl: chlorite, Grt: garnet, Mar: marialite, Svl: silvialite, Sil: sillimanite, Cal: calcite, Fap: fluorapatite, Fl: fluorite, GoF: goodness of fit

Petrography

The mineral phases documented during the petrographic study are summarized in Table 7, which lists silicate minerals followed by carbonates, sulphates, phosphates, oxides and halides. Opaques are summed together in the last column. Detailed images of each polished thin section (plain and cross-polarized) are provided in Appendix B along with their petrographic description. A list of samples studied is provided in Table B1 of Appendix B. In some cases, mineralogy was confirmed by SEM analyses and/or EPMA.

The amphibole-group minerals identified include gedrite, hastingsite and hornblende found in amphibolite, mafic and calc-silicate gneiss samples. Typical textures exhibited by two mafic gneiss samples are shown in Fig. 6. For example, a medium-grained, equigranular mafic gneiss with anhedral grains of mostly amphibole and biotite can exhibit a decussate texture (sample PNA12-03C; Fig. 6A), or, mafic gneisses can be very coarse-grained and layered with granoblastic textures (sample PNA11-09A; Fig. 6B). Epidote-group minerals include both allanite and epidote, but only occur in a few samples, mainly in the quartzo-feldspathic gneisses as accessory minerals.

Plagioclase feldspar and K-feldspar occur in almost all the samples except in the calcite marble and fluorite-bearing samples. Garnet occurs in two samples, a metapelite and a mafic gneiss, respectively. Sample PNA11-09C is a metapelite schist which displays evidence of an early fabric (quartz and biotite inclusions) in garnet cores later wrapped by sillimanite foliation (Fig. 6C). With regard to the pyroxene-group minerals, clinopyroxene is common and orthopyroxene was observed in one sample (PNA11-03A). However, the pyroxene is heavily altered, so its presence is not confirmed. Coarse-grained diopside is typical in calc-silicate gneisses (Fig. 6D).

Quartz occurs in most samples, with the exception of the marbles and calc-silicate gneisses. Other silicate minerals detected in some samples include sepiolite, sillimanite, titanite, tourmaline and zircon. The phyllosilicates include biotite, chlorite and muscovite, but biotite is most common. Biotite is locally retrograded to chlorite (e.g., PNA11-09F). Calcite is present in many samples, and in one sample (PNA11-04, calcite marble) a REE-bearing carbonate, synchysite, was analysed. Barite is present in two samples (perthitic pegmatite and quartz-feldspathic gneiss) as an accessory mineral. The phosphate minerals apatite and monazite occur in several samples including quartzo-feldspathic and calc-silicate gneisses. Apatite is also present in the marbles and some pegmatites. The minerals goethite, rutile and fluorapatite occur in a few samples with fluorite mainly in the calcitic marbles and calc-silicate gneisses.

Opaques detected include the sulphides chalcopyrite, galena, pyrrhotite and pyrite and the oxides goethite, hematite, ilmenite, magnetite, uraninite and a REE-bearing oxide. Thorite was also detected in some samples.

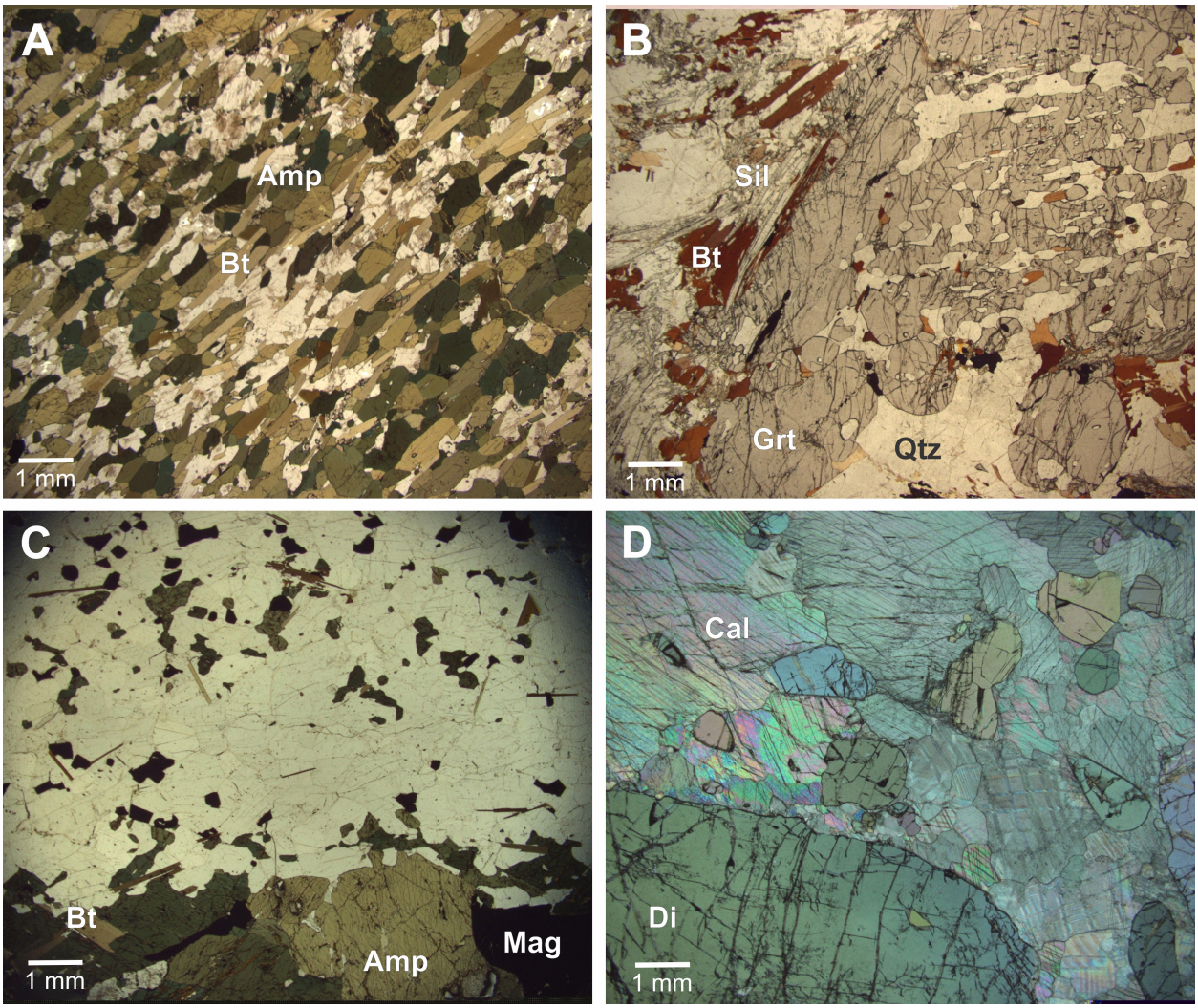

Figure 6. Typical textures exhibited by mafic gneiss, metapelite and calc-silicate gneiss. A) Sample PNA12-03C, equigranular, medium-grained mafic gneiss with decussate texture containing amphibole and biotite (PL); B) Sample PNA11-09C, metapelite schist with garnet porphyroblast with early fabric in core rimmed by sillimanite and biotite (PL); C) Sample PNA11-09A, layered amphibolite gneiss exhibiting granoblastic texture with sutured subhedral grains of quartz, K-feldspar, amphibole (hornblende) and biotite (PL); D) Sample PNA11-08B, calc-silicate gneiss showing very coarse-grained biotite with consertal (sutured) calcite grains (XPL). Magnification 1.25X for all images (Amp: amphibole; Bt: biotite; Cal: calcite; Di: diopside; Mag: magnetite; Qtz: quartz; Sil: sillimanite).

Table 7. Mineral phases documented during petrographic analyses of selected Bancroft samples; many verified by follow-up SEM analyses. For abbreviations see Table B2 in Appendix B, for sample descriptions see Appendix B.

	Silicates												
	Amphibole Gp			Epidote Gp		Feldspar Gp		Garnet Gp	Pyroxene Gp				
Sample ID	Ged	Hs	Hbl	Aln	Ep	Pl	Kfs	Sps	Cpx	Opx	Qtz	Scp	Sil
PNA 10-06A			x			x	x		x		x		
PNA 10-06B	x			x		x	x				x		
PNA 10-06C						x	x				x		
PNA 10-10													
PNA 11-01A									x				
PNA 11-01C		x				x							
PNA 11-03A	x					x	x			x	x		
PNA 11-03C			x			x	x				x		
PNA 11-04													
PNA 11-05A		x							x			x	
PNA 11-05C		x				x	x				x		
PNA 11-06A		x				x	x				x		
PNA 11-06B		x	x	x	x	x			x		x	x	
PNA 11-08B						x	x		x				
PNA 11-09A			x			x	x				x		
PNA 11-09B		x	x			x	x				x		
PNA 11-09C		x		x	x	x	x	x			x		x
PNA 11-09D			x			x	x				x		
PNA 11-09E			x			x	x		x		x		
PNA 11-09F						x	x				x		
PNA 12-03C			x			x	x				x		
PNA 12-03D		x				x	x		x		x	x	
PNA 12-03E		x	x			x	x				x		
PNA 12-06A		x	x			x	x	x		x	x		
PNA 12-06C						x	x		x		x	x	
PNA 12-10B						x	x		x		x		
PNA 12-10D			x			x	x		x		x		
PNA 12-12C			x			x	x		x			x	
PNA 12-12D			x			x	x		?		x		
PNA 12-12G			x			x	x		x		x	x	

Table 7 continued

	Silicates							Carbonates		Phosphates		Sulphates
					Phyllosilicate Gp							
Sample ID	**Thr**	**Ttn**	**Tur**	**Zrn**	**Bt**	**Chl**	**Ms**	**Cal**	**Dol**	**Fap**	**Mnz**	**Brt**
PNA10-06A		x						x		x		
PNA10-06B	x	x	x	x	x			x		x	x	
PNA10-06C				x	x		x	x		x	x	
PNA10-10								x				
PNA11-01A								x				
PNA11-01C					x			x		x		
PNA11-03A		x			x			x		x		
PNA11-03C		x			x					x		
PNA11-04								x, REE		x		
PNA11-05A		x						x				
PNA11-05C		x								x		
PNA11-06A	x											x
PNA11-06B		x	x							x		
PNA11-08B		x		x	x			x				
PNA11-09A		x			x			x		x		
PNA11-09B		x	x	x	x			x		x		
PNA11-09C		x			x							
PNA11-09D		x	x	x	x		x	x				
PNA11-09E		x						x		x		
PNA11-09F				x	x	x			x	x		x
PNA12-03C		x			x							
PNA12-03D		x	x					x				
PNA12-03E					x					x		
PNA12-06A				x	x			x		x		
PNA12-06C		x	x					x				
PNA12-10B		x						x				
PNA12-10D		x	x	x	x			x		x		
PNA12-12C		x								x		
PNA12-12D		x						x				
PNA12-12G		x		x	x					x		

Table 7 continued

	Sulphides				Oxides							Halides	Other
Sample ID	**Ccp**	**Gn**	**Po**	**Py**	**Fe-Oxide**	**Gt**	**Hem**	**Ilm**	**Mag**	**Rt**	**Ur**	**Fl**	
PNA10-06A	x		x	x							x		
PNA10-06B		x		x							x		
PNA10-06C					x								
PNA10-10												x	
PNA11-01A												x	
PNA11-01C				x				x				x	
PNA11-03A				x				x		x	x		Fe-Ti-U oxide
PNA11-03C				x				x					
PNA11-04					x						x	x	REE-oxide
PNA11-05A													
PNA11-05C				x	x								
PNA11-06A				x									
PNA11-06B				x									
PNA11-08B			x										
PNA11-09A							x	x	x				
PNA11-09B				x				x	x	x			
PNA11-09C				x				x	x				
PNA11-09D				x		x			x	x			
PNA11-09E	x		x	x									
PNA11-09F								x		x			
PNA12-03C				x				x					
PNA12-03D	x		x	x									Po>Py>Ccp
PNA12-03E			x	x				x	x				
PNA12-06A				x	x								unk incl Py
PNA12-06C			x	x									graphite?
PNA12-10B				x			x		x				
PNA12-10D					x								
PNA12-12C				x									
PNA12-12D					x								
PNA12-12G				x					x				

Scanning Electron Microscopy

Scanning electron microscopy was used to verify the minerals identified in the petrographic study. These phases are noted in the petrographic descriptions provided in Appendix B.

Electron Probe Microanalysis

For the inverse geochemical modelling reported in Desbarats *et al.* (2016), the composition of some of the mineral phases was determined using EPMA. For example, biotite grains were analysed from samples from the Croft and Rare Earth No. 2 mines, amphibole from Croft, Rare Earth No. 2 and Halo mines, as well as scapolite and pyroxene from the Halo Mine. The amphibole was determined to be hastingsite or magnesiohastingsite and the scapolite was determined to be a phase intermediate between marialite (Na variety) and meionite (Ca variety) (formerly known as mizzonite: $(Na,Ca)_4(Al,Si)_{12}O_{24}(Cl,CO_3)$).

The results of REE-bearing minerals including allanite, (fluor)apatite, bastnäsite, synchysite and monazite are given in Table 8 with summary formulae in Table 10. For example, the composition of allanite is calculated to be $(Ca,Na,Mg,Mn)_{2.42}(Y,Th)_{1.0}REE_{2.73}Fe_{1.16}Al_{1.75}Si_{3.25}O_{12}(OH)$ based on 13 oxygens. These minerals tend to be LREE-enriched with minor to trace UO_2 and ThO_2. Both bastnäsite and synchysite have high F contents, 6 and 5.3 wt.%, respectively. The SEM photomicrographs of these minerals are shown in Fig. 7.

The composition of U- and Th-bearing minerals as determined by EPMA are provided in Table 9. The main minerals analysed include uraninite, thorite and brannerite. The uraninite grains associated with these deposits tend to be Pb-, Th- and REE-bearing with up to 9 wt.% ThO_2, 12 wt.% PbO and 7 wt.% ΣREE. A summary composition is provided in Table 10. The presence of these cations is not unusual, Janeczek and Ewing (1992) have reported that up to 20 wt.% of these cations can be found and accommodated in uraninite. The two thorite grains analysed contain from 11-20 wt.% U and thus could be considered as uranothorite grains (*cf*., Robinson and Abbey, 1957). They also contain minimal REE and trace Pb. A summary composition is also provided in Table 10. Brannerite, a Ti-and U-bearing mineral contains some trace amounts of REE and appears to have a more typical composition. A summary composition is provided in Table 10.

Autoradiography

Autoradiograph images are shown in Appendix B and a brief summary of results is presented in Table 11. Activity ranges from Nil to High (Fig. 8) with most of the samples in the very low range. Those showing faint or dark spots contain radioactive minerals such as uraninite, thorite or zircon. In some samples, the grain boundaries and textures may become highlighted due to this process, indicating the possibility of some very-fine grained radioactive minerals along grain boundaries.

Table 8. EPMA results for REE-bearing minerals in selected samples from the Bancroft area.

Mineral	Allanite	Apatite*	Bastnäsite	Synchysite	Synchysite?	Monazite	Monazite
Sample ID	PNA10-06A	PNA11-04	PNA11-04	PNA11-04	PNA11-04	PNA11-09C	PNA10-06B
No. Sites	(n=10)	(n=6)	(n=8)	(n=9)	(n=3)	(n=4)	(n=9)
SiO_2 (wt.%)	31.5	0.5	n.d.	n.d.	n.d.	n.d.	n.d.
TiO_2	0.2	n.d.	n.d.	n.d.	n.d.	n.d.	n.d.
Al_2O_3	14.4	n.d.	n.d.	n.d.	n.d.	n.a.	n.a.
FeO	13.4	n.d.	n.d.	n.d.	6.5	0.2	n.d.
V_2O_3	n.d.	n.a.	n.a.	n.a.	n.a.	n.a.	n.a.
MnO	0.5	n.a.	n.a.	n.a.	n.a.	n.a.	n.a.
MgO	0.4	n.d.	n.d.	n.d.	n.d.	n.d.	n.d.
CaO	12.8	53.1	0.1	8.6	18.6	0.7	0.3
Na_2O	0.1	n.a.	n.a.	n.a.	n.a.	n.a.	n.a.
CO_2	n.a.	n.a.	28.1	29.7	34.5	n.a.	n.a.
F*	n.a.	3.61	6.0	5.3	n.a.	n.a.	n.a.
Cl	n.a.	n.d.	n.a.	n.a.	n.a.	n.a.	n.a.
P_2O_5	n.d.	39.1	n.d.	n.d.	n.d.	33.5	34.0
SrO	n.d.	n.a.	n.a.	n.a.	n.a.	n.a.	n.a.
Y_2O_3	0.5	0.4	0.2	0.2	4.5	2.0	0.3
ZrO_2	n.a.	0.1	n.d.	n.d.	n.d.	0.1	0.1
Nb_2O_5	n.a.	n.d.	n.d.	n.d.	n.d.	n.d.	n.d.
La_2O_3	2.7	0.3	24.3	18.7	8.3	12.8	22.0
Ce_2O_3	9.6	0.9	32.1	29.7	16.3	28.3	34.4
Pr_2O_3	1.3	n.a.	n.a.	n.a.	n.a.	n.a.	n.a.
Nd_2O_3	4.2	0.4	7.4	8.3	7.0	13.6	8.6
Sm_2O_3	n.d.	0.1	0.6	0.8	1.5	2.7	1.2
Yb_2O_3	n.d.	n.d.	n.d.	n.d.	n.d.	n.d.	n.d.
PbO	n.d.	n.d.	n.d.	n.d.	n.d.	0.2	n.d.
ThO_2	0.5	0.1	0.1	n.d.	0.6	2.6	0.3
UO_2	n.d.	n.d.	n.d.	n.d.	n.d.	0.6	n.d.
Total	**92.2**	**97.13**	**98.9**	**101.5**	**97.9**	**97.3**	**101.2**

*Sample was re-analysed to determine F content; these results are combination of majors (new) and traces (old); total accounts O=F.

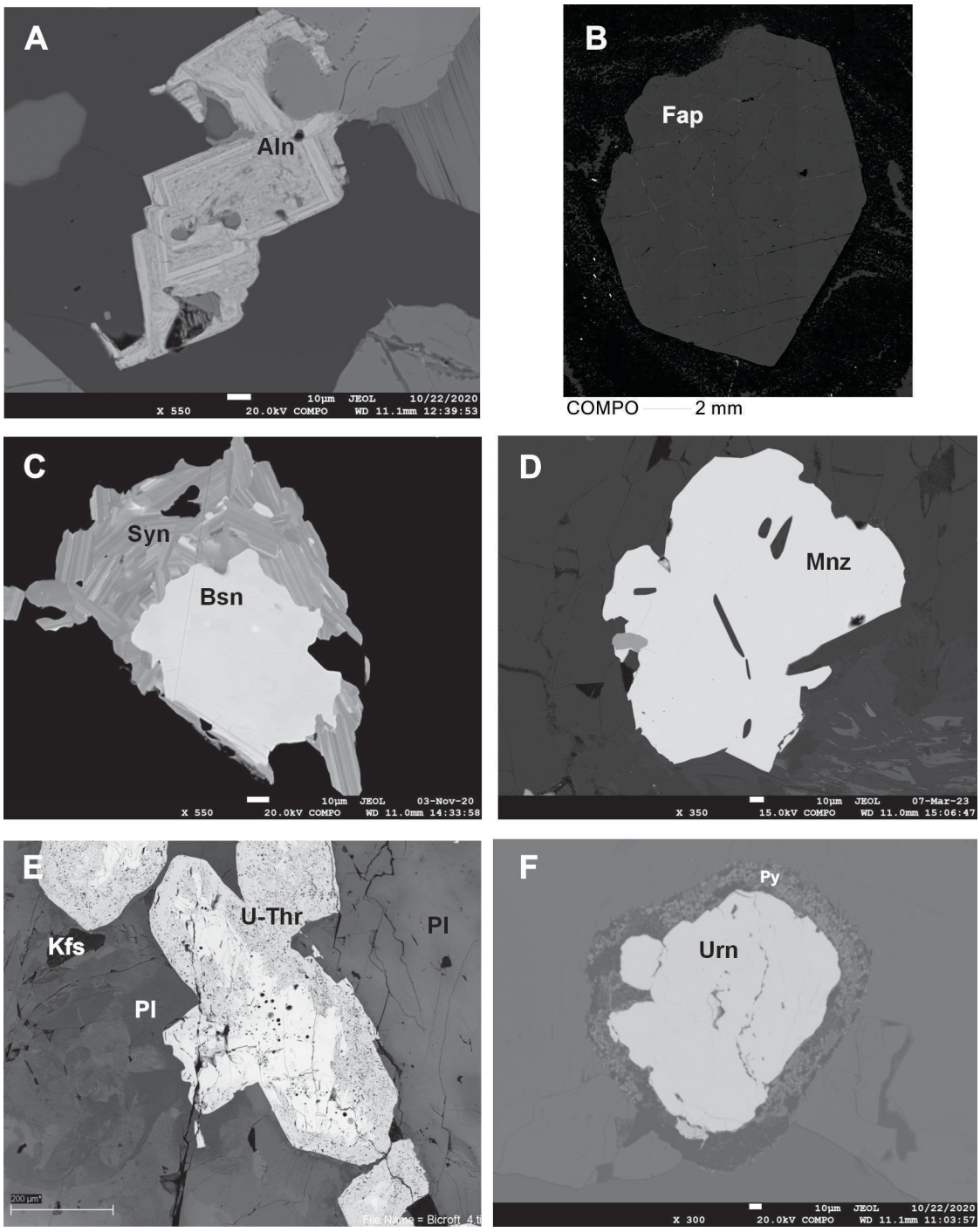

Figure 7. Backscattered photomicrographs of mineral phases analysed by EPMA or SEM. A) highly altered allanite (Aln) in sample PNA10-06B; B) REE-bearing fluorapatite (Fap) in sample PNA11-04-note image is a composite of 54 images as grain is 1.5 cm wide; C) basnäsite (Bsn) surrounded by synchysite (Syn) in sample PNA11-04; D) monazite (Mnz) in sample PNA11-06B; E) uranothorite (U-Thr) in polished slab from the Bicroft Mine (Robinson and Abbey, 1957; National Mineral Collection-uncatalogued); F) uraninite (Urn) rimmed by pyrite (Py) in sample PNA10-06B.

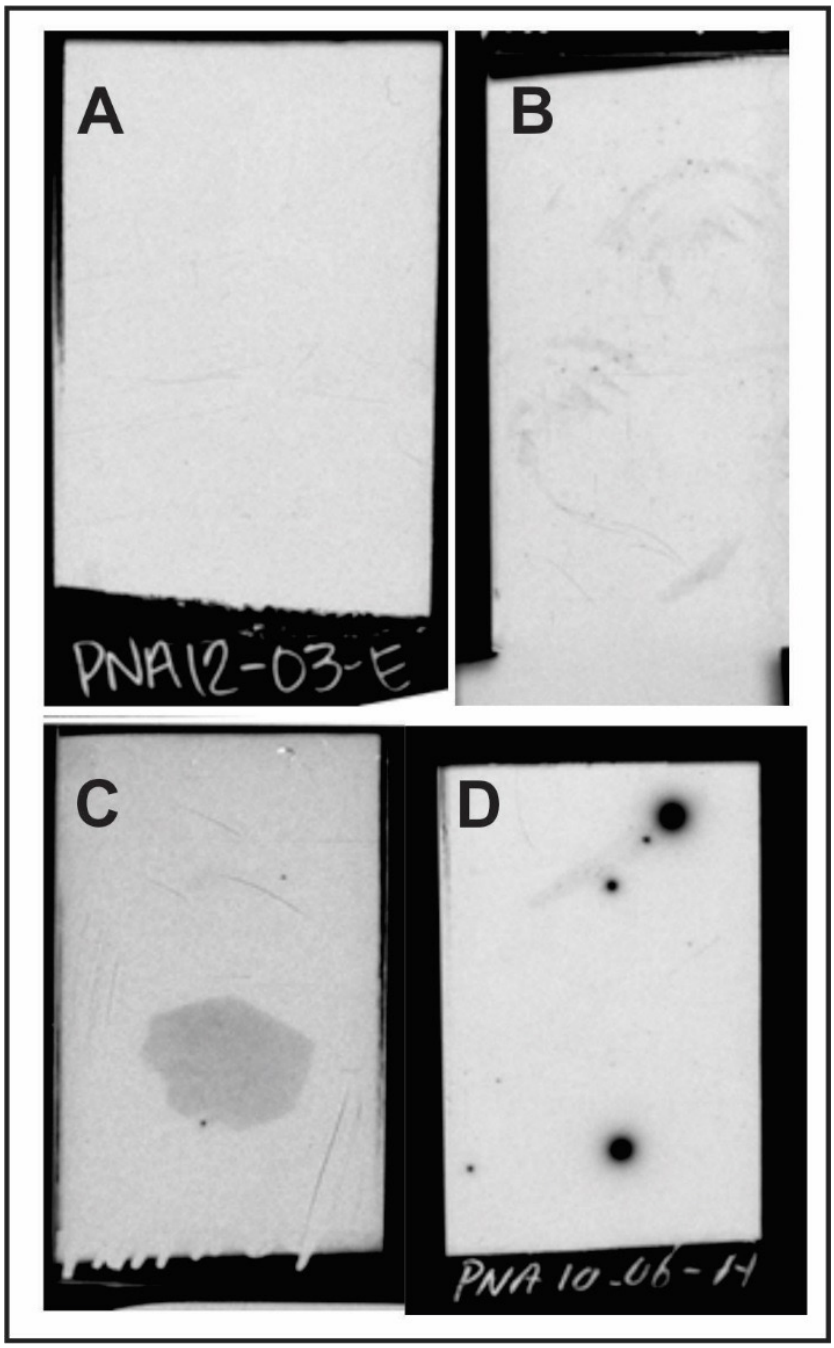

Figure 8. Examples of autoradiographs showing A) nil (PNA12-03E); B) very low (PNA10-06C); C) low (PNA11-04); and D) high radioactivity (PNA10-06A). Dark spots represent radioactive minerals such as uraninite, thorite or zircon. Textural features can be brought out by the autoradiography process.

Table 9. EPMA results for U- and Th-bearing minerals in selected samples from the Bancroft area.

Mineral	**Uraninite**	**Uraninite**	**Uraninite**	**Uraninite**	**Thorite**	**Thorite**	**Brannerite**
Sample ID	**PNA10-06A**	**PNA10-06B**	**PNA11-03A**	**PNA11-04**	**PNA10-06B**	**PNA11-06A**	**PNA11-03A**
No. Sites	**(n=11)**	**(n=5)**	**(n=5)**	**(n=7)**	**(n=5)**	**(n=2)**	**(n=4)**
SiO_2 (wt.%)	n.d.	n.d.	0.1	n.d.	21.4	15.5	8.6
TiO_2	0.1	0.1	0.1	0.1	0.1	n.d.	40.5
FeO	n.d.	n.d.	n.d.	1.2	0.1	1.4	16.9
MgO	n.d.	n.d.	0.1	n.d.	n.d.	n.d.	0.1
CaO	0.8	0.5	0.2	0.6	2.7	0.2	1.2
P_2O_5	n.d.	n.d.	n.d.	n.d.	0.1	0.1	n.d.
Y_2O_3	4.9	2.9	2.5	3.0	0.5	2.6	1.0
ZrO_2	n.d.	n.d.	n.d.	n.d.	n.d.	0.1	n.d.
Nb_2O_5	n.d.	n.d.	n.d.	0.1	n.d.	n.d.	0.3
La_2O_3	n.d.	n.d.	n.d.	0.1	0.1	0.2	n.d.
Ce_2O_3	0.5	0.5	0.2	1.5	0.1	2.0	0.3
Nd_2O_3	0.6	0.3	0.2	1.4	n.d.	1.5	0.2
Sm_2O_3	0.3	0.1	0.2	0.5	n.d.	0.3	0.1
Yb_2O_3	0.6	0.4	0.2	0.3	n.d.	0.2	n.d.
PbO	10.9	11.2	11.8	10.3	1.0	0.1	n.d.
ThO_2	5.0	7.5	7.3	9.2	42.4	49.7	n.d.
UO_2	72.2	73.1	74.2	67.3	19.5	11.6	22.2
Total	**95.8**	**96.8**	**97.2**	**95.7**	**88.1**	**85.7**	**91.4**

Table 10. Mineral formulae of selected U-, Th- and REE-bearing minerals from Bancroft samples based on EPMA results (see Tables 8 and 9).

Mineral	**Ideal Formula**	**This Study**
Allanite	$(Ce,Ca,Y)(Al_2Fe^{2+})(Si_2O_7)(SiO_4)O(OH)$	$(Ca,Na,Mg,Mn)_{2.42}(Y,Th)_{1.0}REE_{2.73}Fe_{1.16}Al_{1.75}Si_{3.25}O_{12}(OH)$
Fluorapatite	$Ca_5(PO_4)_3F$	$Ca_5(REE_{0.1})(PO_4)_3F$
Bastnäsite	$Ce(CO_3)F$	$(Ce_{0.39}, La_{0.30}, Nd_{0.09})(C_{1.27}O_3)F_{0.63}$
Brannerite	UTi_2O_6	$(U_{0.28}Ca_{0.07})(Ti_{1.77}Fe_{0.82}Si_{0.50})O_6$
Monazite	$(Ce,Nd,Y,Dy,Sm,Nd,Th)(PO_4)$	$Ce_{0.40}Nd_{0.19}La_{0.18}Sm_{0.04}Th_{0.0}2P_{1.1}O_4$
Synchysite	$CaCe(CO_3)_2F$	$Ca_{0.50}(Ce_{0.59}, La_{0.37}, Nd_{0.16})(C_{1.09}O_3)_2F_{0.90}$
Thorite/Uranothorite	$(Th,U)SiO_4$	$Th_{0.52}U_{0.23}Pb_{0.01}Ca_{0.16}Si_{1.15}O_4$
Uraninite	UO_2	$U_{0.81}Th_{0.08}Pb_{0.16}Y_{0.03}O_2$

Table 11. Qualitative assessment of autoradiographs.

Sample ID	Activity	Comments
PNA10-06A	High	Several large dark spots: uraninite
PNA10-06B	High	Several large dark spots: uraninite, thorite
PNA10-06C	Nil	
PNA10-10	Very low	Grain boundaries faintly outlined
PNA11-01A	Very low	Grain boundaries faintly outlined
PNA11-01C	Low	Small spots indicate possible radioactive minerals
PNA11-03A	High	Dark spots: uraninite, U-bearing Ti-Fe-oxide
PNA11-03C	Nil	
PNA11-04	Low	Few dark spots: uraninite, REE-carbonate, REE-oxide; apatite grain visible in image
PNA11-05A	Very low	Grain boundaries faintly outlined
PNA11-05C	Nil	
PNA11-06A	Low	One dark spot: thorite; faint spots also present
PNA11-06B	Very low	Few faint spots
PNA11-08B	Low	Small spots: zircon; faint grain boundaries
PNA11-09A	Very low	Grain boundaries faintly outlined, some faint spots
PNA11-09B	Very low	Grain boundaries faintly outlined, some faint spots
PNA11-09C	Low	Few dark spots indicate possible radioactive minerals
PNA11-09D	Low	Few dark spots indicate possible radioactive minerals
PNA11-09E	Low	Few dark spots indicate possible radioactive minerals
PNA11-09F	Nil	
PNA12-03C	Very low	Grain boundaries faintly outlined, some faint spots
PNA12-03D	Very low	Grain boundaries faintly outlined, some faint spots
PNA12-03E	Very low	Grain boundaries faintly outlined
PNA12-06A	Very low	Grain boundaries faintly outlined
PNA12-06C	Very low	Grain boundaries faintly outlined
PNA12-10B	Low	Few dark spots indicate possible radioactive minerals
PNA12-10D	Very low	Grain boundaries faintly outlined
PNA12-12C	Nil	
PNA12-12D	Low	Few faint spots indicate possible radioactive minerals
PNA12-12G	Nil	

DISCUSSION

Mineralogy

The hand samples examined in this study area are representative of the types of rocks that were explored and mined in the Bancroft region from the 1880s to the early 1980s. The commodities exploited included non-radioactive (apatite, calcite, fluorite, feldspar, magnetite, mica, quartz, sodalite) and radioactive (uraninite, uranothorite ± allanite, betafite, and others) materials (Satterly, 1957, Sabina, 1986). This study focuses on understanding the impact of radioactive minerals and their long-lived radioactivity on the environment in the post-mining phase. Thus, the modal mineralogy and mineral chemistry are important constraints in predicting potential environmental issues.

Results from the XRD analyses quantify the major and minor mineral phases in the host rocks collected. Mostly these are typical rock-forming minerals of the pegmatites and gneisses including quartz, plagioclase, K-feldspar, amphibole and pyroxene-group minerals, garnet, phyllosilicates (chlorite, biotitic mica) plus common accessory minerals such as tourmaline, sillimanite and scapolite-group minerals. The fluorite-bearing pegmatites are rich in calcite, fluorite and fluorapatite. The XRD results were complemented by detailed petrographic analyses of a myriad of trace minerals (see Table 7 and Appendix B). Some of the observed trace minerals host contaminants of interest and therefore are useful for determining a geochemical signature. These include the radioactive ore minerals uraninite, uranothorite, thorite and brannerite and the accessory REE-bearing minerals allanite, apatite, bastnäsite, synchysite and monazite. Other radioactive minerals detected include minor to trace thorite, cyrtolite, pyrochlore, betafite and fergusonite. According to Robinson and Abbey (1957), uranothorite may be more easily weathered than uraninite. Note that these minerals were singled out following detailed SEM analyses with subsequent EPMA analyses to provide more precise mineral compositions (Table 9). These minerals, along with the gangue minerals noted above, define a mineralogical footprint for this geological environment and its granitic pegmatite-hosted U-Th-REE deposits.

Mineralogical Signature

Geoenvironmental ore deposit models reported in Plumlee and Nash (1995) and updates in Seal and Foley (2002) are descriptions that provide guidance on potential risks associated with a variety of ore deposits. The closest model that fits the Bancroft region is that of Armbrustmacher *et al.* (1995) who describes the geological characteristics of Th and REE vein deposits. Table C1 (Appendix C) provides a direct comparison with the factors outlined by Armbrustmacher *et al.* (1995) with what is known from this study and previous studies in the Bancroft area. The results from this study provide quantitative evidence of the downstream environmental impacts.

The sources and sinks for elements of interest are known through the detailed mineralogical and chemical analyses of the rocks present at a mine site (Hammarstrom and Smith, 2002). In the Bancroft area, uraninite contains from 5-10 wt.% ThO_2, up to 12 wt.% PbO and < 7 wt.% REEs, whereas thorite/uranothorite contains between 11-20 wt.% UO_2 and much less REE (< 6 wt.%, including Y). Thus, dissolution of U and Th under oxidizing conditions will contribute to surface runoff in shallow groundwater systems, but Th will remain close to its source due to strong sorption

to soil particles (Torstenfelt, 1986; Desbarats and Percival, 2016; Desbarats *et al.*, 2016; Patel *et al.*, 2023). In general, U-bearing minerals have low solubility under reducing conditions, but under oxic conditions, U will form stable uranyl complexes with carbonate or phosphate ligands and can be mobile. In groundwaters around the Bancroft deposits, Th concentrations range from 0.02-0.12 µg/L (n=28) in filtered water and from 0.03-11.56 µg/L in unfiltered water, whereas U ranges from 0.59-2580 µg/L (n=41) in filtered water and 1.19-2530 µg/L in unfiltered water (Desbarats *et al.*, 2016). In contrast, maximum total REE concentrations in filtered and unfiltered groundwater were measured at 24.2 µg/L and 126.5 µg/L, respectively. Desbarats *et al.* (2016) suggested that contributions of REE in groundwaters are related to breakdown of metamict minerals such as allanite. In addition, carbonate (synchysite) and phosphate (monazite) minerals tend to contain limited LREE in their structure, but both minerals are considered to have low solubility.

Contributions to the environment also arise from lake and stream sediments as well as waste rock and tailings dumps. Although the main minerals in these materials are similar to the gangue minerals reported here, trace phases will also be present and can release contaminants to the surface waters. For example, the regional lake and stream sediments contain from 0.4-140 mg/kg U and 1.2-110 mg/kg U, respectively and concentrations of uranium in tailings at the Bicroft Mine were determined to be from 3.1-210 mg/kg and in downstream sediments up to 730 mg/kg (Parsons *et al.*, 2013). Thorium concentrations in tailings can be as high as 1030 mg/kg at Bicroft and range from 100-495 mg/kg in downstream sediments (Parsons *et al.*, 2014). Also, following extraction of U, some of the daughter products remain in the tailings and waste rock. As an example, radon gas surveys of soils in the vicinity of the Bicroft Mine show values up to 770 kBq/m^3 whereas regional values range from 3.2 to 48 kBq/m^3. However, tailings from the Bicroft Mine have radon gas measurements from 1800 to 12,000 kBq/m^3 (Parsons *et al.*, 2013).

The mineralogical footprint of these mine wastes and contaminated sediments is localized near the mine workings. The mineralized bedrock, waste rock dumps and tailings continue to contribute contaminants to ground and surface waters through weathering. Further remediation may be required to limit the environmental impact of these sites.

SUMMARY AND CONCLUSIONS

Bancroft, Ontario is renowned for its collecting localities of a wide variety of industrial and ore-related minerals. Situated in the Grenville Province of the Canadian Shield, there is a legacy of U-Th-REE mines and prospects, along with fluorite and mica mines that have been explored and mined since the late 1880s.

This study focused on characterizing the mineralogy and petrography of representative samples from a range of lithologies as part of the Environmental Geoscience Program (EGP) project on the geoenvironmental characteristics of granitic pegmatite-hosted U-Th-REE deposits of the Grenville Province. Samples were collected from 14 sites and include veins, dykes, pegmatites, gneisses (quartzo-feldspathic, amphibolite/mafic, metapelite, calc-silicate) and marbles. The gneissic samples contain quartz, feldspar and mafic minerals (clinopyroxene, amphibole) and micas. Calcite is dominant in the calc-silicate gneisses and marbles; fluorite occurs in pegmatites.

Accessory minerals include sulphides (chalcopyrite, galena, pyrrhotite and pyrite) and oxides (goethite, hematite, ilmenite, magnetite, uraninite, uranothorite, thorite) as well as a host of other silicate minerals (sepiolite, sillimanite, titanite, tourmaline, zircon). Monazite and apatite occur in calc-silicate gneisses and quartzo-feldspathic gneisses.

Mineral phases containing elements of interest in this area include the radioactive minerals uraninite, thorite/uranothorite and brannerite and those rich in REE such as allanite, bastnäsite, fluorapatite, monazite and synchysite. These minerals, especially if weathered or metamict, are contributing uranium, thorium and REE into the receiving environment. They are found locally around the mine sites in waste materials (tailings and rocks), in mineralized bedrock, and scattered core samples. Mine workings contribute these elements into the flowing adits and diamond drill holes. The mineralogical and geochemical signatures of these types of deposits are comparable to the U.S.G.S. geoenvironmental model for Th-REE veins. The host rocks, ore and gangue mineralogy are similar, except that the Bancroft veins and pegmatites are enriched in U relative to Th and do contain REE-bearing minerals.

Although these studies are on abandoned mines, they provide sites and samples to develop new methods for analytical, mineralogical and geochemical characterization. Identifying the factors that control the release and transport of metals and radionuclides will contribute to the development of models for environmental risk assessment of similar U-Th-REE deposits.

ACKNOWLEDGEMENTS

This project was supported by the Geological Survey of Canada's Environmental Geosciences Program (Earth Sciences Sector, Natural Resources Canada). Special thanks to Michael Burns (GSC-O) for lapidary assistance, to Ashley Abraham for laboratory and editorial assistance, to Jessica Tomacic for editorial assistance, to Michael Parsons (GSC-A) for on-going discussions and for critical review of this Open File Report. We want to acknowledge the early (1993) contributions of the late Dr. Y.T.J. (John) Kwong as a strong proponent of coordinating geoscience knowledge from all stages of the mining cycle to address environmental issues.

REFERENCES

Armbrustmacher, T.J., Modreski, P.J., Hoover, D.B. and Klein, D.P. 1995. Th-rare earth element vein deposits. *In* Preliminary Compilation of Descriptive Geoenvironmental Mineral Deposit Models, edited by E.A. du Bray, U.S. Geological Survey Open File Report 95-831, p. 50-53.

Armstrong, J.T. 1988. Quantitative analysis of silicates and oxide minerals: Comparison of Monte-Carlo, ZAF and Phi-Rho-Z procedures. *In* Microbeam Analysis, edited by D.E. Newbury, San Francisco Press, Inc. San Francisco, California, p. 239-246.

Barnett, P.J. 1983. Quaternary geology of the Bancroft area. Ontario Geological Survey Open File 5428, 124 pp.

Bliss, J.D. 1992. Developments in mineral deposit modeling. U.S. Geological Survey Bulletin, 2004, 168 pp.

Bristow, Q. and Bernius, G.R. 1984. Field evaluation of a magnetic susceptibility logging tool. Geological Survey of Canada, Paper 84-1A, p. 453-462.

Bullis, A.R. 1965. Geology of Metal Mines Ltd. (Bancroft Division). Transactions of the Canadian Institute of Mining and Metallurgy (CIMM) and Mining Society of Nova Scotia, v. LXVIII, p. 195-203.

Burgess, M.M., Percival, J.B., Jefferson, C.W. and Kwong, Y.T.J. 2003. Using geoscience expertise to achieve sustainable development: Federal contributions to environmental and resource assessments. Geological Association of Canada-Mineralogical Association of Canada Annual Meeting, Vancouver, May (Abstract) (http://gac.esd.mun.ca/gac_2003/search_abs/).

Carr, S.D., Easton, R.M., Jamieson, R.A. and Culshaw, N.G. 2000. Geologic transect across the Grenville orogen of Ontario and New York. Canadian Journal of Earth Sciences, v. 37, p. 193-216.

Corriveau, L., Perreault, S. and Davidson, A. 2007. Prospective metallogenic settings of the Grenville Province. *In* Mineral Deposits of Canada: A Synthesis of Major Deposit-Types, District Metallogeny, the Evolution of Geological Provinces, and Exploration Methods, edited by W.D. Goodfellow, Geological Association of Canada, Mineral Deposits Division, Special Publication No. 5, p. 819-847.

Cox, D.P. and Singer, D.A. 1986. Mineral deposit models. U.S. Geological Survey Bulletin, v. 1693, 379 pp.

Davidson, A. 1986. New interpretations in the southwestern Grenville Province. *In* The Grenville Province, edited by J.M. Moore, A. Davidson and A.J. Baer. Geological Association of Canada, Special Paper 31, p. 61-74.

Desbarats, A.J. and Percival, J.B. 2016. Groundwater chemistry of uranium-thorium-rare earth element deposits, Bancroft area, Ontario. Geological Survey of Canada, Open File 7992, 65 pp (doi: 10.4095/297779).

Desbarats, A.J., Percival, J.B. and Venance, K.E. 2016. Trace element mobility in mine waters from granitic pegmatite U-Th-REE deposits, Bancroft area, Ontario. Applied Geochemistry, v. 67, p. 153-167.

Easton, R.M. 1986. Geochronology of the Grenville Province. *In* The Grenville Province, edited by J.M. Moore, A. Davidson and A.J. Baer. Geological Association of Canada, Special paper 31, p. 271-280.

Easton, R.M. 1992. The Grenville Province and Proterozoic history of central and southern Ontario. *In* Geology of Ontario, edited by P.C. Thurston, H.R. Williams, R.H. Sutcliffe and G.M. Scott. Ontario Geological Survey Special Volume 4, Part 2, p. 715-904.

Easton, R.M. and Davidson, A. 1994. Terrane boundaries and lithotectonic assemblages within the Grenville Province, eastern Ontario. Field Trip A1: Guidebook, Geological Association of Canada-Mineralogical Association of Canada Annual Meeting, May 12-15, Waterloo, Ontario

Ford, K.L., Holman, P.B., Grant, J.A., Carson, J.M. and Heteu, R. 1992. Airborne radioactivity maps of the Central metasedimentary belt of eastern Ontario and part of western Québec. Geological Survey of Canada FORUM, Abstracts volume 1992, p. 10.

Goodman, C. and Thompson, G.A. 1943. Autoradiography of minerals. American Mineralogist, v. 28, p. 456-467.

Gordon, J.B., Rybak, U.C. and Robertson, J.A. 1981. Uranium and thorium deposits of southern Ontario. Ontario Geological Survey, Open File Report 5311, 665 pp.

Griffith, J.W. 1986. Uranium deposits of the Bancroft area, Ontario. *In* Uranium Deposits of Canada, edited by E.L. Evans, The Canadian Institute of Mining and Metallurgy, Special Vol. 33, p. 57-61.

Hammarstrom, J.M. and Smith, K.S. 2002. Geochemical and mineralogical characterization of solids and their effects on waters in metal-mining environments. *In* Geoenvironmental Models of Mineral Deposits, edited by R.R. Seal II and N.K. Foley. U.S. Geological Survey Open File Report 02-195, p. 8-54.

Janeczek, J. and Ewing, R.C. 1992. Structural formula of uraninite. Journal of Nuclear Materials, v. 190, p. 128-132.

Killeen, P.G. 1986. A system of deep test holes and calibration facilities for developing and testing new borehole geophysical techniques. *In* Borehole Geophysics for Mining and Geotechnical Applications, edited by P.G. Killeen, Geological Survey of Canada, Paper 85-27, p. 29-46.

Kretz, R. 1983. Symbols for rock-forming minerals. American Mineralogist, v. 68, p. 277-279.

Kwong, Y.T.J. 1993. Prediction and prevention of acid rock drainage from a geological and mineralogical perspective: MEND Project 1.32.1, Canada Centre for Mineral and Energy Technology (CANMET), Energy, Mines and Resources Canada, Ottawa, 47 p.

Kwong, Y.T.J. 2003. Comprehensive environmental ore deposit models as an aid for sustainable development. Exploration and Mining Geology v. 12, p. 31-36.

Laurin, A.F., Sharma, K.N.M. and Wynne-Edwards, H.R. 1972. The Grenville Province of the Precambrian in Quebec. Guidebook for Excursion A46 and C46, International Geological Congress, Montreal Quebec, 56 pp.

Lentz, D. 1991. Radioelement distribution in U, Th, Mo, and rare-earth-element pegmatites, skarns, and veins in a portion of the Grenville Province, Ontario and Quebec. Canadian Journal of Earth Sciences, v. 28, p. 1-12.

Lentz, D. 1996. U, Mo, and REE mineralization in late-tectonic granitic pegmatites, southwestern Grenville Province, Canada. Ore geology Reviews, v. 11, p. 197-227.

Lumbers, S.B., Heaman, L.M., Vertolli, V.M. and Wu, T.-W. 1990. Nature and timing of Middle Proterozoic magmatism in the Central Metasedimentary Belt, Grenville Province, Ontario. *In* Mid-Proterozoic Laurentia-Baltica, edited by C.F. Gower, T. Rivers and A.B. Ryan. Geological Association of Canada, Special Paper 38, 243-276.

Moore, J.M. 1982. Stratigraphy and tectonics of the Grenville Orogen in eastern Ontario. Friends of the Grenville, 1982 Grenville Workshop, Rideau Ferry, Ontario, Abstracts, p. 7.

Moore, J.M. 1986. Introduction: The 'Grenville problem' then and now. *In* The Grenville Province, edited by J.M. Moore, A. Davidson and A.J. Baer. Geological Association of Canada Special Paper 31, p. 1-11.

Moore, J.M. and Pride, C. 1979. Geochemical signatures and metallogeny, Grenville Orogen. *In* Geoscience Research Grant Program, Summary of Research, 1978-1979, Ontario Geological Survey, Miscellaneous Paper 87, p. 104-107.

Ontario Geological Survey. 1991. Bedrock geology of Ontario, southern sheet. Ontario Geological Survey Map 2544, scale 1:1,000,000.

Parsons, M.B., Friske, P.W.G., Ford, K.L. and LeBlanc, K.W.G. 2013. Transport and fate of uranium, rare earth elements, and radionuclides from decommissioned tailings at the historical Bicroft uranium mine, Ontario. Geological Association of Canada-Mineralogical Association of Canada Joint Annual Meeting, Programs with Abstracts, v. 36, p. 157-158.

Parsons, M.B., Friske, P.W.B., Laidlow, A.M., and Jamieson, H.E. 2014. Controls on uranium, rare earth element, and radionuclide mobility at the decommissioned Bicroft Uranium Mine, Ontario; Geological Survey of Canada, Scientific Presentation 24, poster. doi:10.4095/293623.

Patel, K.S., Sharma, S., Maity, J.P., Martin-Ramos, P., Fiket, Z., Bhattacharya, P. and Zhu, Y. 2023. Occurrence of uranium, thorium and rare earth elements in the environment: A review. Frontiers in Environmental Science, Open Access (doi: 10.3389/fenvs2022.1058053).

Percival, J.A. and Easton, R.M. 2007. Geology of the Canadian Shield in Ontario: An update. Ontario Geological Survey Open File Report 6196 and Geological Survey of Canada, Open File 5511, Ontario Power Generation, Report 068819-REP-01200-10158-R)), 65 pp.

Percival, J.B., Parsons, M.B., Kwong, Y.T.J., Beauchemin, S., and Desbarats, A.J. 2011. The role of mineralogy in geo-environmental ore deposit models. Geological Association of Canada-Mineralogical Association of Canada Annual Meeting, Program With Abstracts, v. 34, p. 169.

Percival, J.B., Desbarats, A.J., Venance, K.E. and Parsons, M.B. 2015. The role of mineralogical research in mine site characterization. Geological Association of Canada-Mineralogical Association of Canada-American Geophysical Union Annual Meeting, May 2015.

Plumlee, G.S., and Nash, J.T., 1995. Geoenvironmental models of mineral deposits – fundamentals and applications. *In* Preliminary Compilation of Descriptive Geoenvironmental Mineral Deposit Models, edited by E.A. du Bray, U.S. Geological Survey Open File Report 95-831, pp. 1-9.

Plumlee, G.S., Smith, K.S. and Ficklin, W.H. 1994. Geoenvironmental models of mineral deposits, and geology-based mineral-environmental assessments of public lands. U.S. Geological Survey Open File Report 94-203, 7 pp.

Rivers, T., Martignole, J., Gower, C.F. and Davidson, A. 1989. New tectonic divisions of the Grenville Province, southeast Canadian Shield. Tectonics, v. 8, p. 63-84.

Rivers, T., Culshaw, N., Hynes, A., Indares, A., Jamieson, R. and Martignole, J. 2012. The Grenville Orogen – A post-LITHOPROBE perspective. Ch. 3. *In* Tectonics Styles in Canada: The LITHOPROBE Perspective, edited by J.A. Percival, F.A. Cook and R.M. Clowes. Geological Association of Canada, Special Paper 49, p. 97-236.

Robinson, S.C. 1952. Autoradiographs as a means of studying distribution of radioactive minerals in thin sections. American Mineralogist, v. 37 (5&6), Notes and News, p. 544-547.

Robinson, S.C. 1960. Economic uranium deposits in granitic dykes Bancroft District, Ontario. Canadian Mineralogist, v. 6 (part 4), p. 513-521.

Robinson, S.C. and Abbey, S. 1957. Uranothorite from eastern Ontario. Canadian Mineralogist, v. 6, p. 1-14.

Robinson, S.C. and Sabina, A.P. 1955. Uraninite and thorianite from Ontario and Quebec. American Mineralogist, v. 40, p. 624-633.

Sabina, A.P. 1986. Rocks and Minerals for the Collector: Bancroft-Parry Sound area and southern Ontario. Geological Survey of Canada, Miscellaneous Report 39, 182 pp.

Satterly, J. 1957. Radioactive mineral occurrences in the Bancroft area. Ontario Department of Mines, 65th Annual Report, Part 6 (1956), 181 pp.

Seal, R.R. II and Foley, N.K. (eds.). 2002. Progress on geoenvironmental models for selected mineral deposit types. U.S. Geological Survey Open File Report 02-195 (https://pubs.usgs.gov/of/2002/of02-195/).

Sparkes, G. W. 2013. A re-evaluation of the application of CR-39 autoradiographs in the textural analysis of uranium-bearing samples and thin sections. Exploration and Mining Geology, v. 21, p. 79-83.

Staatz, M.H. 1992. Descriptive model of thorium-rare-earth veins. *In* Developments in Mineral Deposit Modelling, edited by J.D. Bliss, U.S. Geological Survey Bulletin 2004, p. 13-15.

Stephens, M.B., Bergström, U. and Wahlgren, C.-H. 2020. Regional context and lithotectonic framework of the 1.1-0.9 Ga Sveconorwegian orogen, southwestern Sweden. Geological Society, London, Memoirs v. 50, p. 337-349.

Torstenfelt, B. 1986. Migration of the actinides thorium, protactinium, uranium, neptunium, plutonium and americium in clay. Radiochimica Acta, v. 39, p. 105-112 (doi:10.1524/ract.1986.39.2.105).

Vandergraaf, T.T., Abry, D.R.M. and Davis, C.E. 1982. The use of autoradiography in determining the distribution of radionuclides sorbed on thin sections of plutonic rocks from the Canadian Shield. Chemical Geology, v. 36, p. 139-154.

Warr, L.N. 2021. IMA-CNMNC approved mineral symbols. Mineralogical Magazine v. 85, p. 291-320.

Wynne-Edwards, H.R. 1972. The Grenville Province. *In* Variations in Tectonic Styles in Canada, edited by R.A. Price and R.J.W. Douglas. Geological Association of Canada, Special Paper 11, p. 263-334.

APPENDIX A

Study Sites

A brief description of each study site where samples were collected is provided (see Fig. 2 for locations). Table A1 summarizes the possible minerals that can be found at each of the sites visited during the 2010-2013 field campaigns.

Study Sites

Bicroft Mine

In 1955, Bicroft Uranium Mines, Limited formed due to the amalgamation of Centre Lake Uranium Mines, Limited, and Croft Uranium Mines, Limited (Satterly, 1957). Uraniferous granitic pegmatites occur in a zone of syenitized paragneiss and amphibolite which is overlain by marble to the east and underlain by leucogranite (alaskite) of the Cardiff batholith (Satterly, 1957; Gordon *et al*., 1981). The metasediments are comprised of biotite paragneiss, amphibolite, scapolite-biotite gneiss, garnet-sillimanite-biotite paragneiss and a band of silicified marble. The metasediments were intruded and replaced by grey albite syenite, yellow-brown sodic syenite and granite containing alkaline hornblende or pyroxene and titanite and pink potassic syenite and granite. Radioactive minerals such as uranothorite, uraninite, allanite, thorite, pyrochlore and betafite generally occur in the yellow-brown or red sodic granite and syenite pegmatites (Satterly, 1957). Satterly (1957) provides detailed descriptions of the various lithologies, wall-rock alteration and the ore and Sabina (1986) provides a synopsis of the primary and accessory minerals associated with this U and Th deposit. Exploration was conducted through trenching, development of a 53.4 m adit and two shafts (71.4 m and 562 m) (Sabina, 1986). Exploration by Kerr-Addison continued until about 1975 through diamond drilling. However, production ceased by 1963; over 2 million kg of U_3O_8 were extracted from 2,233,067 t of ore (see Table 2) (Gordon et al., 1981; Sabina, 1986).

Canadian Dyno Mine

This deposit occurs between the Cheddar granite on the west and the Centre Lake granite of the Cardiff pluton on the east. It is underlain by amphibolite, pyroxene amphibolite, biotite-diopside-scapolite granulite, garnet-sillimanite paragneiss and marble. The metasediments are intruded and replaced by syenite gneiss and country rocks intruded by N-trending pegmatitic leucogranite dykes (Satterly, 1957; Gordon *et al*., 1981). It was mined for uranium and thorium between 1954 and 1960 with a total production of 599,523 t of ore with 453,592 t in reserve (see Table 2). In all, 360,524 kg of U_3O_8 were produced (Gordon *et al*., 1981; Griffith, 1986; Sabina, 1986). Ore minerals include uraninite and uranothorite associated with allanite, uranophane, crytolite (zircon) and thorite from magnetite-rich zones in the pegmatites. Sabina (1986) reported that the U-bearing minerals occur in deep red to purplish zones due to intense hematization. Accessory minerals include titanite, apatite, pyrite and molybdenite. Pegmatites also contain albite (peristerite), microcline, smoky quartz, pyroxene and amphibole (Sabina, 1986).

Cardiff Mine (Prospect)

The Cardiff prospect was initially explored for fluorite in 1943 by the Cardiff Fluorite Mines Limited and exploration for uranium and thorium began in 1953 by Cardiff Uranium Mines Limited (Satterly, 1957; Sabina, 1986). Both the uraninite and fluorite occur in calcite veins within a band of calcareous paragneiss and amphibolite near the contact with crystalline limestone (Satterly, 1957). The limestone (marble) underlies the western part of the prospect and is overlain by scapolitic amphibolite, calcareous paragneiss and biotite amphibolite. The gneisses are syenitized and intruded by syenite and granite pegmatites. Veins tend to be lenticular, pod-shaped or irregular in shape but strike conformably with the country rock (Satterly, 1957). No production occurred although two adits and a shaft (83.8 m) were developed in the south zone. Minerals associated with the calcite veins include apatite, biotite, pyroxene, scapolite, titanite, molybdenite and quartz. The shaft of this mine, sealed using waste rock from the original site, is shown in Fig. A1-B.

Croft Mine (Prospect)

The Croft deposit occurs in the same belt of syenitized paragneiss and amphibolite which hosts the Bicroft Mine. The metasediments include hornblende gneiss, amphibolite, biotite paragneiss, biotite-garnet-sillimanite gneiss (augen gneiss) cut and replaced by syenite and granite dykes (Satterly, 1957; Gordon *et al*., 1981). Development of this deposit included surface trenches, extensive diamond-drilling and an adit. Exploration of the adit level revealed four lenticular *en échelon* pegmatite bodies, along the contacts of pods of biotite-garnet-sillimanite gneiss. The dykes are biotite granite pegmatite with porphyroblastic textured feldspar (Gordon *et al*., 1981). The main mineral is uranothorite in association with secondary uranium minerals (*e.g*., allanite, betafite, uranophane, pyrochlore), zircon (cyrtolite), pyrite and molybdenite. Kerr-Addison Mines Limited carried out further exploration in the 1970s and estimated reserves at 888,867 tonnes (see Table 2) grading at 0.6 kg/tonne (Gordon et al., 1981). Figure A1-C shows the adit where water was sampled for the groundwater part of this study and Fig. A1-D shows AD downloading data from the submersed data-logger placed in an artesian borehole for the duration of the study.

Desmont Mine

This prospect is underlain by marble with inter-bands of diopside-bearing rock, calc-silicate rock and rusty mica-bearing gneisses (Satterly, 1957). The surface workings of pits, trenches and strippings are extensive over a distance of 1150 m (Sabina, 1986). The minerals uranothorite occurs in diopside or diopside-calcite rock within marble and uraninite in calc-silicate bands in marble or mica-bearing marble. Other minerals in calcite veins include uncommon stillwellite and hydroxybastnäsite. Sabina (1986) reported a long list of minerals that can be found at this site for mineral collectors (Table A1, Appendix A). Assays indicated 0.004% U_3O_8 and 0.016-0.44% MoS_2 (Gordon *et al*., 1981). The most recent exploration between 1976 and 1977 was carried out by Highland Mercury Mines, Limited (Gordon *et al*., 1981).

Dwyer Fluorite Mine

This deposit was developed for fluorite in 1918 by P.J. Dwyer with production listed as 33.5 t (see Table 2). The fluorite is in calcite veins that cut granite. Accessory minerals include apatite, hornblende and clinopyroxene (Sabina, 1986).

Halo Mine

This deposit occurs along the western side of the Cardiff dome in a curving belt of amphibolite and paragneiss with interbedded marble and metamorphic pyroxenite (Satterly, 1957; Gordon *et al.*, 1981). Uranium mineralization occurs in pegmatite, syenite, metamorphic pyroxenite and calcite-fluorite veins and consists of uraninite, uranothorite, thorite and betafite. Accessory minerals include chlorite, tourmaline, titanite, amphibole, molybdenite, pyrite and pyrrhotite (Sabina, 1986). Several prospects were explored and developed: Northwest zone, Lake zone, Pyroxenite zone and South zone. Adits were developed in the Northwest and Lake zones only. The Northwest zone is comprised of west- to northwest-striking biotite paragneiss or biotite-garnet paragneiss with uraninite occurring in granite or syenite pegmatite bodies that strike north or northwest. The Lake zone consists of paragneiss and garnet-biotite paragneiss with a narrow band of metamorphic pyroxenite and interbedded marble. Uranothorite occurs in irregular-shaped lenticular bodies within a leucogranite pegmatite (Satterly, 1957; Gordon *et al*., 1981). Including other prospects at this site, reserves were estimated at 428,191 tonnes grading 0.112% U_3O_8 (see Table 2; Gordon *et al*., 1981). The adit and remains of an exploration trench found at this site are shown in Figs. A1-E and -F, respectively.

Kenmac-Chibougamou Mine

Uranium-bearing minerals uranothorite and allanite occur with magnetite in numerous pegmatite dykes that cut amphibolite, biotite-rich paragneiss and marble (Satterly, 1957; Gordon *et al*., 1981). Accessory minerals include zircon, apatite, scapolite, calcite and biotite (Sabina, 1986). Reserves in 1957 were estimated at 181,436 tonnes at 0.20% U_3O_8 (see Table 2). Development included trenching, surface stripping, diamond-drilling and an 84-m long adit (Gordon *et al*., 1981).

Millar's Mine

This deposit was opened in about 1900 as a radioactive (thorite, thorianite, uranophane) and phosphate (apatite) prospect. The minerals occur in calcite veins cutting graphic granite pegmatite. Development included trenching and a 9 m long adit driven into a ridge (Sabina, 1986).

OTC Highway 118

In 1979 the GSC drilled two holes (60 mm diameter; BN-79-4 and BN-79-5) along Highway 118, southwest of Bancroft (near Monck Road) in a Kerr-Addison property. These boreholes were drilled to intersect uranium-and thorium-bearing mineralized zones to test and develop new logging systems, starting with gamma ray spectral logging. In 1981 two 100 mm holes (HQ; BN-81-1 and BN-81-2) were drilled 60 m apart in the same location to test and evaluate a new borehole

XRF probe (Killeen, 1986). In addition, magnetic susceptibility, IP and resistivity were tested as well as an assessment of the volume of rock between holes. The logs of these boreholes show numerous narrow pegmatite intersections within strongly banded biotite gneiss and hornblende biotite gneiss lithologies. Based on the tests, the pegmatite intersections show high counts for U and Th using both the gamma ray spectral logging tool as well as the downhole XRF probe (Killeen, 1986). Magnetic susceptibility tended to be negligible for the pegmatites in comparison with the gneisses (Bristow and Bernius, 1984).

Rare Earth Mine 2

The deposit is underlain by amphibolite and marble bands that were intruded by metagabbro and granite or granite pegmatite. Uranothorite, uraninite and uranophane occur in the granite or granite pegmatite in lenticular bodies which parallel the gneissic fabric of the metagabbro. Accessory minerals include fergusonite, zircon, allanite, with minor titanite, pyroxene, smoky quartz, hematized feldspar and peristerite (Satterly, 1957; Sabina, 1986). This deposit was developed by shaft, adit and several trenches. Reserves in 1957 were estimated at 265,305 tonnes with a grade of between 0.095 and 0.12% U_3O_8 (see Table 2; Gordon *et al*., 1981). There was no production from this mine.

Richardson Fission Mine (Prospect)

Uraninite was discovered on this property by W.M. Richardson in 1922, the first discovery in the Wilberforce area. The uranium minerals occur in calcite-fluorite-apatite veins or pegmatite bodies. The deposit is found on the northwest side of the Cardiff plutonic complex. Country rocks are syenitized metasediments comprised of amphibolite, biotite-scapolite granulite and syenitized gneiss striking northeast, cut and replaced by granite and syenite pegmatites rich in fluorite and calcite. In this deposit, uraninite is found in the calcite-fluorite veins whereas uraninite plus uranothorite occur in pyroxene-fluorite syenite pegmatite dykes (Satterly, 1957; Gordon *et al*., 1981). Sabina (1986) noted that deep purple fluorite associated with uraninite gives off a foul odour when crushed and that the emerald green clinoamphibole is suitable for lapidary purposes. Other accessory minerals include magnetite, allanite, zircon, titanite, molybdenite, pyrite, pyrrhotite, thorite and melanocerite. In addition, Sabina (1986) reports uranophane, betafite and euxenite in the deposit. Reserves were estimated as 272,155 tonnes of 26% fluorite and some zones containing up to 0.07% U_3O_8 (see Table 2; Gordon *et al*., 1981).

Silver Crater Mine

The Silver Crater deposit, also known as the Basin property, was originally mined for black mica (lepidomelane) in the 1920s by the Bancroft Mining Company for use in the roofing industry (Sabina, 1986). Between 1947 and 1951, 426 tonnes of mica were produced from an open pit. Exploration for radioactive minerals occurred between 1953 and 1955 by Silver Crater Mines Limited through trenching and a development of a 70 m long adit south of the original mica pit. The main uranium mineral discovered was betafite in association with zircon, fluorite, titanite, molybdenite, pyrrhotite and pyrochlore. The deposit is found within a carbonate lens, surrounded by a band of amphibolite in a trough of syenitic and nepheline syenite gneisses (Satterly, 1957;

Gordon *et al*., 1981). Satterly (1957) provides very detailed descriptions of the adit and cross-cuts at this site.

Tripp (Nu-Age) Mine

This deposit containing uraninite, uranothorite, allanite and thorite is located in an amphibolite and syentized gneiss belt, northwest of the Cardiff plutonic complex (Satterly, 1957, Gordon *et al*., 1981). Originally worked for fluorite by Industrial Minerals Corporation and then later explored for radioactive minerals by Nu-Age Uranium Mines, Limited (Sabina, 1986). The former company hand-picked 1.8 tonnes of fluorspar grading 98% CaF_2, which sold for $32 in 1924 (Satterly, 1957). Satterly (1957) reported that the radioactive anomalies were produced by uraninite in red syenitzed gneiss, uranothorite in pegmatite and both minerals in calcite-fluorite-apatite veins.

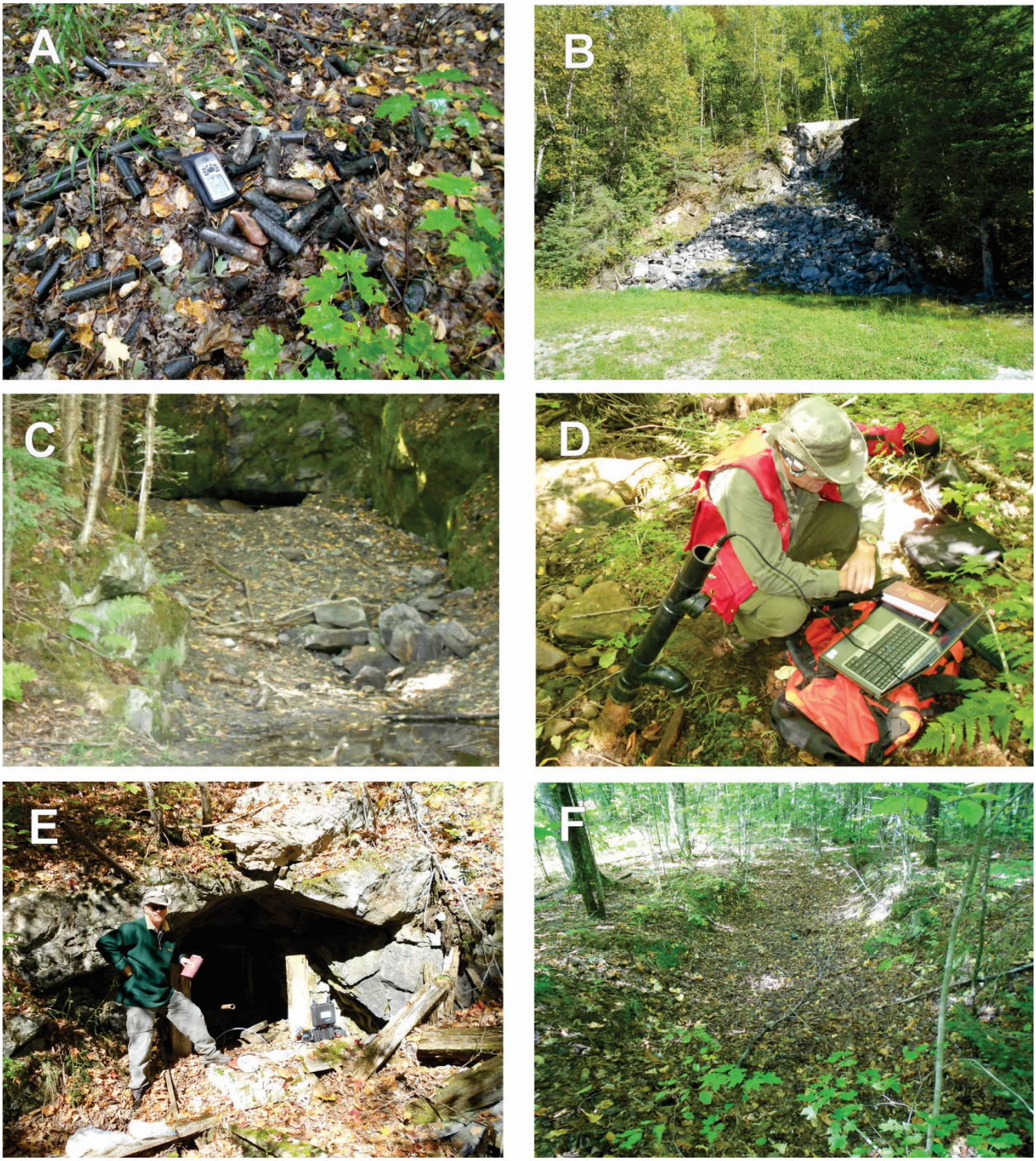

Figure A1: (A) typical drill core dump, Tripp (Nu-AGE) mine (NRCan Photo 2023-689); (B) rehabilitated shaft, Cardiff Mine (NRcan Photo 2023-690); (C) adit, Croft mine (NRCan Photo 2023-691); (D) AD downloading data from borehole-submersed data-logger, Croft mine (NRCan Photo 2023-692); (E) AD in front of adit, Halo mine (NRCan Photo 2023-693); (F) remains of an exploration trench, Halo mine (NRCan Photo 2023-694). All photos by J.B. Percival

Table A1. Possible mineral phases found at each mine site and prospect visited in the Bancroft area (after Sabina, 1986).

Mine Site	Radioactive Minerals (U/Th)	Silicates	Carbonates	Phosphates/ Sulphates/ Borates	Oxides/ Selinides	Sulphides	Other
Bicroft Mine	allanite, betafite, euxenite, pyrochlore, uraninite, uranothorite	amphibole, scapolite, garnet, microcline, peristerite, pyroxene, quartz, sillimanite, titanite, tourmaline, zircon	bastnäsite, calcite	apatite	anatase, magnetite, umangite	molybdenite, pyrite, pyrrhotite	fluorite, graphite
Canadian Dyno Mine	allanite, kasolite, uraninite, uranophane, uranothorite	amphibole, microcline, peristerite, pyroxene, quartz, titanite, zircon		apatite	magnetite	molybdenite, pyrite	
Cardiff Mine (prospect)	allanite, betafite, euxenite, pyrochlore, uraninite, uranothorite	nordbergite, phlogopite, pyroxene, scapolite, sepiolite, serpentine, talc, titanite, tourmaline	calcite	apatite, fluoborite		molybdenite, pyrite, pyrrhotite	fluorite, graphite
Croft Mine (prospect)	allanite, betafite, pyrochlore, uraninite, uranothorite	chlorite, clinopyroxene, garnet, sillimanite, titanite, tourmaline, zircon	calcite	apatite, monazite		molybdenite, pyrite, pyrrhotite	sulphur
Desmont Mine	allanite, thorianite, uranothorite	chondrodite, clinoamphibole, clinopyroxene, garnet, K-feldspar, perrierite, plagioclase, quartz, scapolite, serpentine, stillwellite, titanite, tourmaline	ancylite, calcite, hydroxylbastnäsite	apatite, monazite, gypsum	goethite, magnetite	marcasite, molybdenite, pyrite, pyrrhotite, sphalerite	graphite, sulphur

Table A1 continued

Mine Site	Radioactive Minerals (U/Th)	Silicates	Carbonates	Phosphates/ Sulphates/ Borates	Oxides/ Selinides	Sulphides	Other
Dwyer Fluorite Mine	—	clinoamphibole, clinopyroxene	calcite	apatite			fluorite, graphite
Halo Mine (prospect)	betafite, thorite, thorogummite, uraninite, uranothorite	amphibole, chlorite, pyroxene, titanite, tourmailine, zircon	calcite			molybdenite, pyrite, pyrrhotite	fluorite
Kenmac Chibougamou	allanite, uranothorite	biotite, pyroxene, scapolite, zircon	calcite	apatite	magnetite		
Millar's Mine	thorianite, thorite, uranophane	biotite, chondrodite, clinoamphibole, clinopyroxene, orthoclase, quartz, serpentine, talc, titanite	calcite			pyrite	
Blue Rock Rare Earth Mine 2	allanite, uraninite, uranophane, uranothorite	amphibole, clinopyroxene, corundum, garnet, peristerite, scapolite, talc, titanite, vesuvianite, zircon	calcite, bastnäsite		fergusonite	galena, molybdenite, pyrite, pyrrhotite	graphite
Richardson Fission Mine (prospect)	allanite, betafite, euxenite, uraninite, uranophane, uranothorite	biotite, chlorite, clinoamphibole, clinopyroxene, feldspar, melanocerite, titanite, zircon	calcite	apatite	hematite, magnetite	chalcopyrite, molybdenite, pyrite, pyrrhotite	fluorite

Table A1 continued

Mine Site	Radioactive Minerals (U/Th)	Silicates	Carbonates	Phosphates/ Sulphates/ Borates	Oxides/ Selinides	Sulphides	Other
Silver Crater Mine	betafite, euxenite	albite, amphibole, lepidomelane, titanite, tourmaline, zircon	calcite	apatite	magnetite	molybdenite, pyrite, pyrrhotite	fluorite
Tripp (Nu-Age) Mine	allanite, thorite, uraninite, uranothorite	biotite, clinoamphibole, clinopyroxene, feldspar, peristerite, scapolite, zircon	calcite	apatite	magnetite	chalcopyrite, pyrite	fluorite

APPENDIX B

Petrography

Petrographic descriptions of polished thin sections are summarized below. Table B1 lists the sample number, lithology and location. The description of each sample is accompanied by scanned images in plane light, cross-polarized light and autoradiograph. Images are accompanied by description of the minerals and textures observed. Table B2 lists the minerals, their commonly used symbols and formulae for minerals identified petrographically.

Table B1. List of samples selected for petrographic study.

Sample No.	Lithology	Location
PNA10-06A	Calc-Silicate Gneiss	Dyno Mine
PNA10-06B	Quartzo-Feldspathic Gneiss	Dyno Mine
PNA10-06C	Calc-Silicate Gneiss	Dyno Mine
PNA10-10	Calcite-Fluorite Marble	Cardiff Mine
PNA11-01A	Calcite Marble	Silver Crater Mine
PNA11-01C	Calc-Silicate Gneiss	Silver Crater Mine
PNA11-03A	Quartzo-Feldspathic Gneiss	Blue Rock Rare Earth Mine 2
PNA11-03C	Mafic Gneiss	Blue Rock Rare Earth Mine 2
PNA11-04	Calcite Marble	Richardson-Fission Mine
PNA11-05A	Calc-Silicate Gneiss	Halo Mine
PNA11-05C	Mafic Gneiss	Halo Mine
PNA11-06A	Pegmatitic Perthite	Halo Mine
PNA11-06B	Calc-Silicate Gneiss	Halo Mine
PNA11-08B	Calc-Silicate Gneiss	Cardiff mine
PNA11-09A	Layered Mafic Gneiss	Croft Mine
PNA11-09B	Mafic Gneiss	Croft Mine
PNA11-09C	Garnet-Sillimanite Metapelite	Croft Mine
PNA11-09D	Quartzo-Feldspathic Gneiss	Croft Mine
PNA11-09E	Mafic Gneiss	Croft Mine
PNA11-09F	Quartzo-feldspathic Gneiss	Croft Mine
PNA12-03C	Mafic Gneiss	Blue Rock Rare Earth Mine 2
PNA12-03D	Calc-Silicate Gneiss	Blue Rock Rare Earth Mine 2
PNA12-03E	Mafic Gneiss	Blue Rock Rare Earth Mine 2
PNA12-06A	Mafic Gneiss	Saranac Mine
PNA12-06C	Calc-Silicate Gneiss	Saranac Mine
PNA12-10B	Calc-Silicate Gneiss	Kenmac Chibougamou
PNA12-10D	Mafic Gneiss	Kenmac Chibougamou
PNA12-12C	Calc-Silicate Gneiss	Tripp (Nu-Age) Mine
PNA12-12D	Layered Mafic Gneiss	Tripp (Nu-Age) Mine
PNA12-12G	Calc-Silicate Gneiss	Tripp (Nu-Age) Mine

Table B2. Mineral group, mineral name, symbol (Kretz, 1983; Warr, 2021) and formula of minerals observed by petrographic study.

Mineral Group/Name	Symbol	Formula
Silicates		
Amphibole Group	Amp	
Gedrite	Ged	$(Mg,Fe^{+2})_5Al_2(Si_6Al_2)O_{22}(OH)_2$
Hastingsite	Hs	$NaCa_2(Fe^{+2},Mg)_4Fe^{+3}(Si_6Al_2)O_{22}(OH)_2$
Hornblende	Hbl	$Ca_2(Fe^{+2},Mg)4Al(Si_7Al)O_{22}(OH,F)_2$
Epidote Group	Ep	
Allanite	Aln	$(Ce,Ca,Y)_2(Al,Fe^{+2},Fe^{+3})_3(SiO_4)_3(OH)$
Epidote	Ep	$Ca2(Fe^{+3},Al)_3(SiO_4)_3(OH)$
Feldspar Group		
Plagioclase Feldspar	Pl	$NaAlSi_3O_8 – CaAl_2Si_2O_8$
K-Feldspar	Kfs	$KAlSi_3O_8$
Garnet Group	Grt	
Spessartine*	Sps	$Mn_3{}^{+2}Al_2(SiO_4)_3$
Pyroxene Group	Px	
Diopside	Cpx/Dp	$CaMgSi_2O_6$
Enstatite**	Opx/En	$Mg_2Si_2O_6$
Quartz	Qtz	SiO_2
Scapolite group	Scp	
Marialite*	Mar	$Na_4Al3_Si_9O_{24}Cl$
Silvialite*	Svl	$(Ca,Na)_4Al_6Si_6O_{24}(CO_3,SO_4)$
Sillimanite	Sil	$Al2_SiO_5$
Thorite	Thr	$(Th,U)SiO_4$
Titanite	Ttn	$CaTiSiO_5$
Tourmaline Group	Tur	
Schorl**	Srl	$NaFe_3{}^{+2}Al_6(BO_3)Si_6O_{18}(OH)_4$
Zircon	Zrn	$ZrSiO_4$
Phyllosilicates		
Biotite	Bt	$K(Mg,Fe^{+2})_3(Al,Fe^{+3})Si_3O_{10}(OH,F)_2$
Muscovite	Ms	$KAl_2(AlSi_3O_{10})(F,OH)_2$
Chlorite	Chl	$Mg,Fe)_3(Si,Al)_4O_{10}(OH)_2·(Mg,Fe)_3(OH)_6$
Carbonates		
Calcite	Cal	$CaCO_3$
Dolomite	Dol	$CaMg(CO_3)_2$
Phosphates		
Fluorapatite	Fap	$Ca_5(PO_4)_3F$
Monazite	Mnz	$(Ce,La,Nd,Th)PO_4$
Sulphates		
Barite	Brt	$BaSO_4$

Table B2 continued

Mineral	Symbol	Formula
Sulphides		
Chalcopyrite	Ccp	$CuFeS_2$
Galena	Gn	PbS
Pyrrhotite	Po	$Fe_{1-x}S$
Pyrite	Py	FeS_2
Oxides		
Goethite	Gt	α-$Fe^{+3}O(OH)$
Hematite	Hem	α-Fe_2O_3
Ilmenite	Ilm	$Fe^{+2}TiO_3$
Magnetite	Mag	$Fe^{+}2Fe_2^{+3}O_4$
Rutile	Rt	TiO_2
Uraninite	Ur	UO_2
Halides		
Fluorite	Fl	CaF_2

*Best fit from XRD analyses
** Confirmed by SEM-EDS or EPMA analyses

PNA10-06A: Calc-Silicate Gneiss

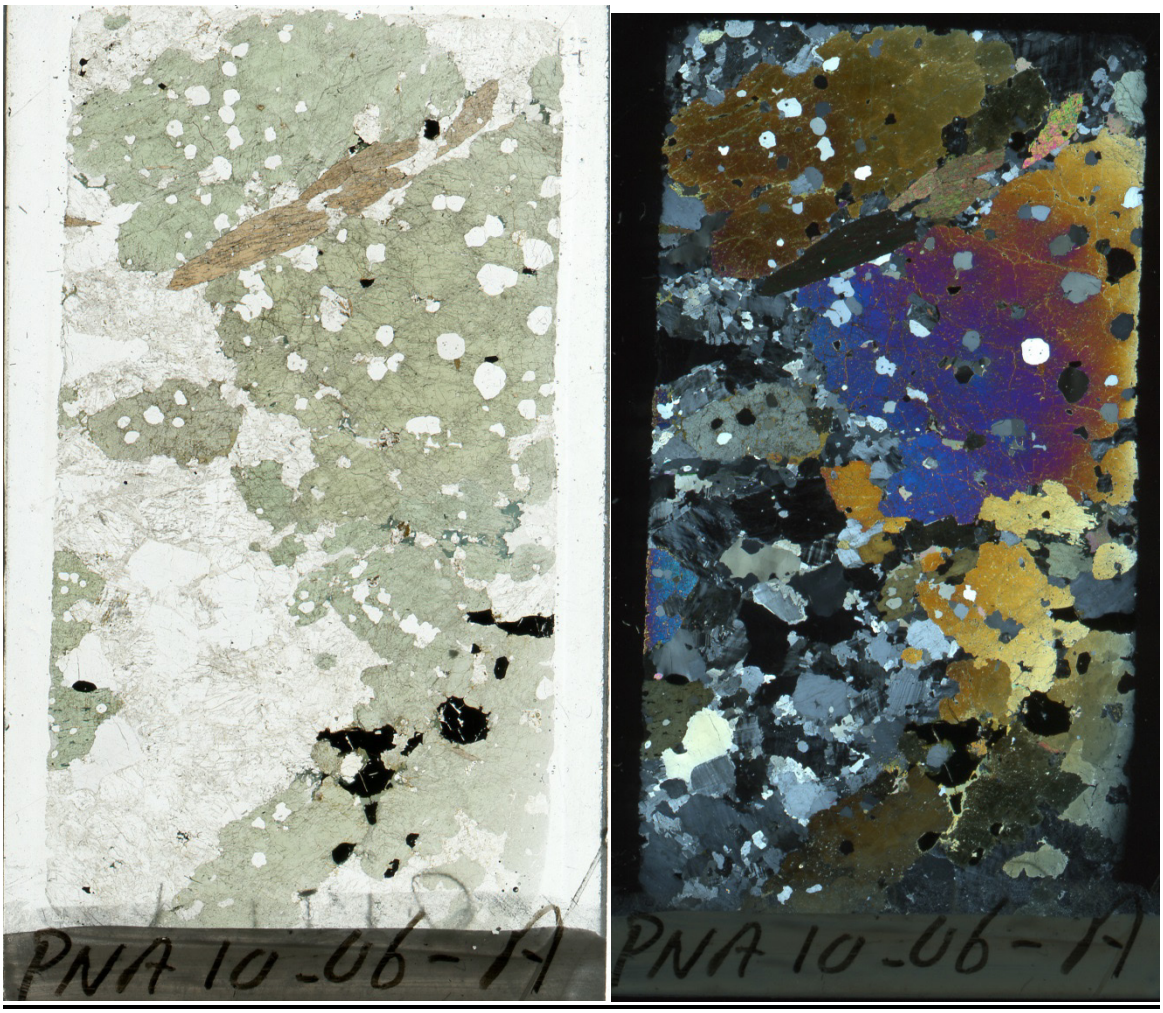

Mineralogy:

Quartz
Potassium Feldspar (Microcline)
Plagioclase
Clinopyroxene (Diopside)
Ca-Amphibole
Calcite
Accessory: Titanite, Apatite, Uraninite, Pyrite, Pyrrhotite, Chalcopyrite

Mineralogy verified by SEM.

Petrography:

Poikiloblasts of diopside include quartz, titanite and plagioclase. Amphibole occurs as overgrowths on diopside, and is associated with late opaque minerals. Coarse-grained titanite is euhedral. Feldspars and quartz have consertal texture; the latter displays undulose extinction. Minor calcite is present.

Autoradiograph: Dark spots are uraninite.

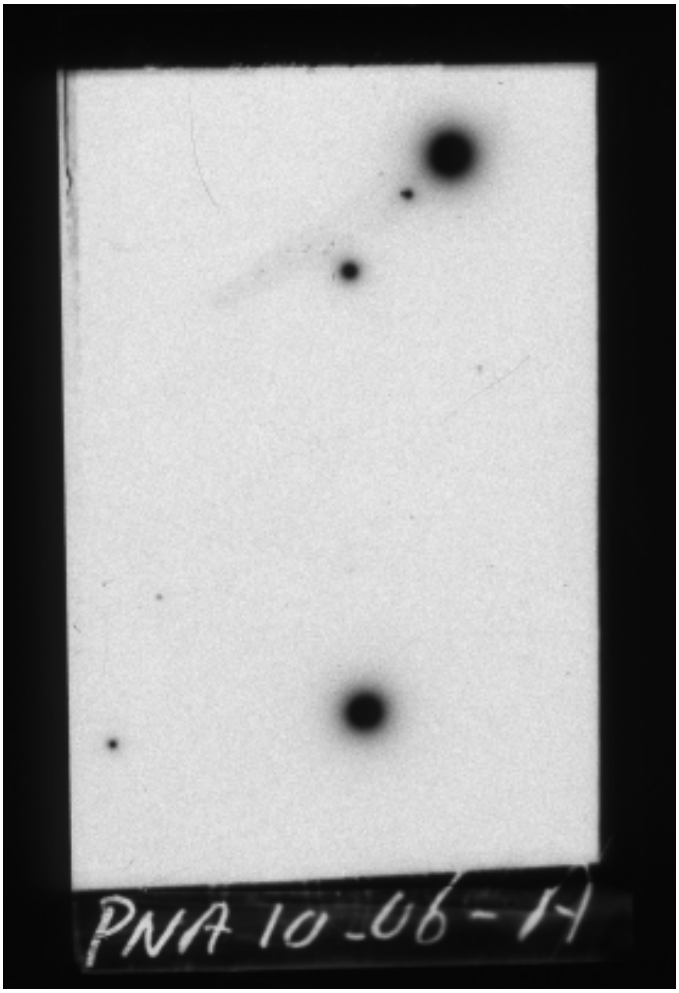

PNA10-06B : Quartzo-Feldspathic Gneiss

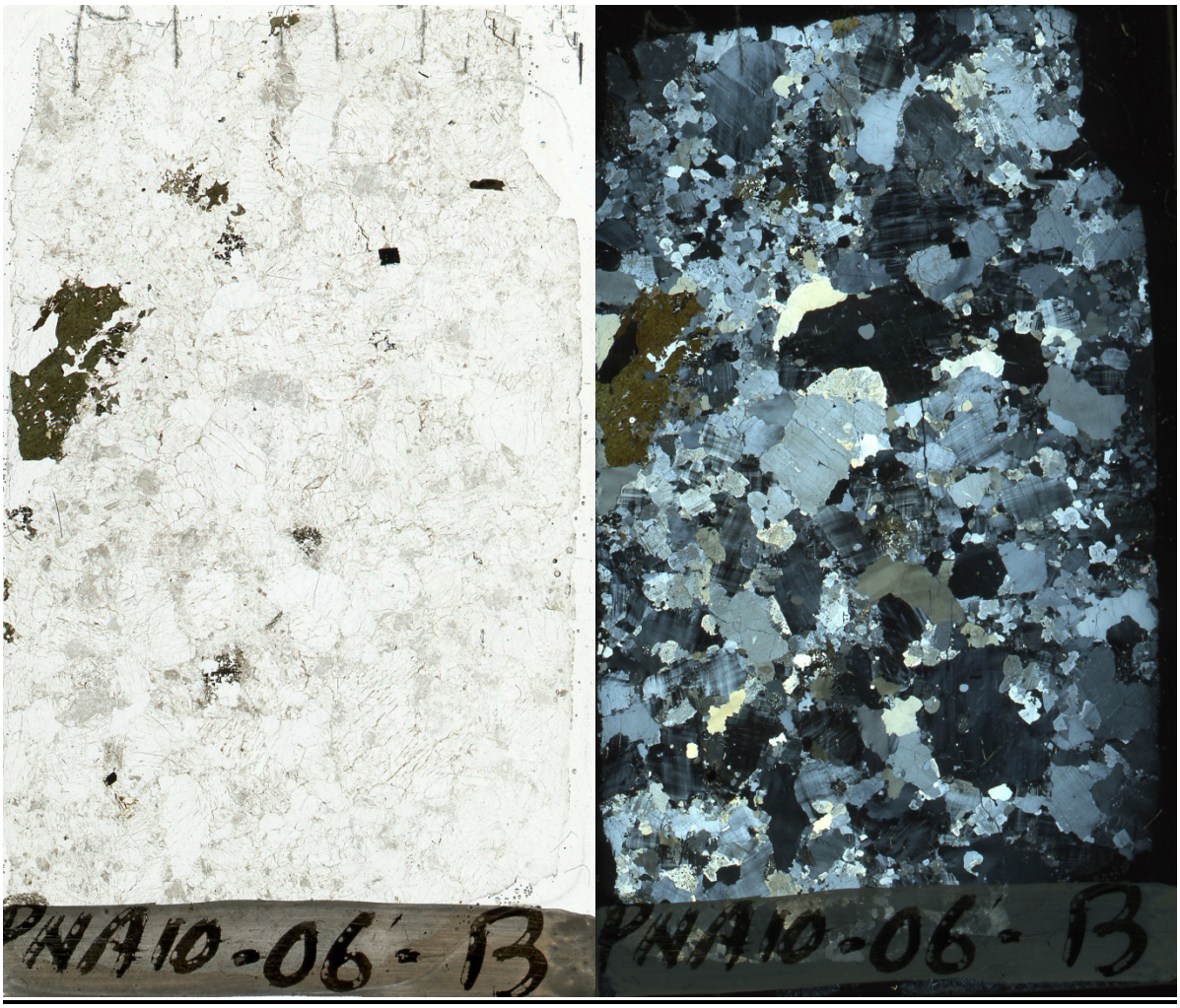

Mineralogy:

Quartz
Potassium Feldspar (Microcline)
Plagioclase
Amphibole (Gedrite)
Biotite
Accessory: Calcite, Titanite, Apatite, Allanite, Monazite, Zircon, Tourmaline, Uraninite, Galena, Thorite, Pyrite

Mineralogy verified by SEM.

Petrography:

Coarse-grained recrystallized, undulose quartz and feldspar have consertal texture; feldspar is moderately altered. There is no oriented fabric. Minor late tourmaline.

Autoradiograph: Dark spots are uraninite, thorite.

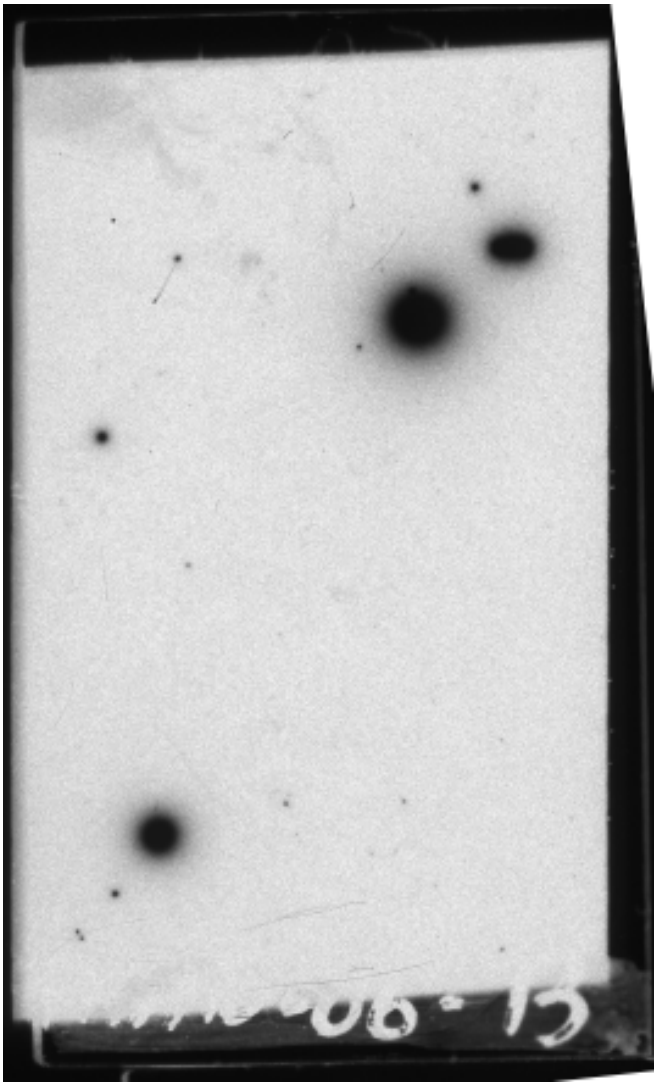

PNA10-06C: Quartzo-Feldspathic Gneiss

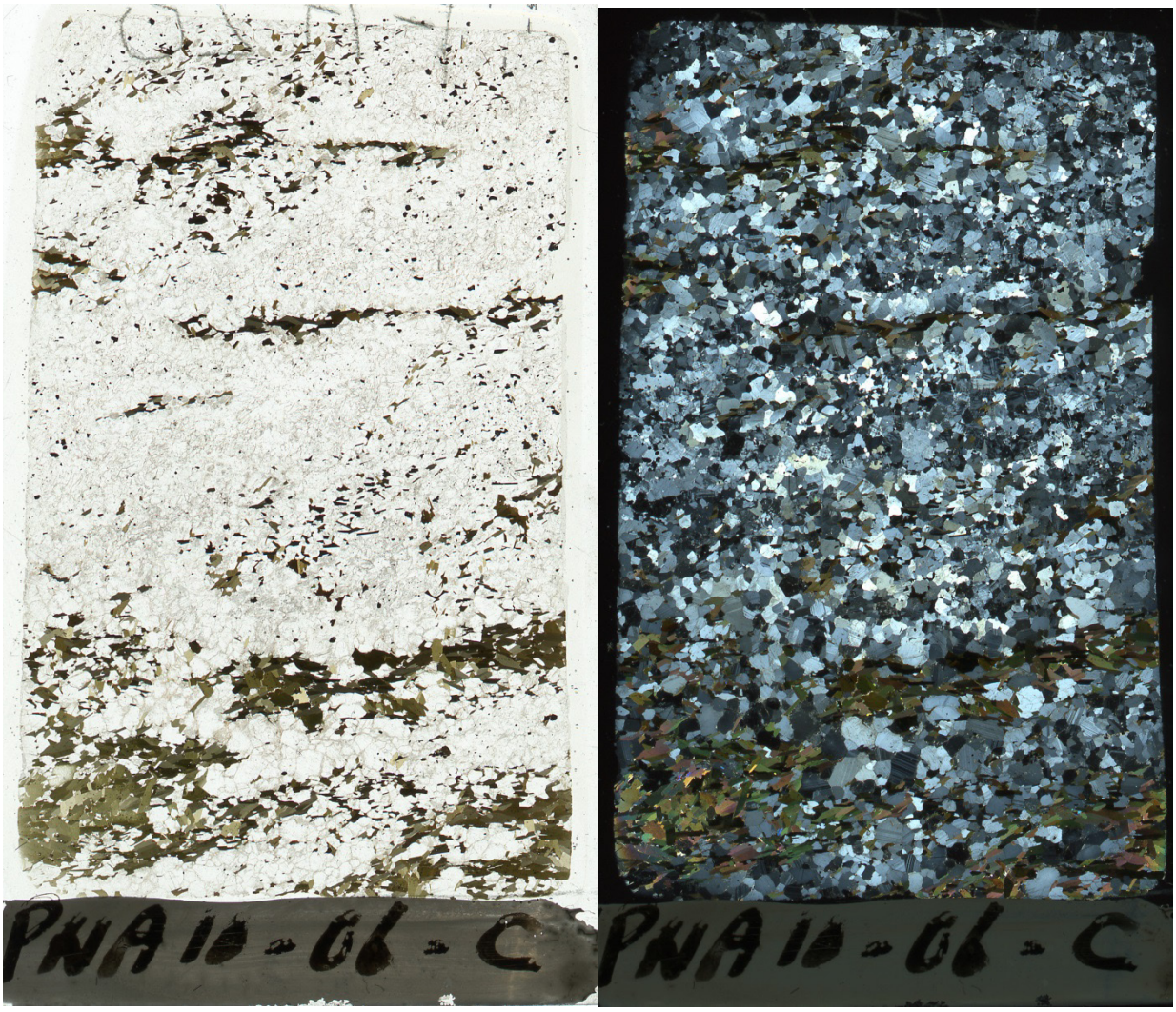

Mineralogy:

Quartz
Potassium Feldspar (Microcline)
Plagioclase
Biotite
Muscovite (trace)
Accessory: Calcite, Apatite, Zircon, Fe-Oxide

Mineralogy verified by SEM.

Petrography:

Granoblastic with no apparent fabric. Biotite (with minor retrograde chlorite) and Fe-oxide lenses occur in layers of quartz and feldspar. Coarse-grained biotite is included in plagioclase cores, surrounded by potassium feldspar.

Autoradiograph: No detectable radioactivity.

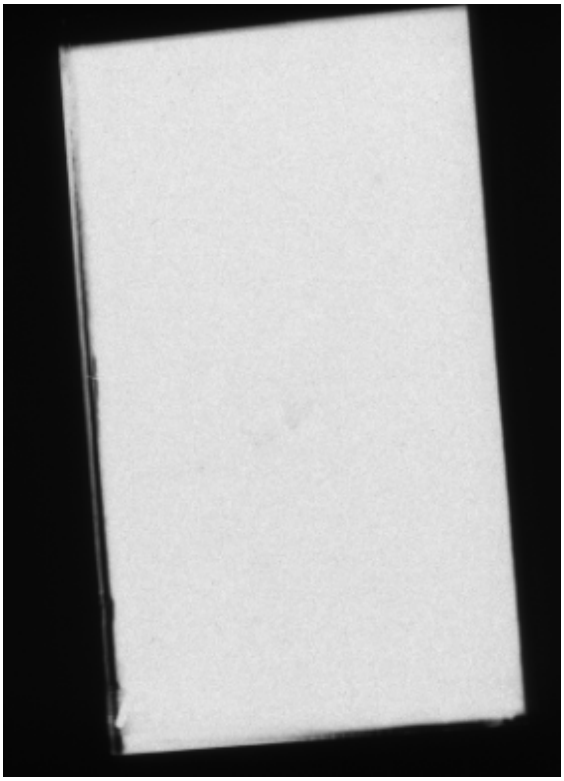

PNA10-10: Calcite Fluorite Marble

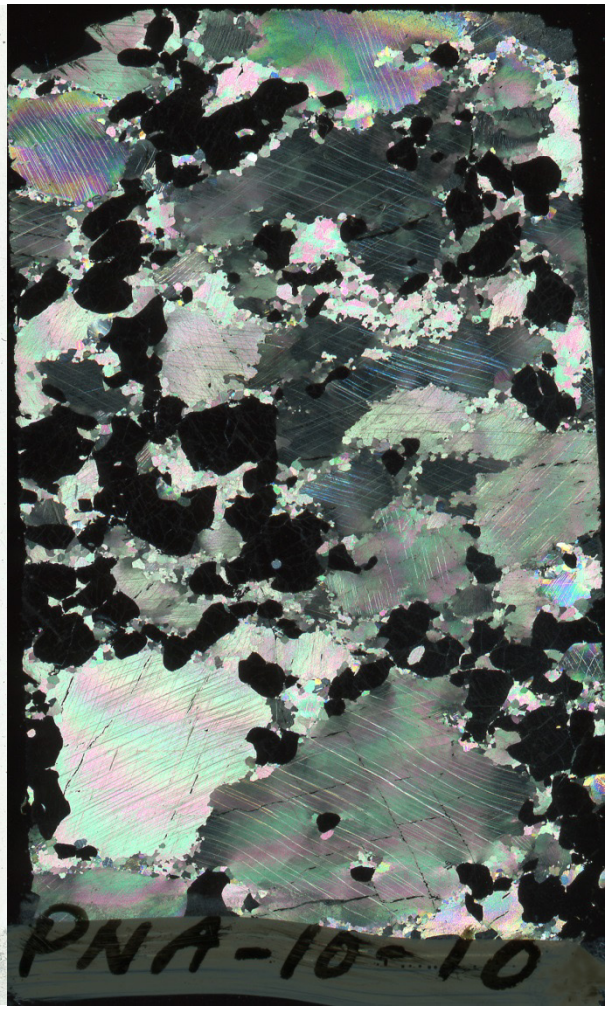

Mineralogy:

Calcite
Fluorite

Petrography:

Coarse-grained anhedral calcite with finer-grained calcite at sutured grain edges. Abundant, coarse-grained, subhedral to anhedral faintly-purple fluorite.

Autoradiograph: No detectable radioactivity.

PNA11-01A Calcite Marble

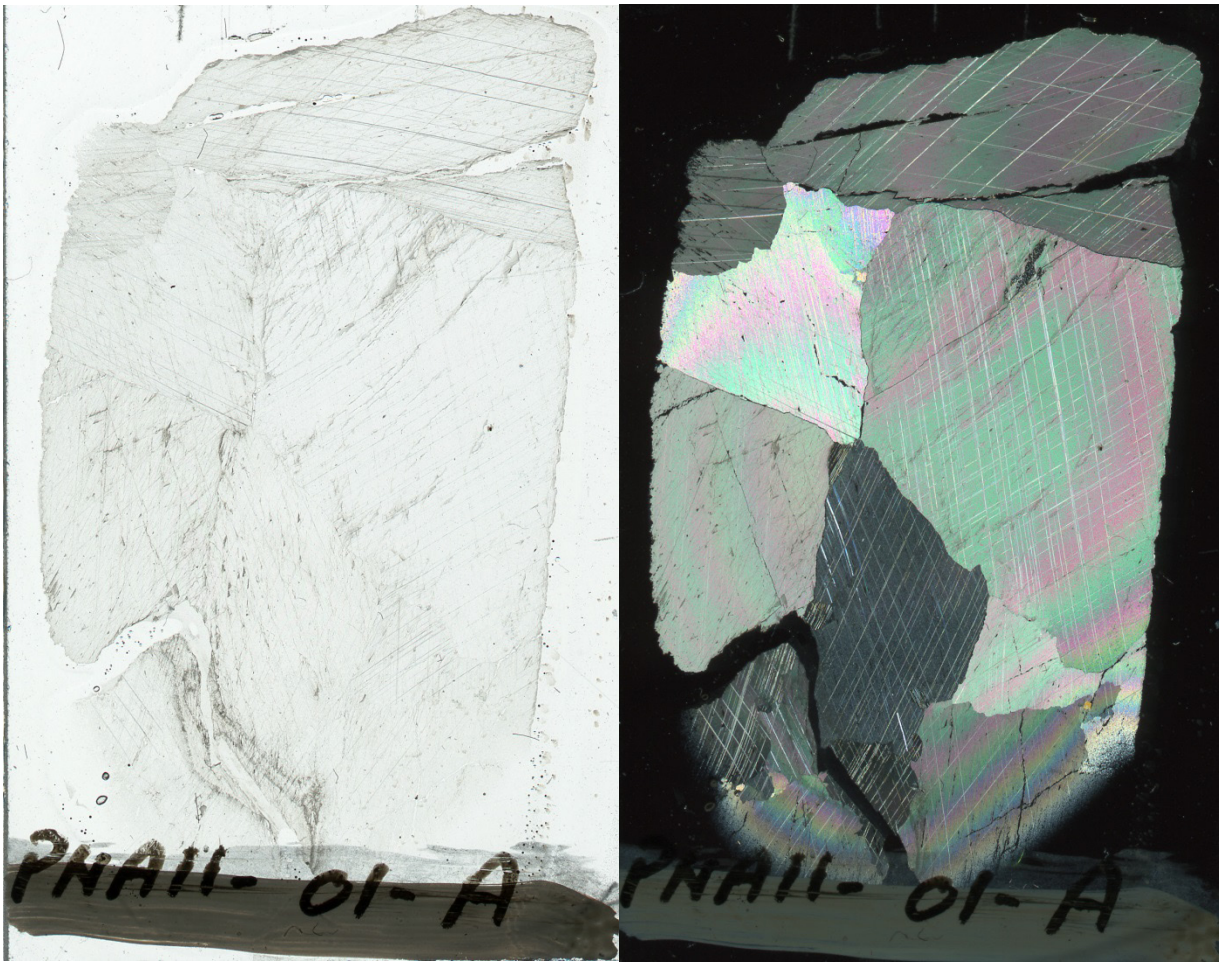

Mineralogy:

Calcite
Fluorite
Clinopyroxene (Diopside)

Petrography:

Very coarse-grained, recrystallized calcite is well-equilibrated with straight edges. There is a trace amount of fracture-filling pale purple fluorite and one grain of clinopyroxene.

Autoradiograph: No detectable radioactivity.

PNA11-01C Calc-Silicate Gneiss

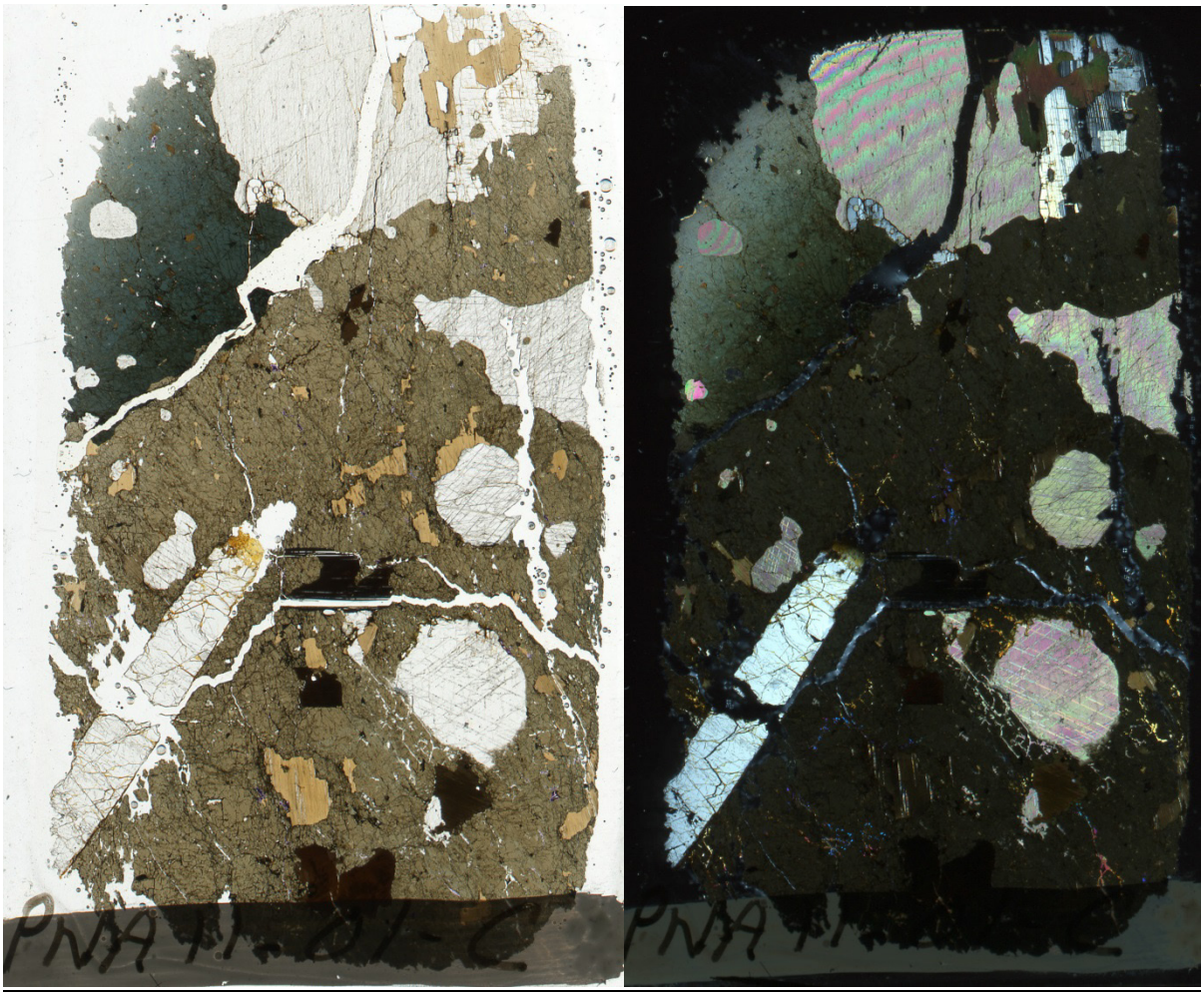

Mineralogy:

Calcite
Ca-Amphibole (Hastingsite)
Plagioclase
Biotite
Apatite
Accessory: Fluorite, Ilmenite, Pyrite

Amphibole chemistry verified by EPMA

Petrography:

Coarse-grained blue-green-brown pleochroic amphibole (hastingsite) contains coarse inclusions of calcite, subhedral apatite, biotite and ilmenite; pyrite is included in biotite. Late fluorite infills fractures and vugs.

Autoradiograph: Faint spots indicate possible radioactive grains.

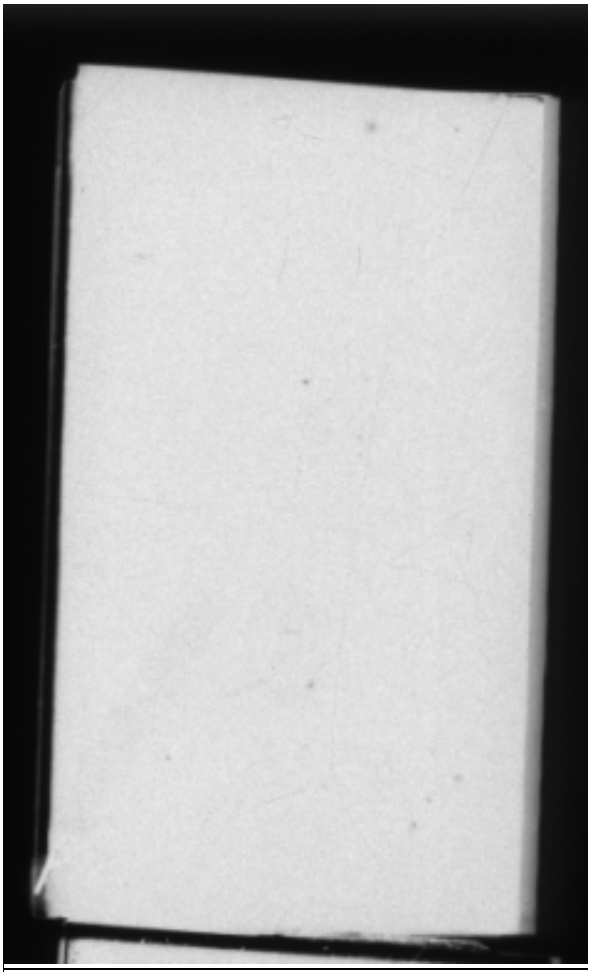

PNA11-03A: Quartzo-Feldspathic Gneiss

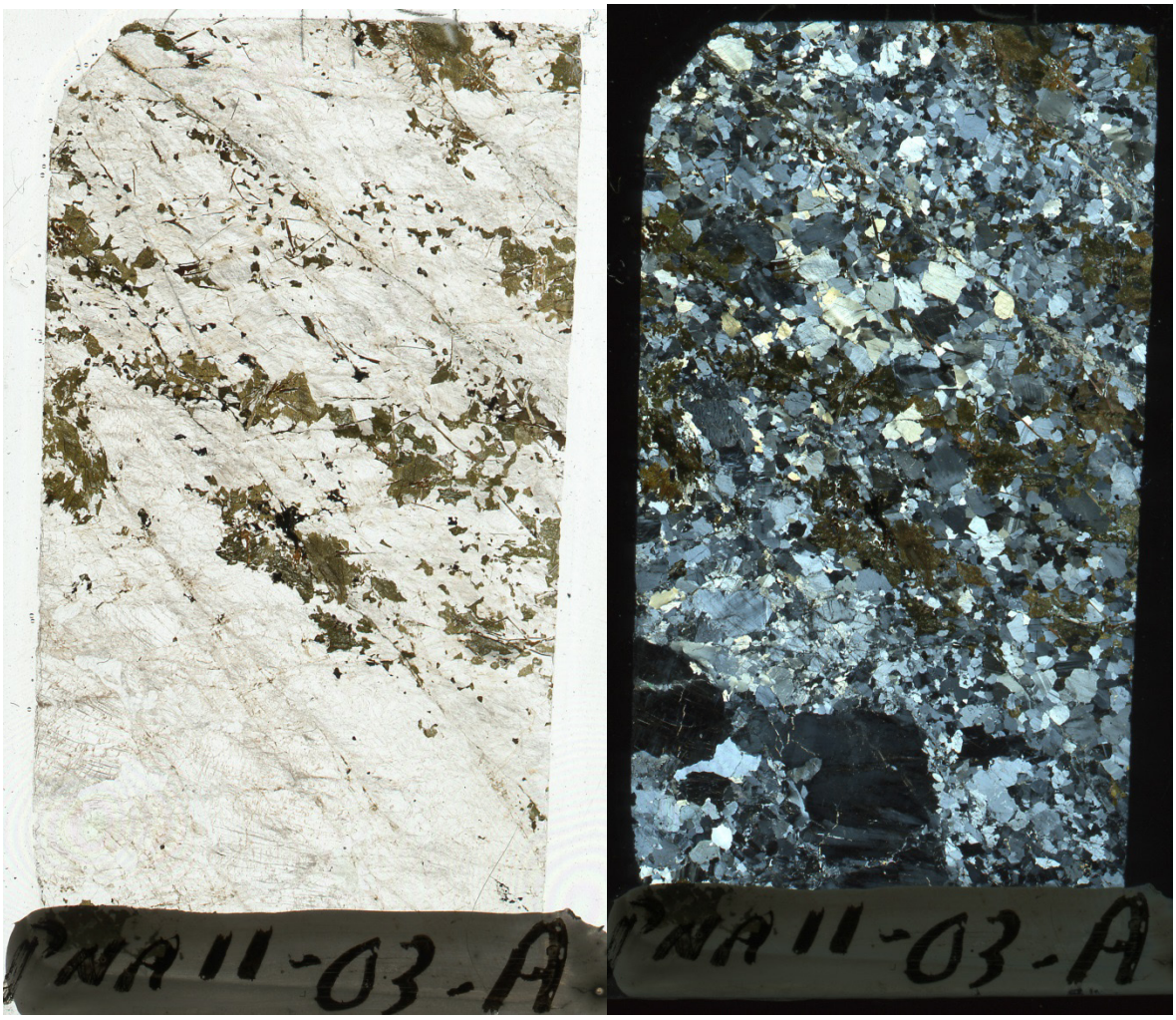

Mineralogy:

Quartz
Potassium Feldspar (Microcline)
Plagioclase
Amphibole (Gedrite)
Orthopyroxene? (severely altered)
Biotite
Titanite
Calcite
Accessory: Apatite, Rutile, Pyrite, Ilmenite, Uraninite, Fe-Ti-U-oxide

Mineralogy verified by SEM.

Petrography:

A matrix of quartz and feldspar is cut by late calcite-filled fractures / foliation.
Mafic layers are comprised of biotite, possible orthopyroxene - it is severely altered (no calcium)-, and titanite rimmed by rutile which is in turn mantled by Fe-Ti-U oxide. A single uraninite grain has a pyrite rim, then mantled by calcite.

Autoradiograph: Dark spots are uraninite, U-bearing Ti-Fe Oxide.

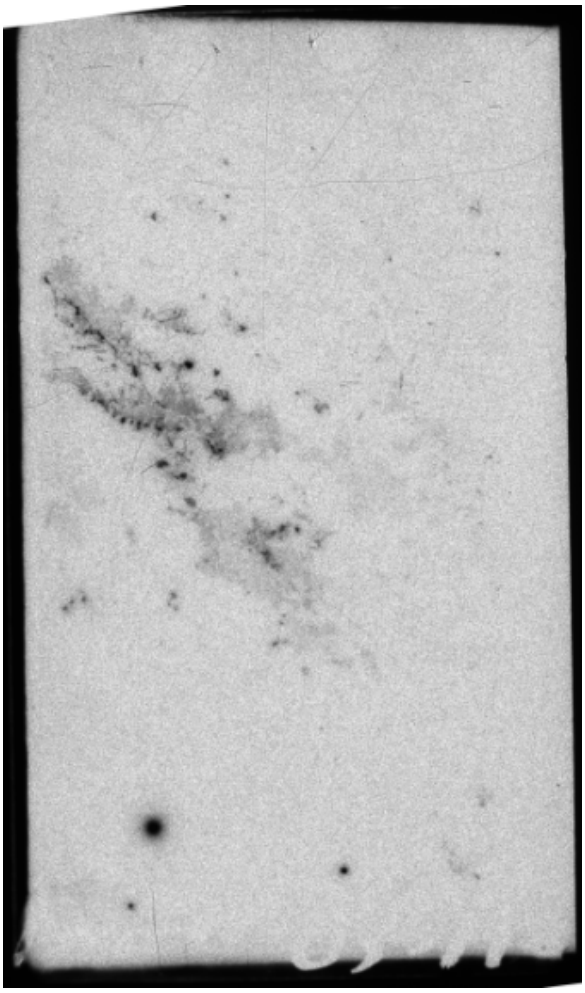

PNA11-03C : Mafic Gneiss

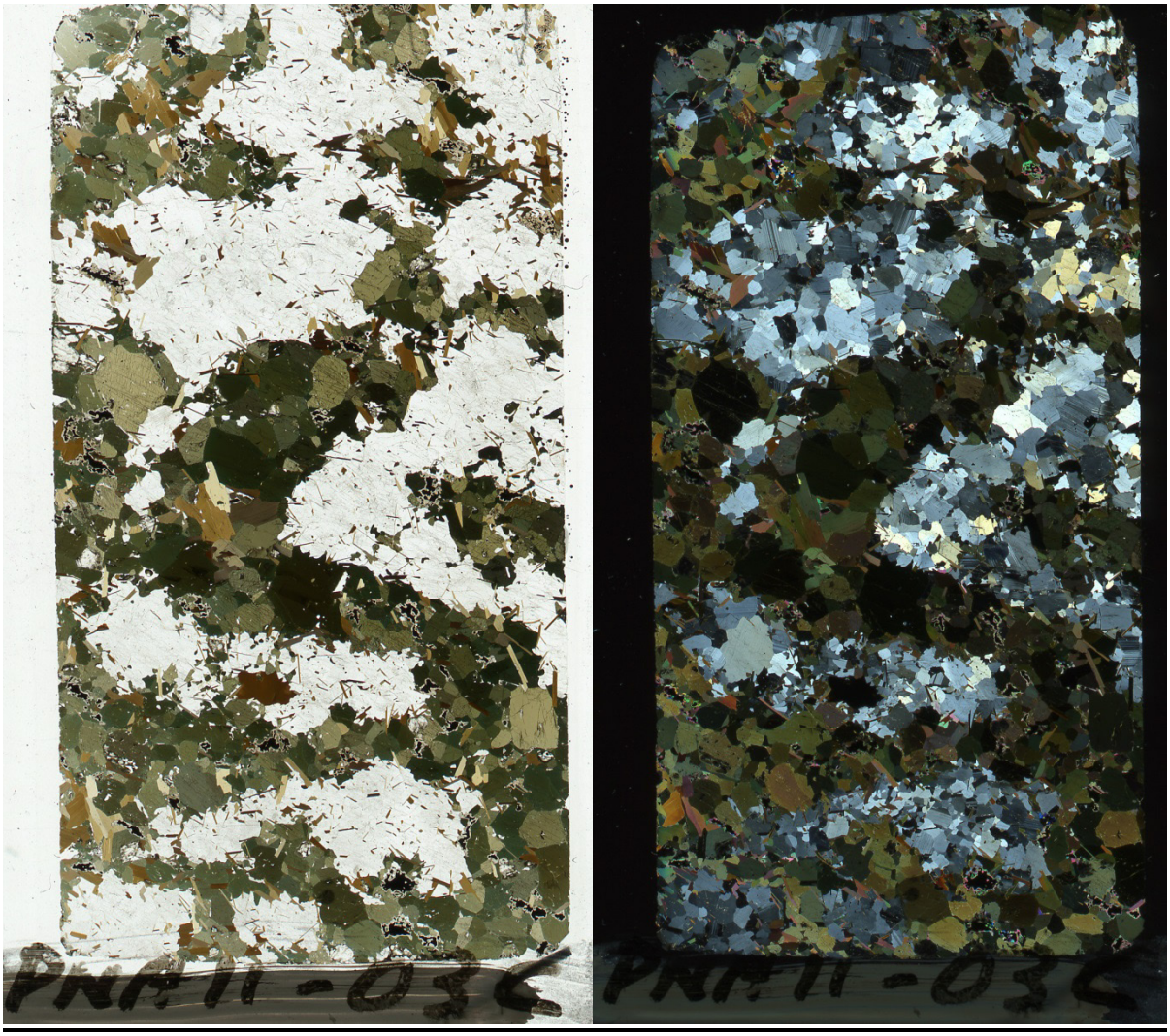

Mineralogy:

Quartz
Potassium Feldspar (Microcline)
Plagioclase
Ca-Amphibole
Biotite
Accessory: Titanite, Apatite, Ilmenite, Pyrite (1 tiny grain)

Mineralogy verified by SEM.

Petrography:

Coarse-grained biotite occurs in mafic lenses with hornblende; finer-grained biotite is in plagioclase-rich lenses. The texture is anhedral with no noticeable fabric. Ilmenite is mantled by titanite.

Autoradiograph: No detectable radioactivity.

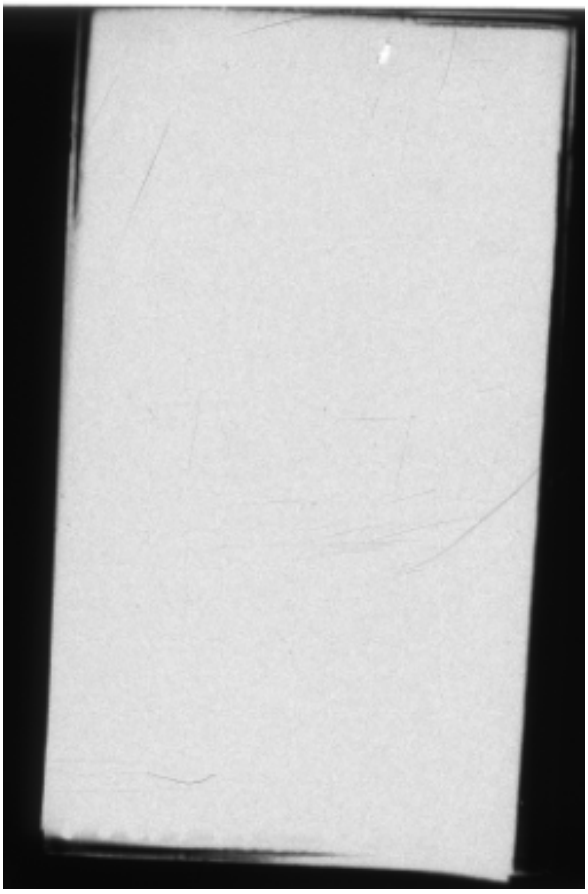

PNA11-04: Calcite Marble

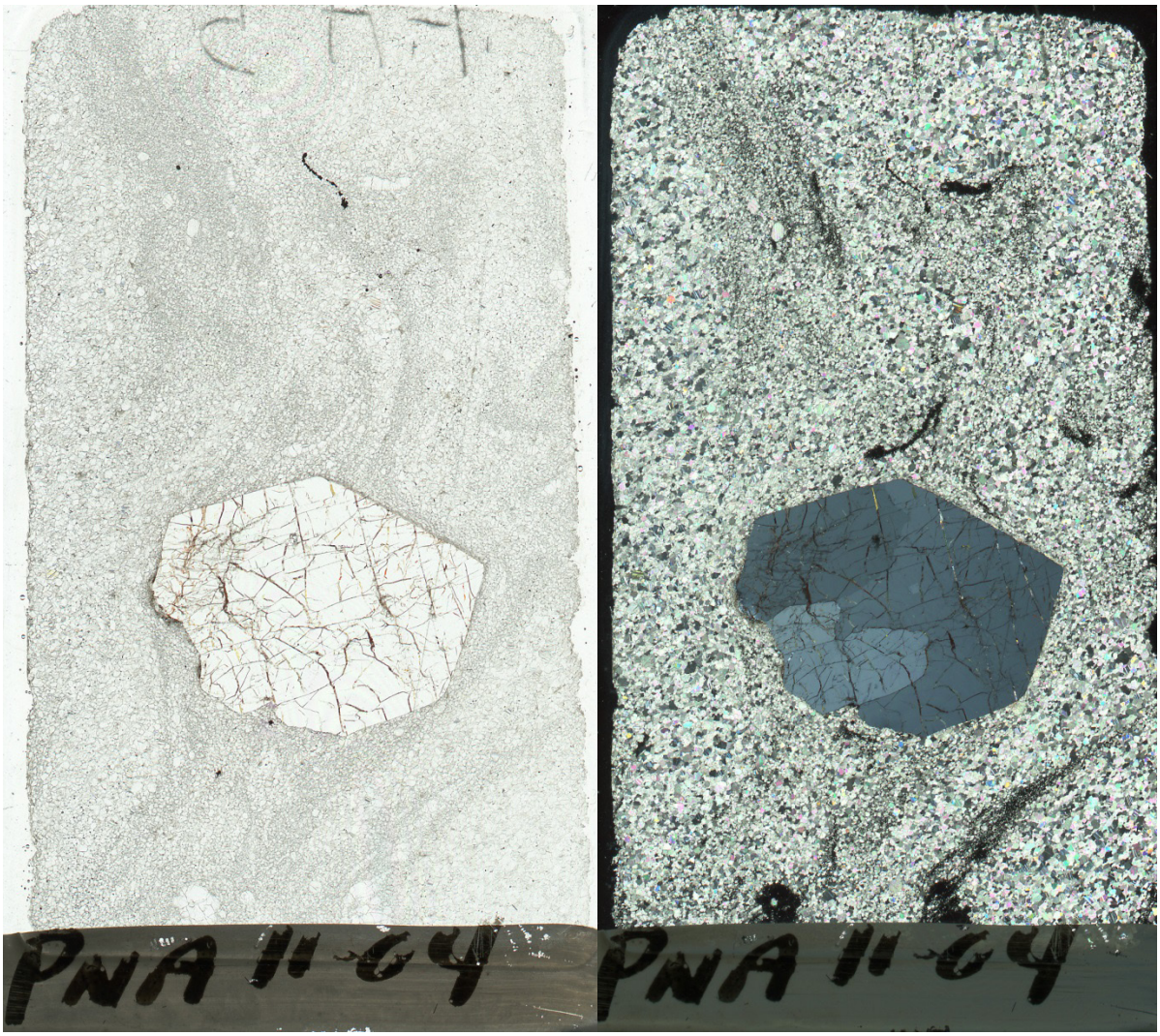

Mineralogy:

Calcite
Apatite
Fluorite
Accessory: REE-carbonate, Fe-Oxide, Uraninite, Pyrite, REE-oxide

Mineralogy verified by SEM.

Petrography:

The matrix is comprised of granoblastic calcite and fluorite. One euhedral apatite porphyoblast has fluorite (and pyrite) growth on rim and in fractures. Pyrite, uraninite, REE carbonate (Ca, Ce, La, Nd) and REE oxide (Ce,Ca,Nd, Pr) occur in trace amounts in the matrix.

Autoradiograph: Dark spots are uraninite,
REE-carbonate, REE-oxide. Note apatite visible in image.

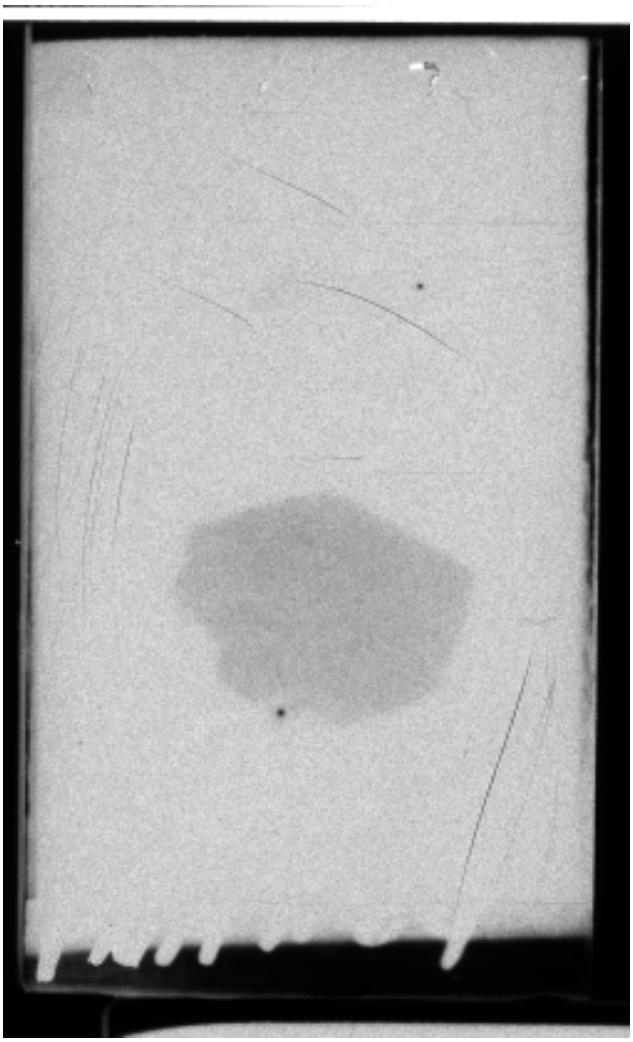

PNA11-05A: Calc-Silicate Gneiss

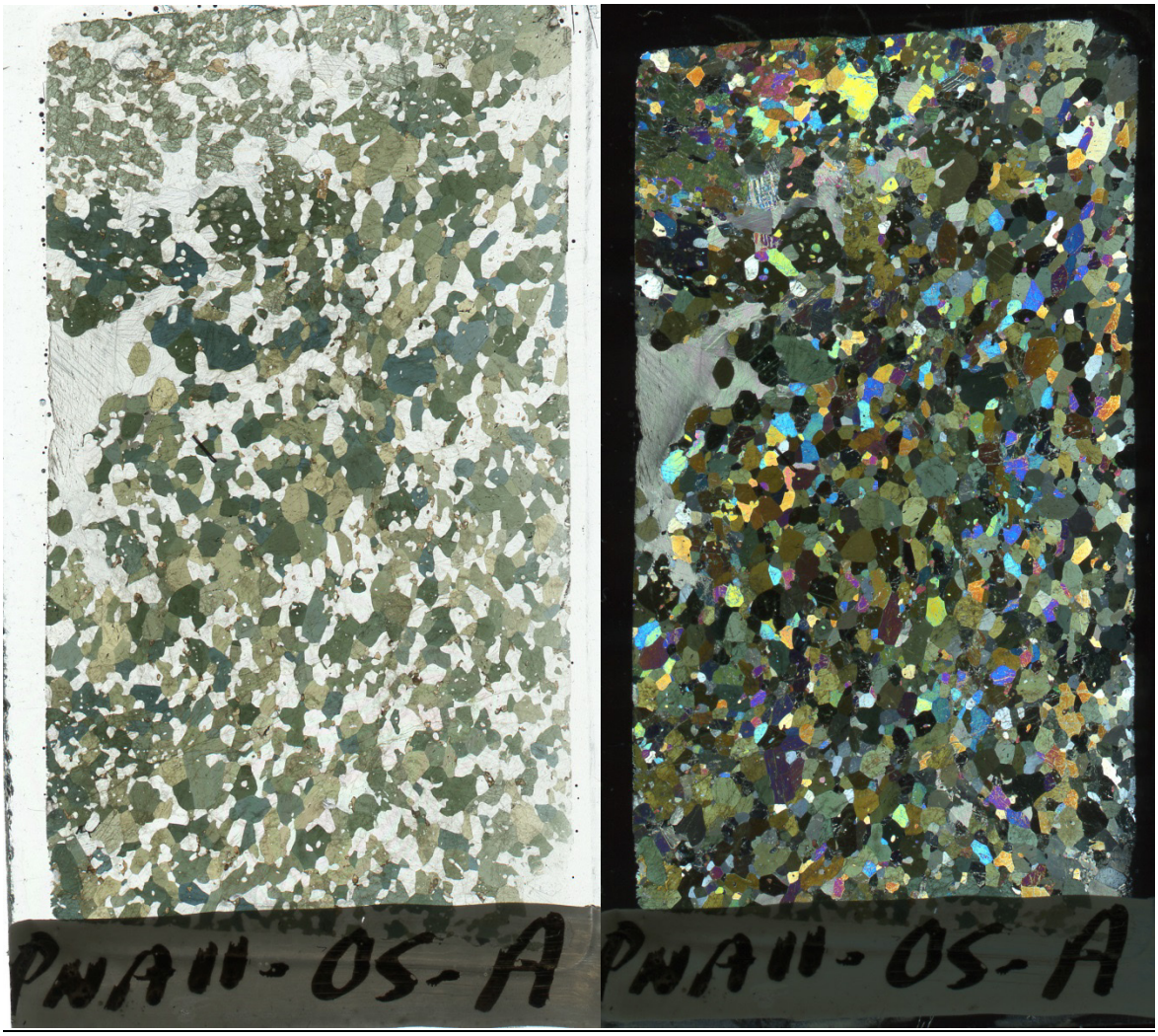

Mineralogy:

Ca-Amphibole (Hastingsite)
Clinopyroxene (Diopside)
Scapolite
Calcite
Titanite

Mineralogy verified by SEM; amphibole chemistry by EPMA analysis.

Petrography:

Medium-to coarse-grained, granoblastic texture; anhedral blue-green-yellow pleochroic amphibole, calcite, diopside, scapolite, and titanite (lamellar twinning) has a weak fabric. One diopside-rich/amphibole-poor layer is comprised of diopside-calcite-titanite-scapolite.

Autoradiograph: No detectable radioactivity.

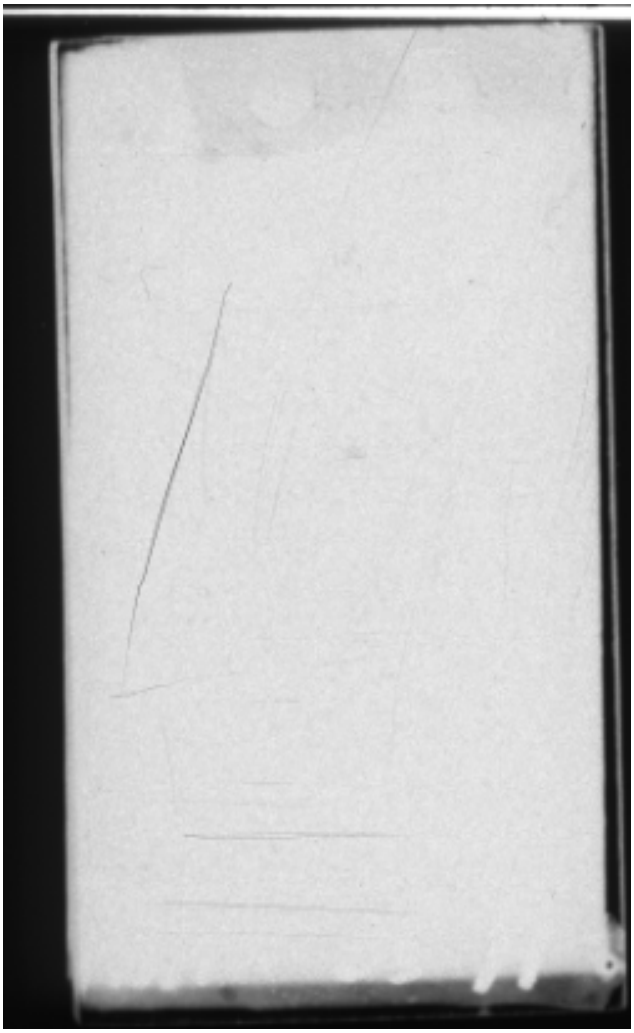

PNA11-05C: Layered Mafic Gneiss

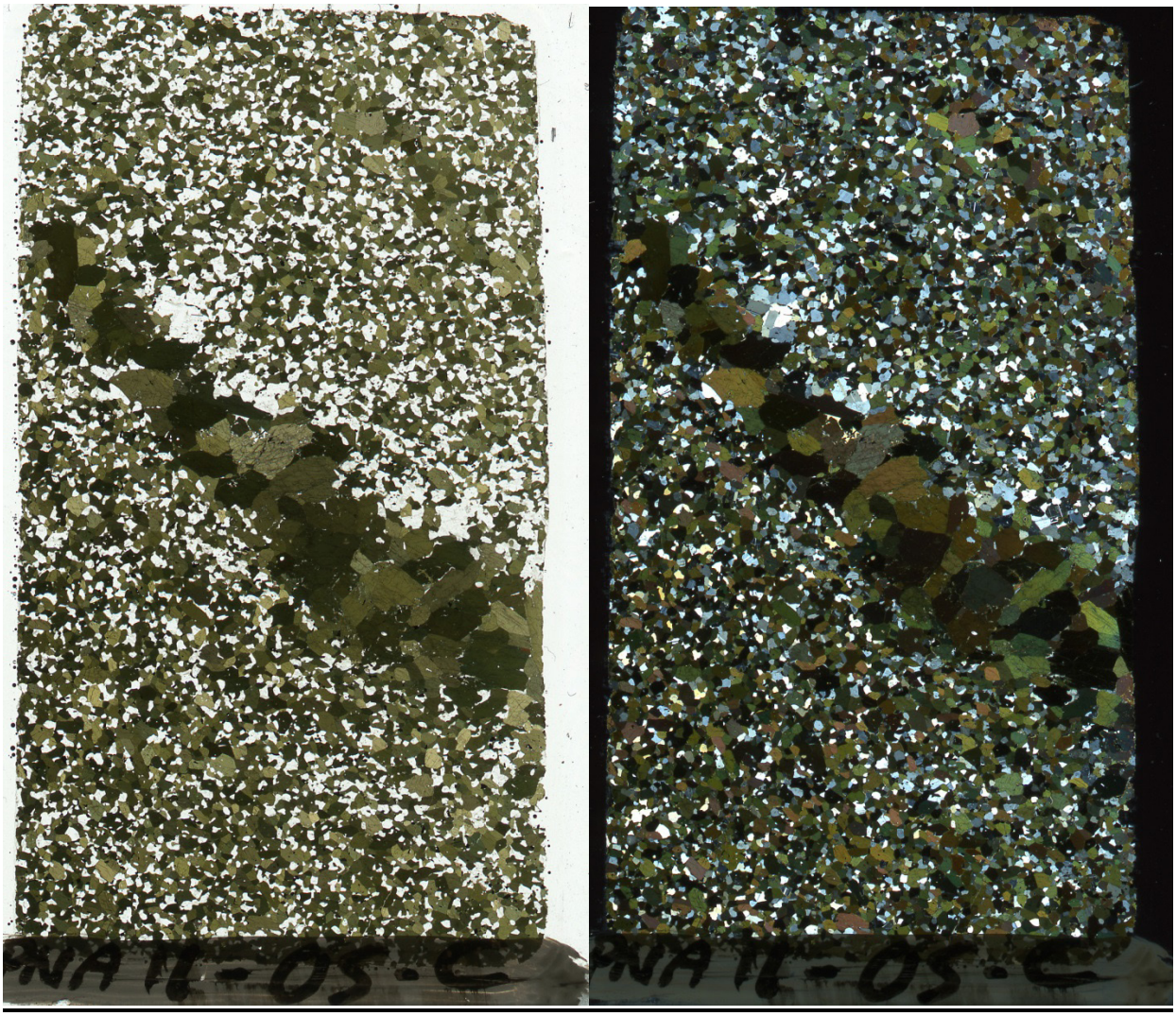

Mineralogy:

Quartz
Potassium Feldspar
Plagioclase
Ca-Amphibole (Hastingsite)
Accessory: Titanite, Apatite, Fe-oxide, Pyrite

Petrography:

Medium-coarse-grained, granoblastic inequigranular banded mafic gneiss, mostly hornblende and feldspar with trace late pyrite.

Autoradiograph: No detectable radioactivity.

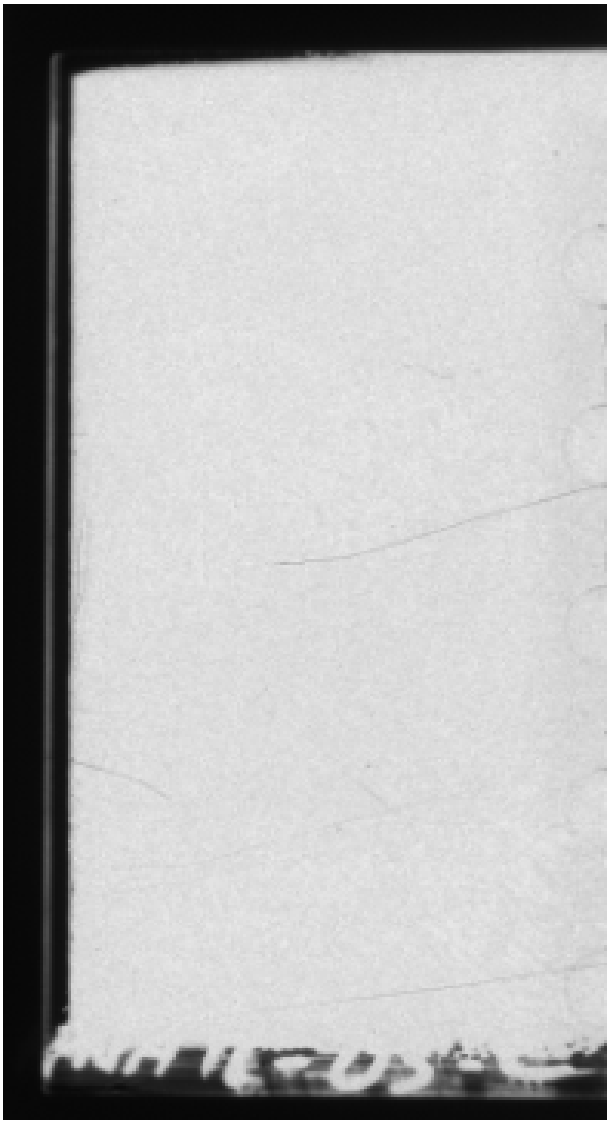

PNA11-06A: Perthite

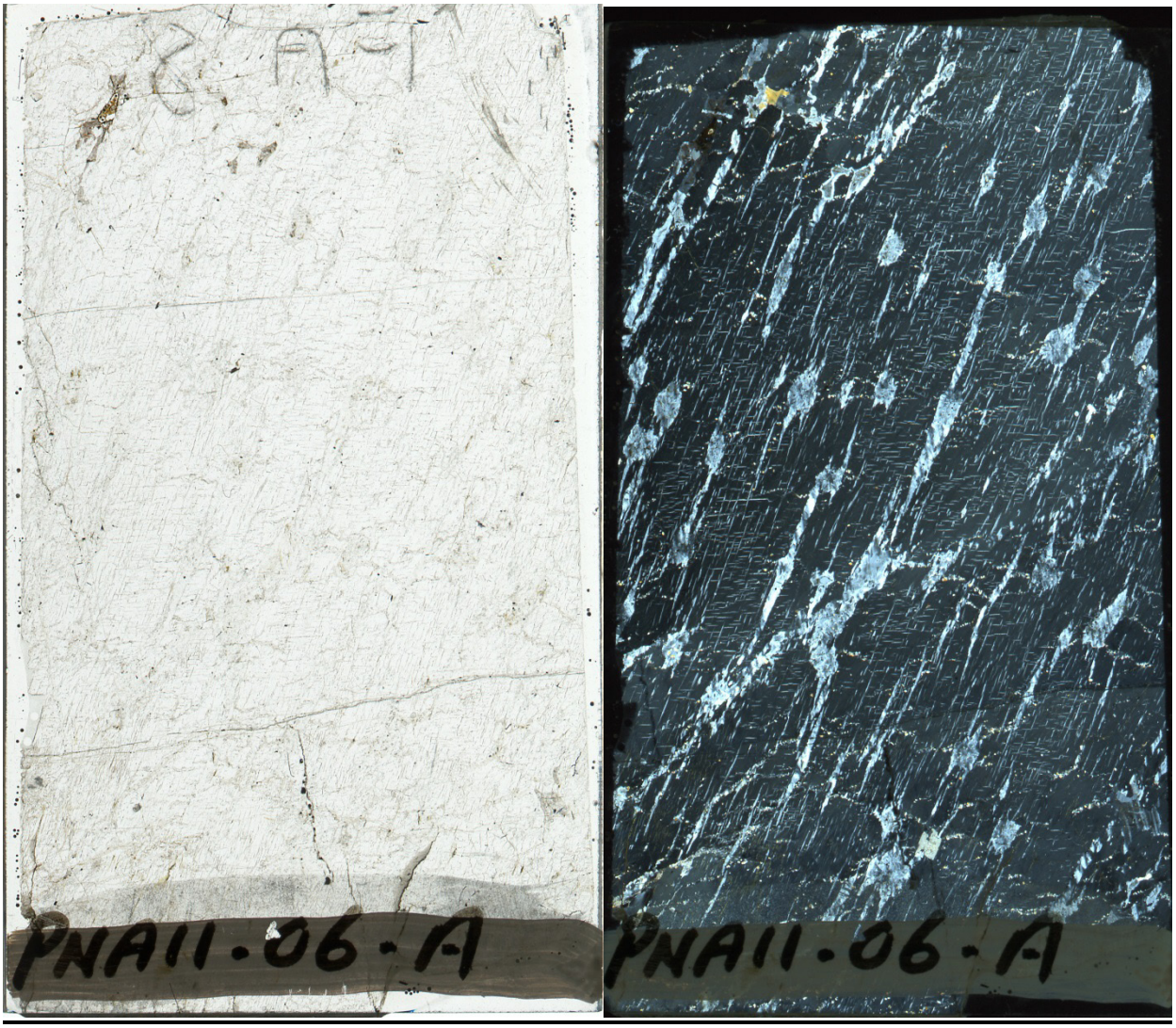

Mineralogy:

Quartz
Potassium Feldspar
Plagioclase
Accessory: Barite, Pyrite, Thorite

Petrography:

A single pegmatitic grain of perthite has microperthitic texture. Late fractures are infilled with fine pyrite; pyrite surrounds a thorite- and barite-filled vug.

Autoradiograph: Dark spot is thorite.

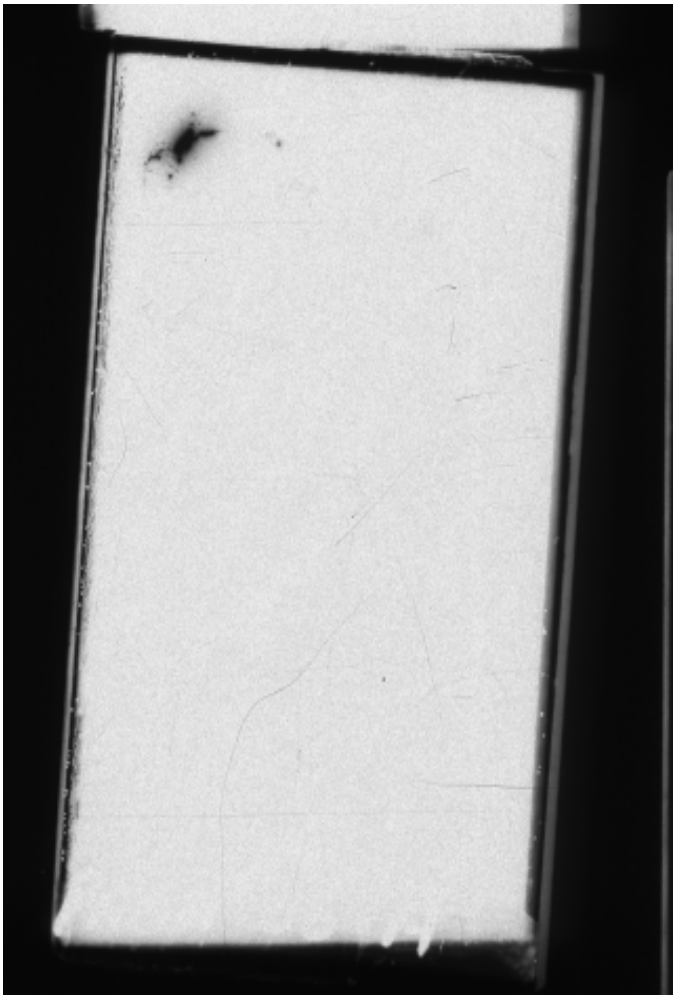

PNA11-06B: Calc-Silicate Gneiss

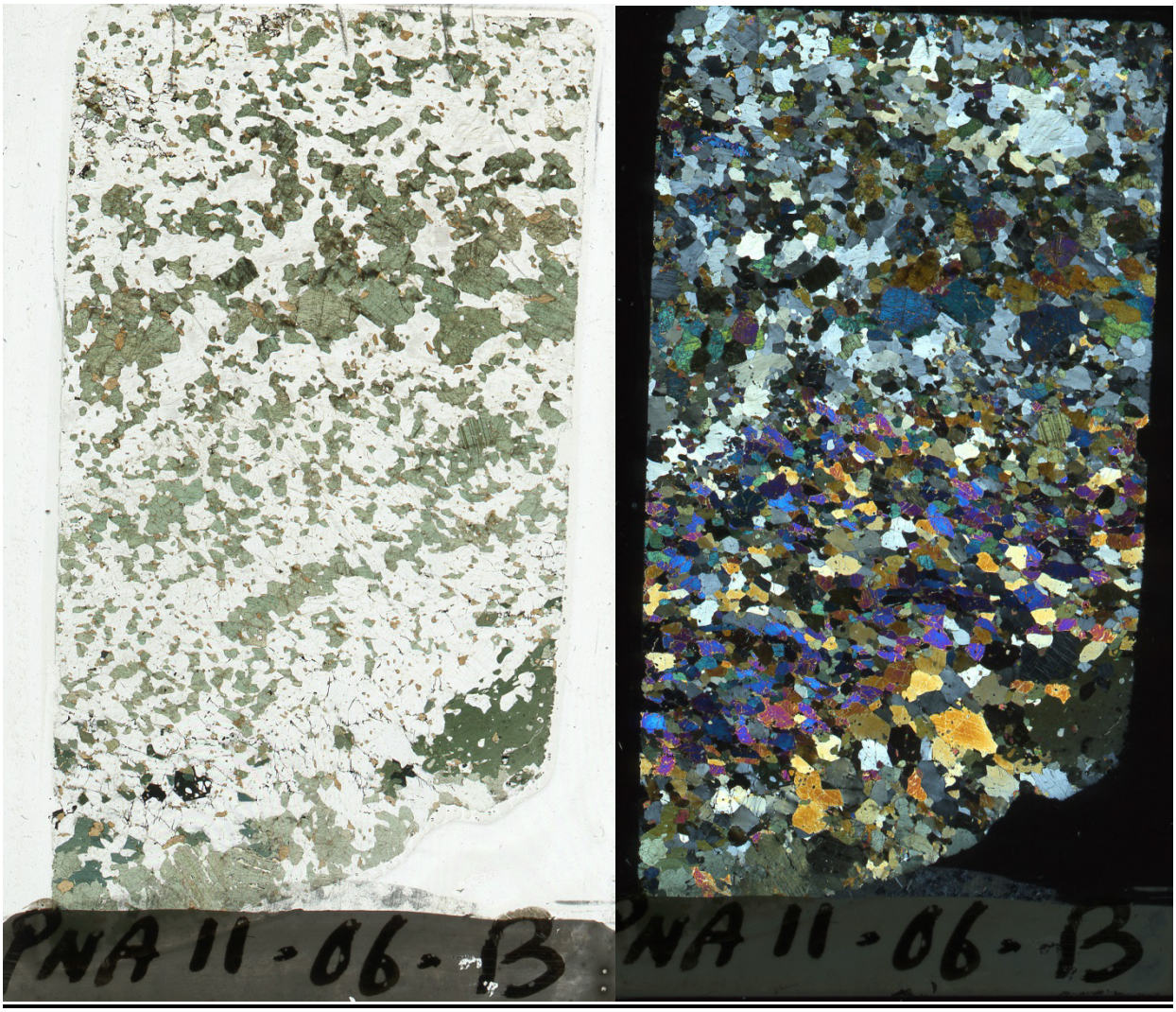

Mineralogy:

Quartz
Feldspar (Plagioclase)
Ca-Amphibole (Hornblende)
Amphibole (Hastingsite)
Scapolite
Clinopyroxene (Diopside)
Titanite
Epidote
Accessory: Allanite, Pyrite, Tourmaline
Mineralogy verified by SEM.

Petrography:

Layered with no obvious fabric. Medium to coarse-grained with subhedral texture. Late, euhedral, black tourmaline includes hornblende and hastingsite amphibole. Scapolite is rimmed by pyrite in fractures. Titanite and allanite are mantled by epidote.

Autoradiograph: Faint spots may indicate radioactive grains.

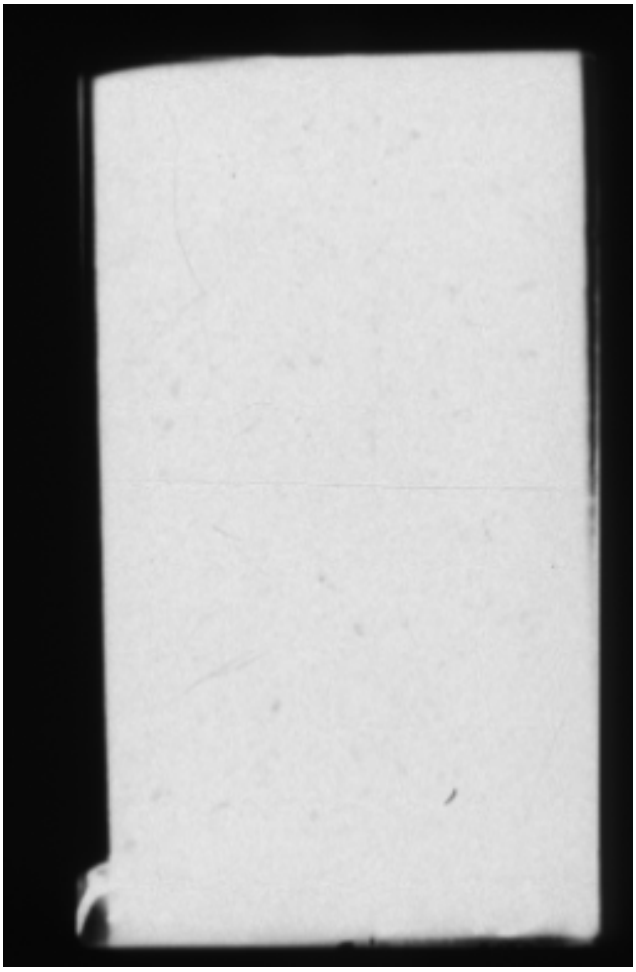

PNA11-08B: Calc-Silicate Gneiss

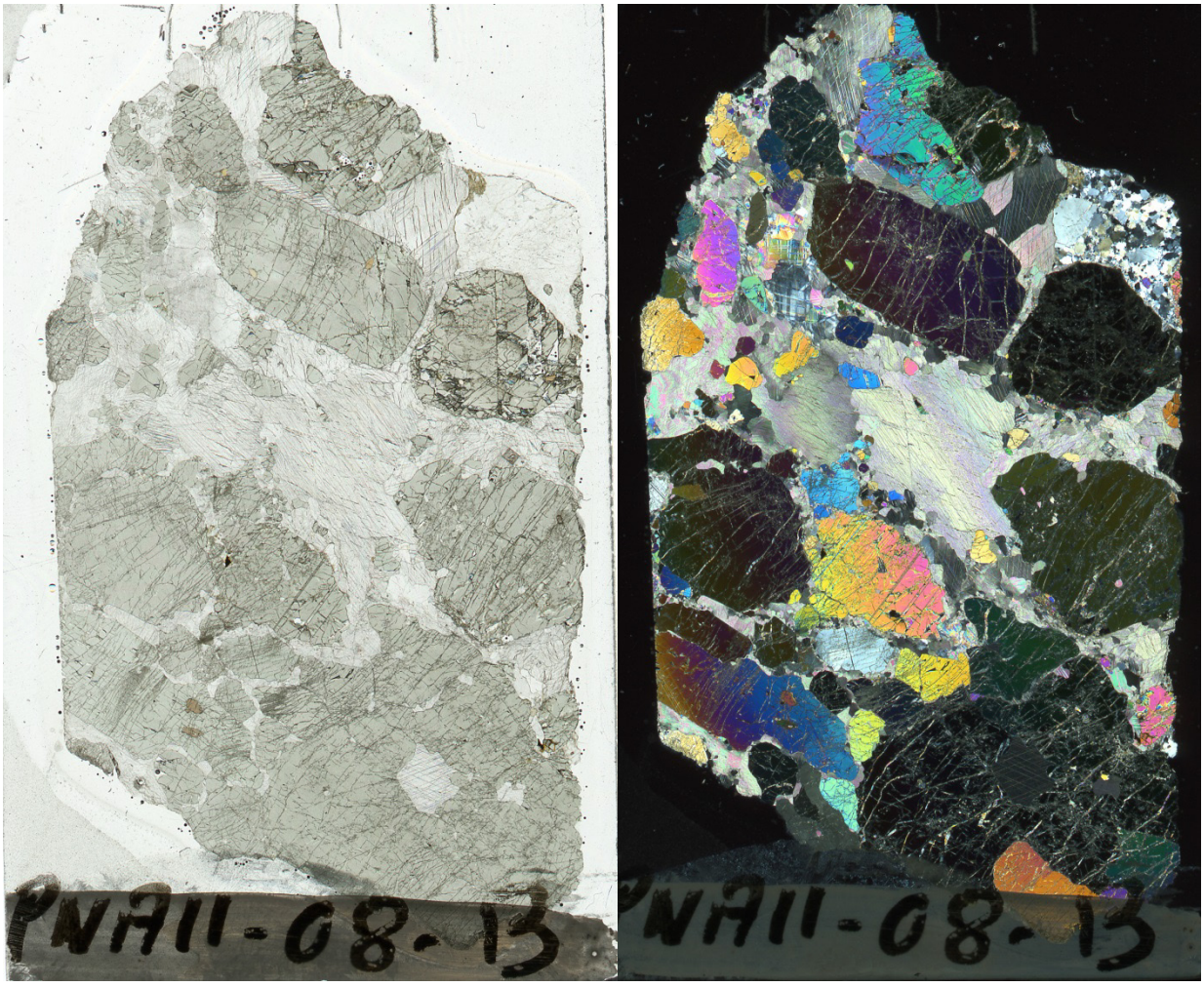

Mineralogy:

Clinopyroxene (Diopside)
Calcite
Potassium Feldspar
Plagioclase
Titanite
Biotite
Accessory: Zircon, Pyrrhotite

Mineralogy verified by SEM.

Petrography:

Biotite is included in very coarse-grained diopside. The matrix of calcite and feldspar has sutured boundaries.

Autoradiograph: Dark spots are zircon.

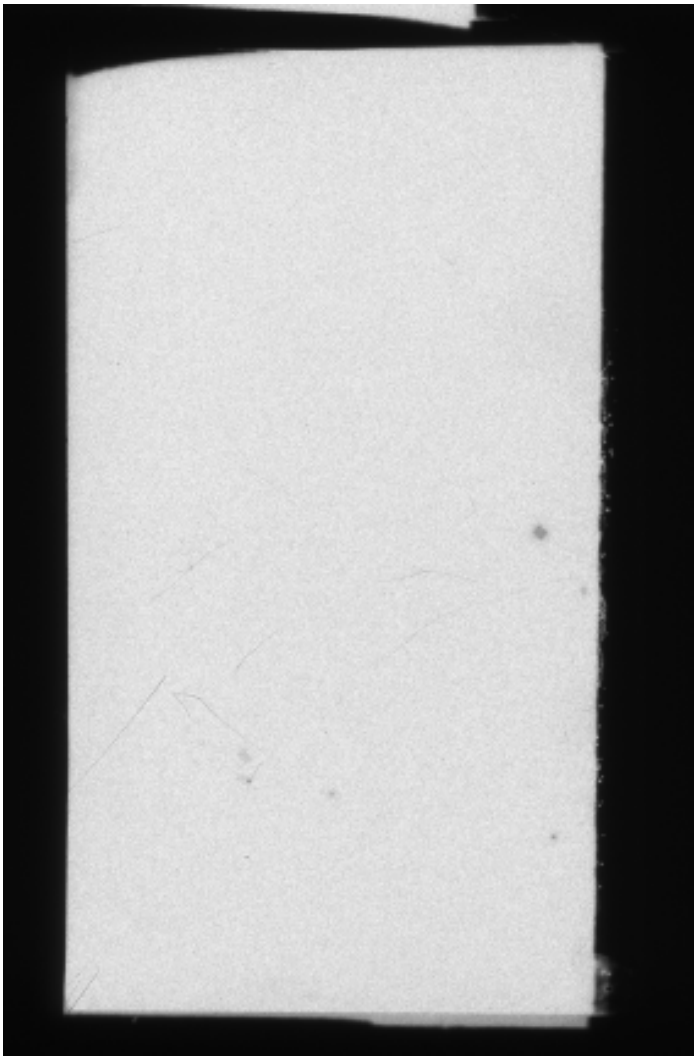

PNA11-09A: Layered Mafic Gneiss

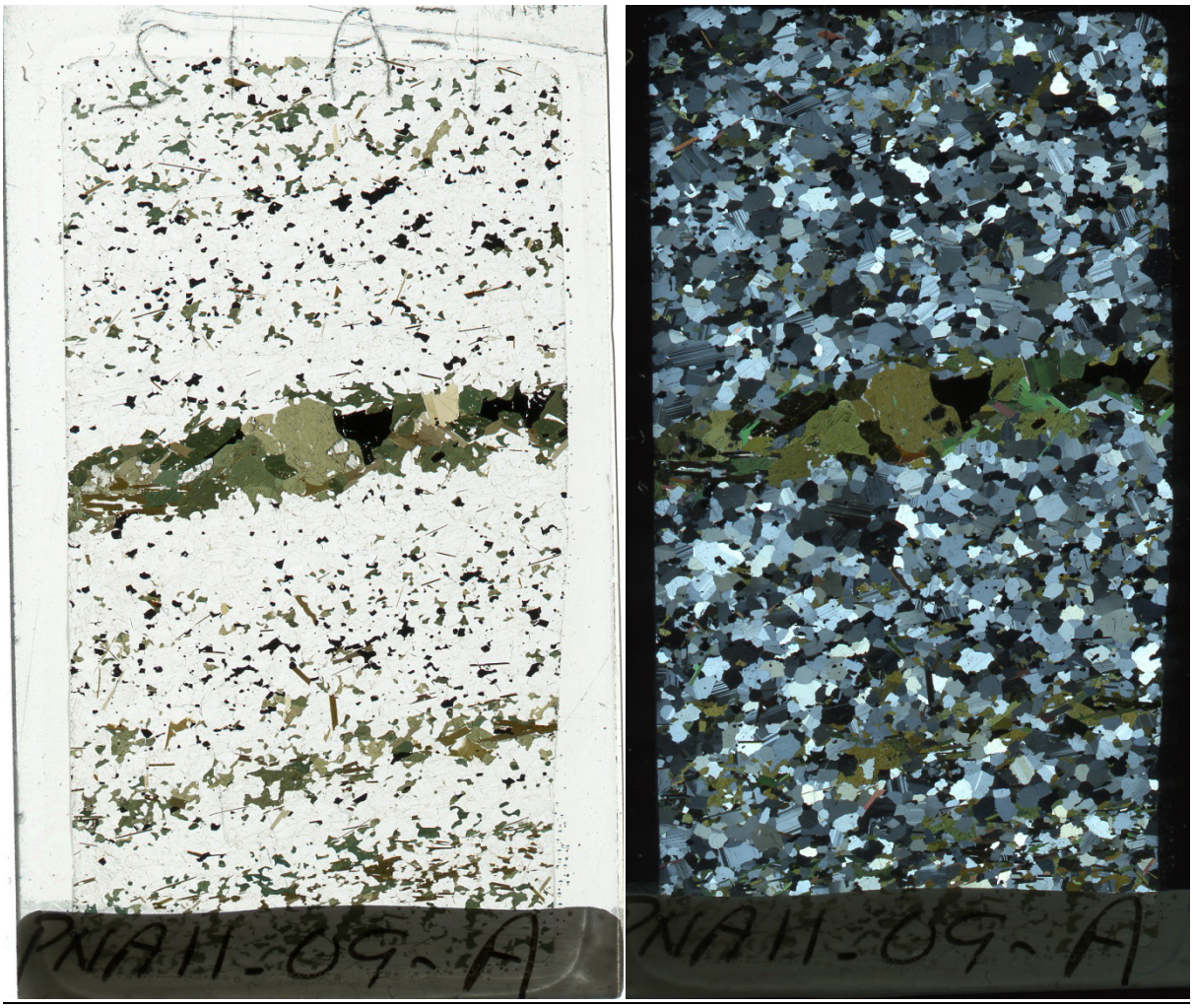

Mineralogy:

Quartz
Potassium Feldspar (Microcline)
Plagioclase
Amphibole (Hornblende)
Biotite
Accessory: Titanite, Calcite, Apatite, Magnetite, Ilmenite, Hematite

Petrography:

Consertal to subhedral texture with no obvious fabric. Compositional layers are variably coarse-grained. The main opaque is subhedral magnetite, with minor ilmenite and hematite in veins. Magnetite is often mantled by titanite.

Autoradiograph: No detectable radioactivity.

PNA11-09B: Mafic Gneiss

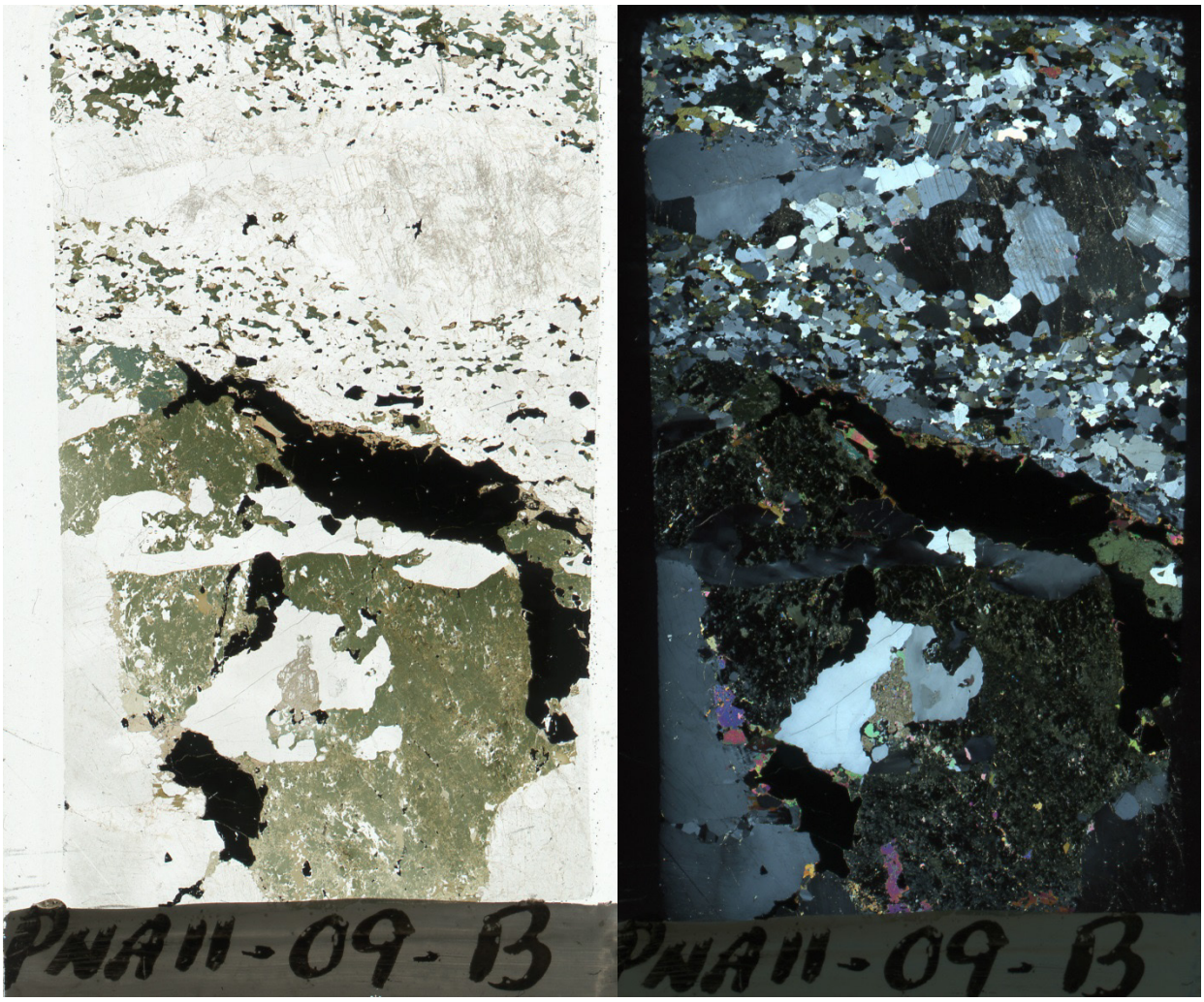

Mineralogy:

Quartz
Potassium Feldspar (Microcline)
Plagioclase
Amphibole (Hornblende, later Hastingsite)
Biotite
Accessory: Titanite, Calcite, Apatite, Tourmaline, Zircon, Rutile, Magnetite, Ilmenite, Pyrite

Petrography:

Layers of quartz and feldspar have consertal texture. Quartz displays undulose extinction. Trace amounts of tourmaline are present as late infill.

Autoradiograph: Faint textural features visible in image.

PNA11-09C: Garnet Sillimanite Metapelite

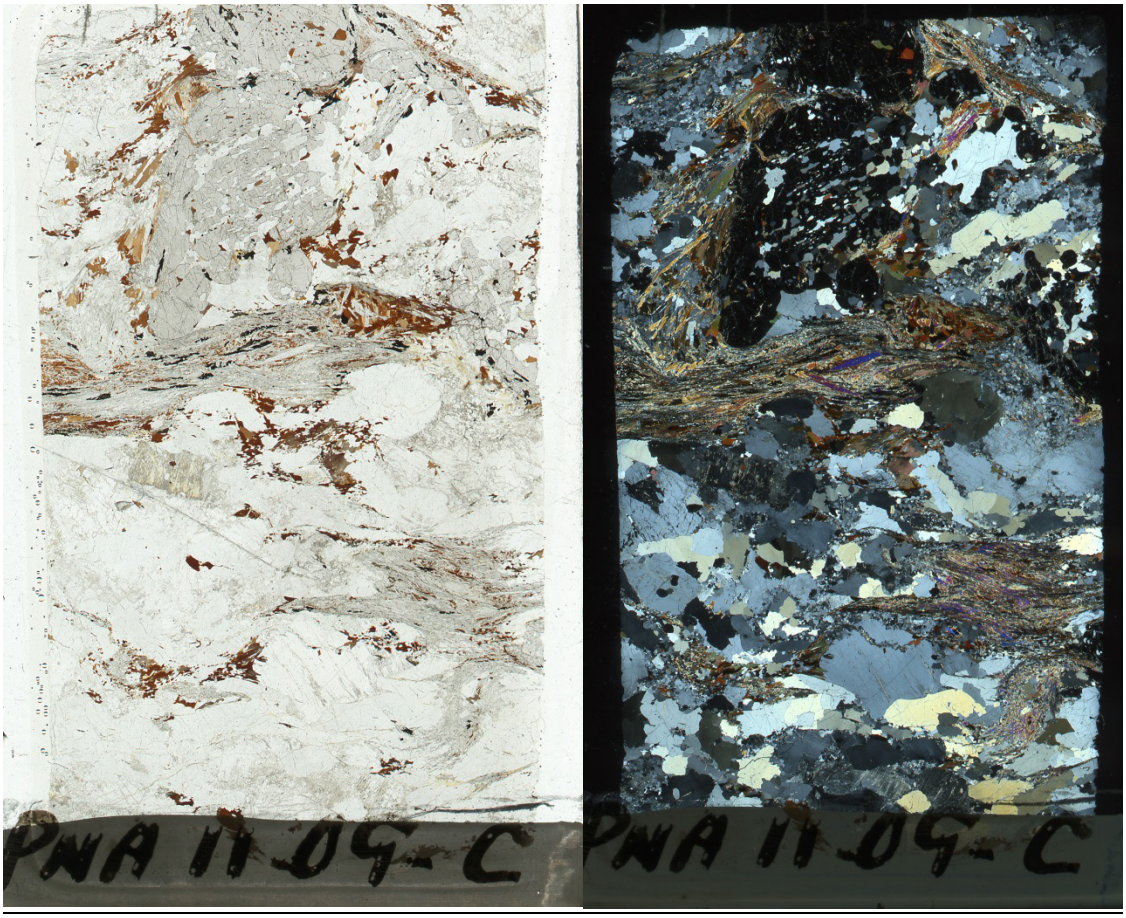

Mineralogy:

Quartz
Potassium Feldspar
Plagioclase
Garnet
Sillimanite
Biotite
Accessory: Epidote, Titanite, Allanite, Pyrite, Magnetite, Ilmenite

Petrography:

A garnet porphyroblast, the core of which has a linear fabric marked by inclusions of quartz and biotite, has a rim zone which contains a later foliation marked by inclusions of sillimanite and biotite. This same fabric continues in a different orientation in the matrix, wrapping around the garnet, and in the matrix is marked by ilmenite and sillimanite. Biotite is contained within this later fabric. Cloudy, coarse-grained plagioclase in the matrix is altered /sericitized. Matrix quartz is coarse-grained and undulose with mostly consertal edges, though some are anhedral.

Autoradiograph: Faint spots indicate some radioactive grains.

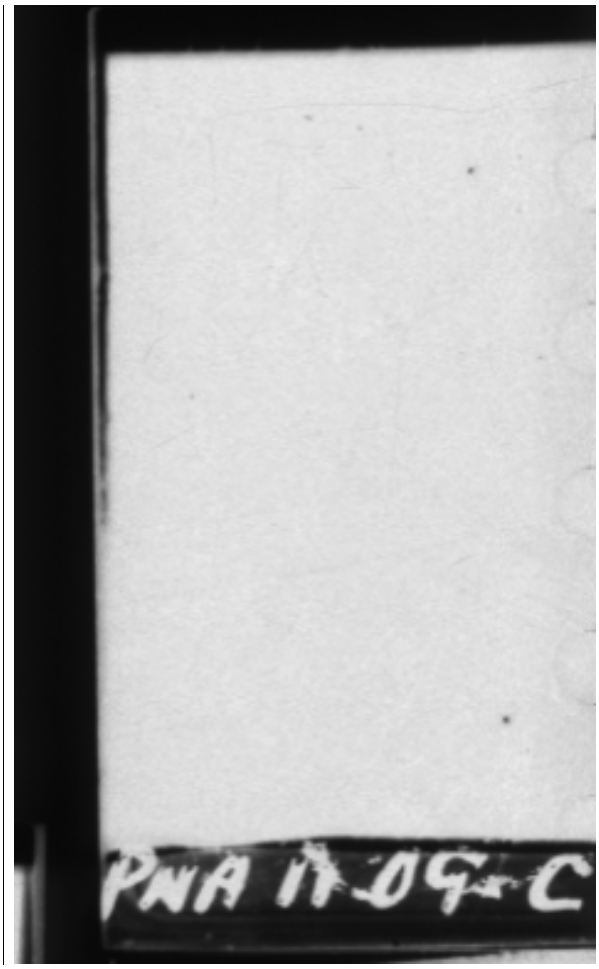

PNA11-09D: Quartzo-Feldspathic Gneiss

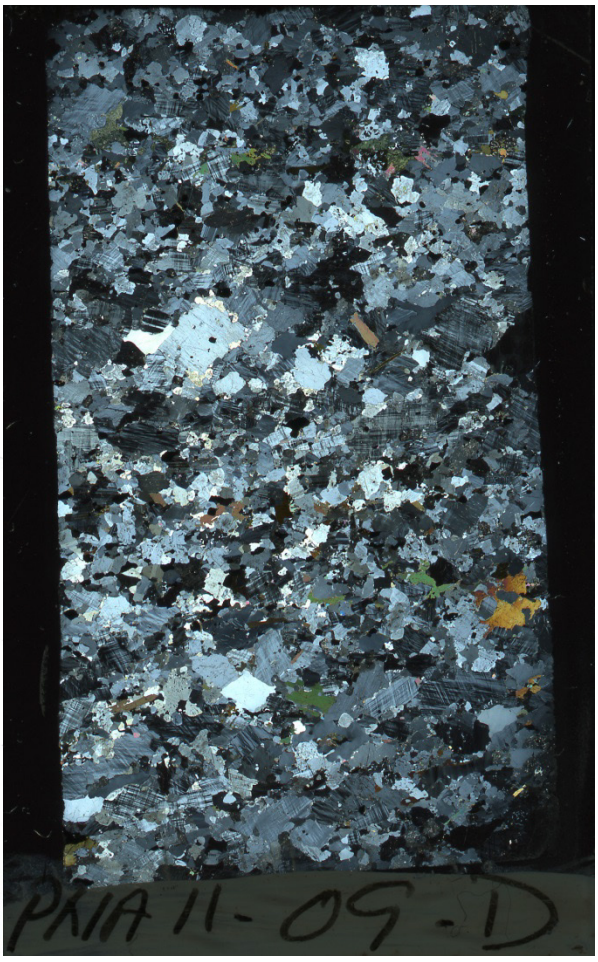

Mineralogy:

Quartz
Potassium Feldspar (Microcline)
Plagioclase
Ca-Amphibole
Biotite
Muscovite (late)
Goethite
Accessory: Zircon, Calcite, Tourmaline (Schorl), Magnetite, Rutile, Pyrite

Mineralogy verified by SEM.

Petrography:

Medium-grained, equigranular, quartz and feldspar with consertal texture. Quartz is undulose. Cores of plagioclase are highly included. Blue-green amphibole (hastingsite) is partially altered to biotite. There are abundant large, zoned subhedral zircons, goethite in crack and minor late tourmaline.

Autoradiograph: Faint spots indicate radioactive grains.

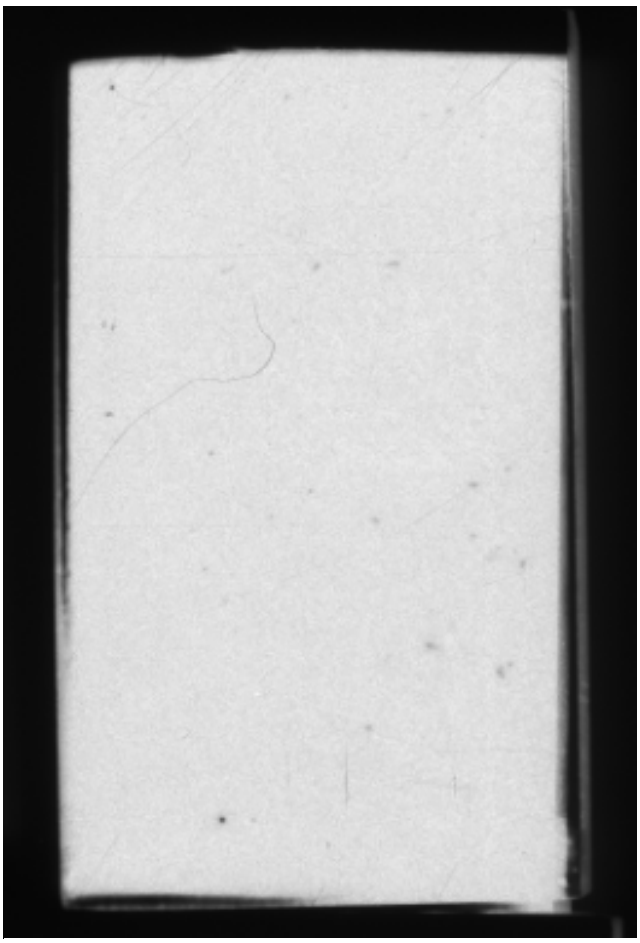

PNA11-09E : Mafic Gneiss

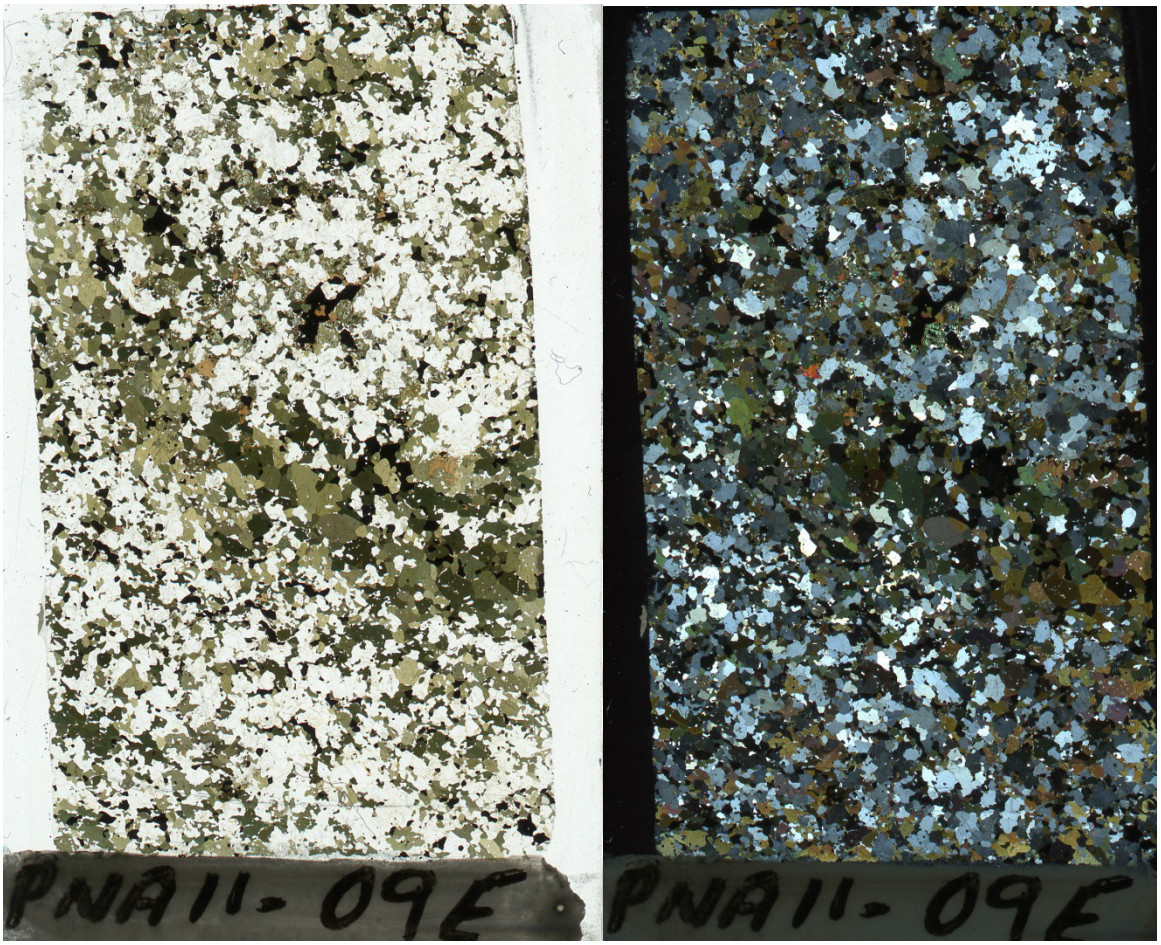

Mineralogy:

Quartz
Potassium Feldspar
Plagioclase
Ca-Amphibole
Clinopyroxene (Diopside)
Accessory: Titanite Apatite, Calcite
Pyrrhotite, Chalcopyrite, Pyrite

Mineralogy verified by SEM.

Petrography:

Medium-grained, equigranular, anhedral amphibole gneiss, with some more mafic-rich lenses. There is no fabric visible. Titanite is usually found as rims on pyrite. Green-pink pleochroic diopside alters to calcite and hornblende. The main opaque is subhedral pyrrhotite, in places partially replaced by pyrite, with minor chalcopyrite.

Autoradiograph: Faint spots indicate some radioactive grains.

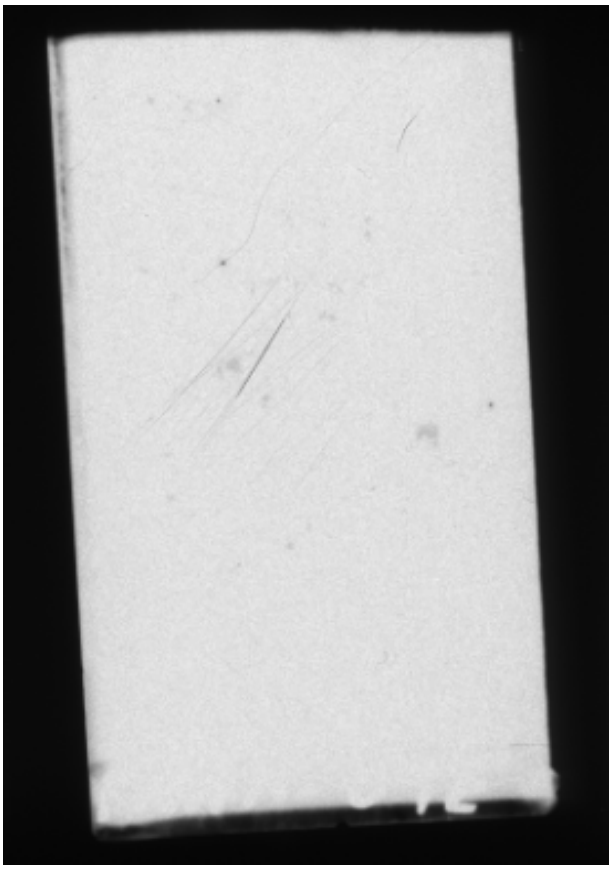

PNA11-09F: Quartzo-Feldspathic Gneiss

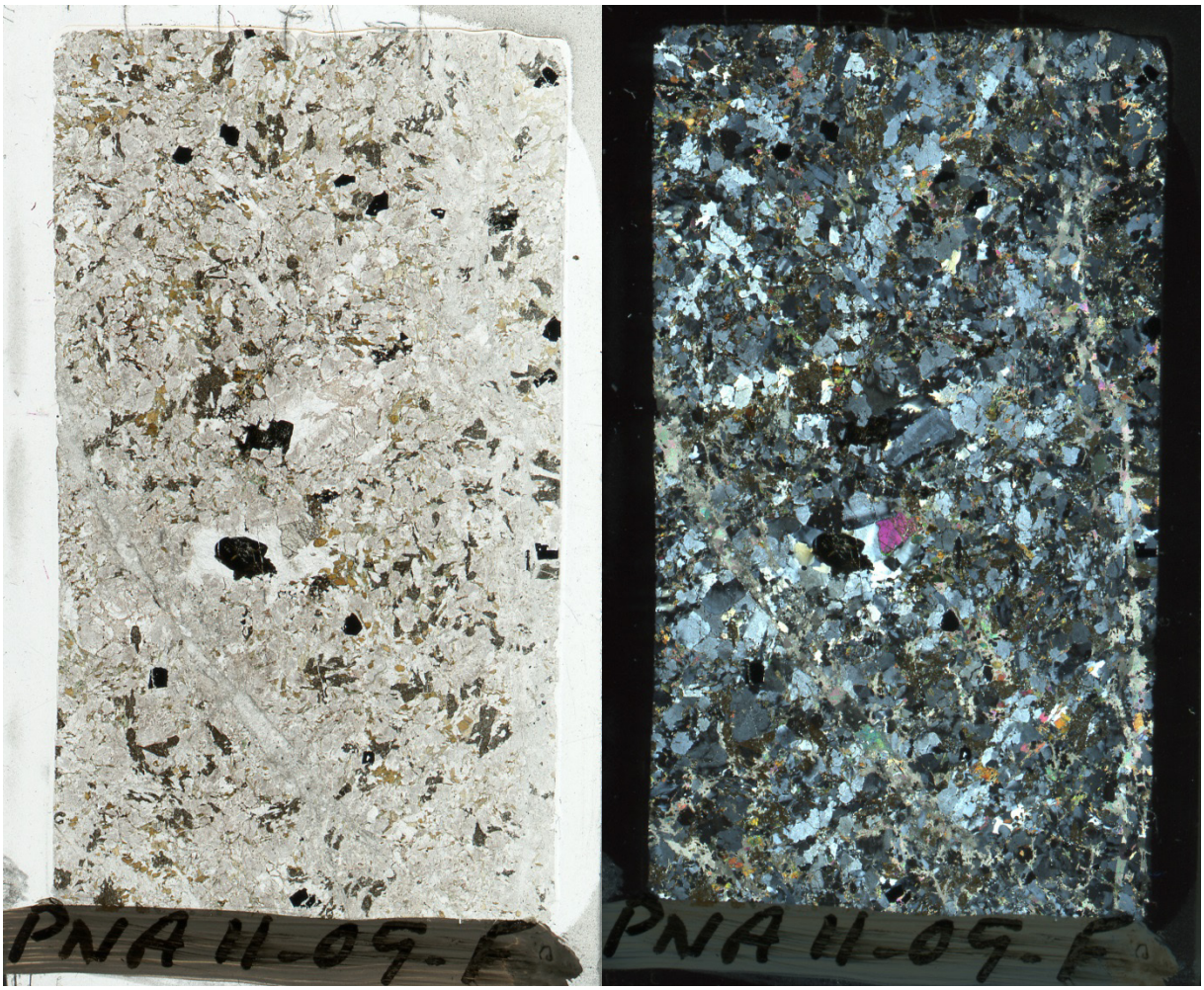

Mineralogy:

Quartz
Potassium Feldspar
Plagioclase
Biotite
Chlorite
Accessory: Apatite, Dolomite, Zircon, Barite, Ilmenite, Rutile

Mineralogy verified by SEM.

Petrography:

The matrix is quartz- and feldspar-rich with no fabric and is ratty and altered. Rutile replaces ilmenite. Biotite is retrograded to chlorite. Feldspar has abundant oriented tiny inclusions of rutile. There is one large fragment of zircon. A late dolomite vein cross-cuts the sample.

Autoradiograph: No detectable radioactivity.

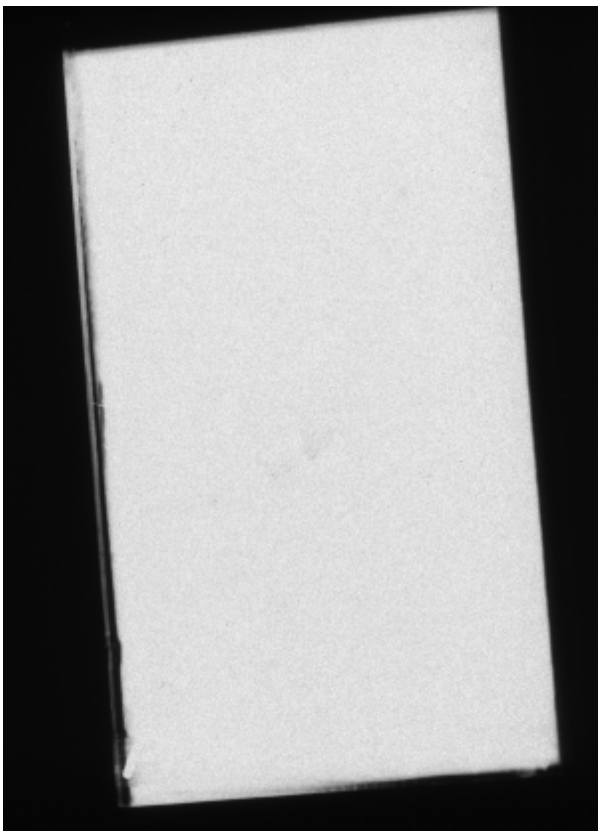

PNA12-03C : Mafic Gneiss

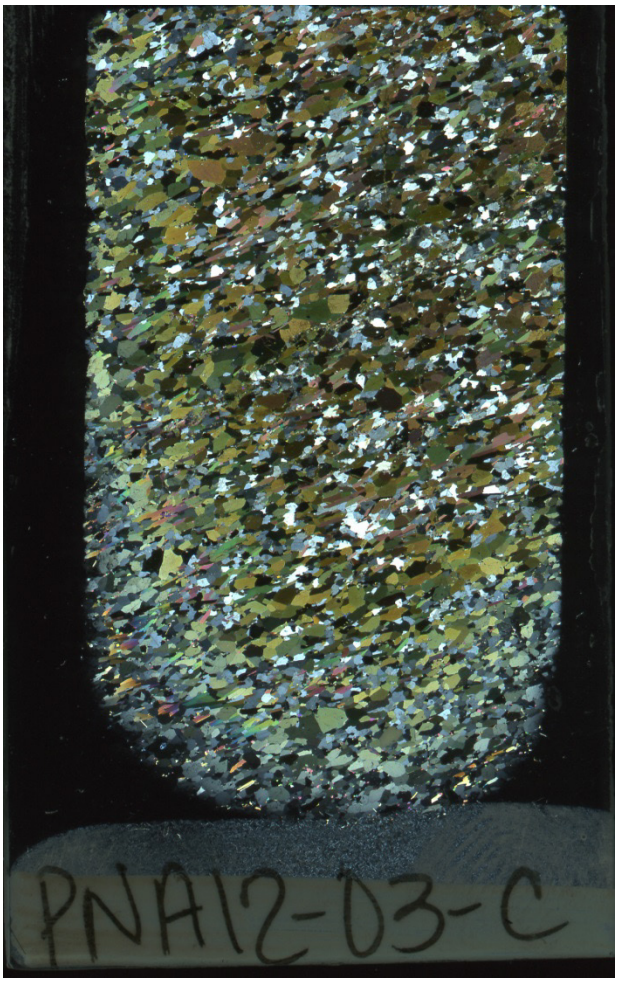

Mineralogy:

Quartz
Potassium Feldspar
Plagioclase
Ca-Amphibole
Biotite
Accessory: Titanite, Pyrite, Ilmenite

Petrography:

Medium-grained, equigranular, anhedral mafic gneiss with decussate texture of mostly amphibole and biotite.

Autoradiograph: No detectable radioactivity.

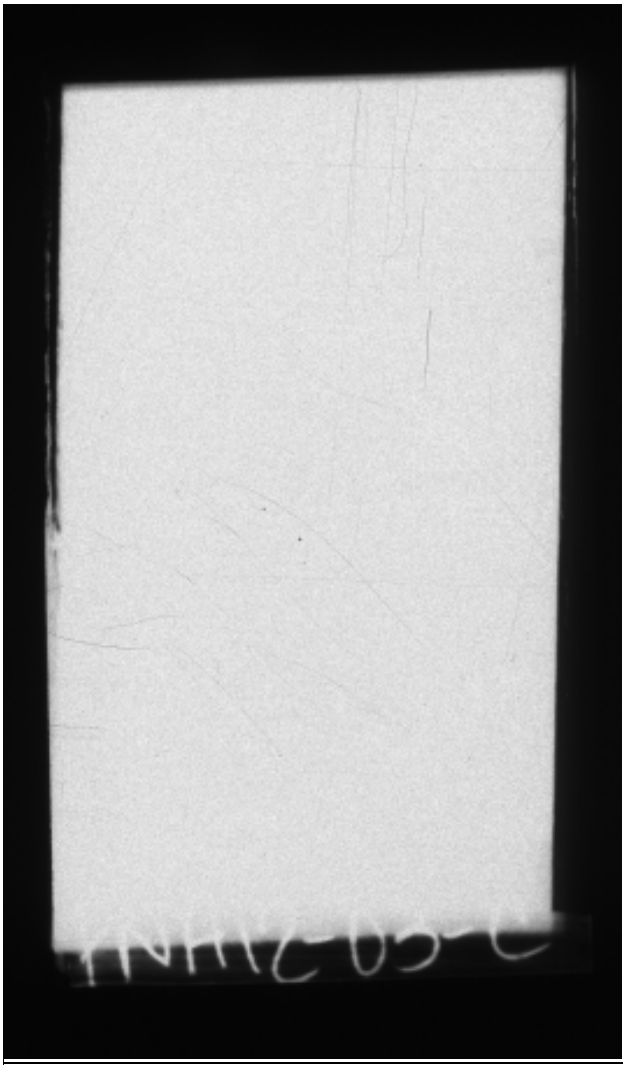

PNA12-03D: Calc-Silicate Gneiss

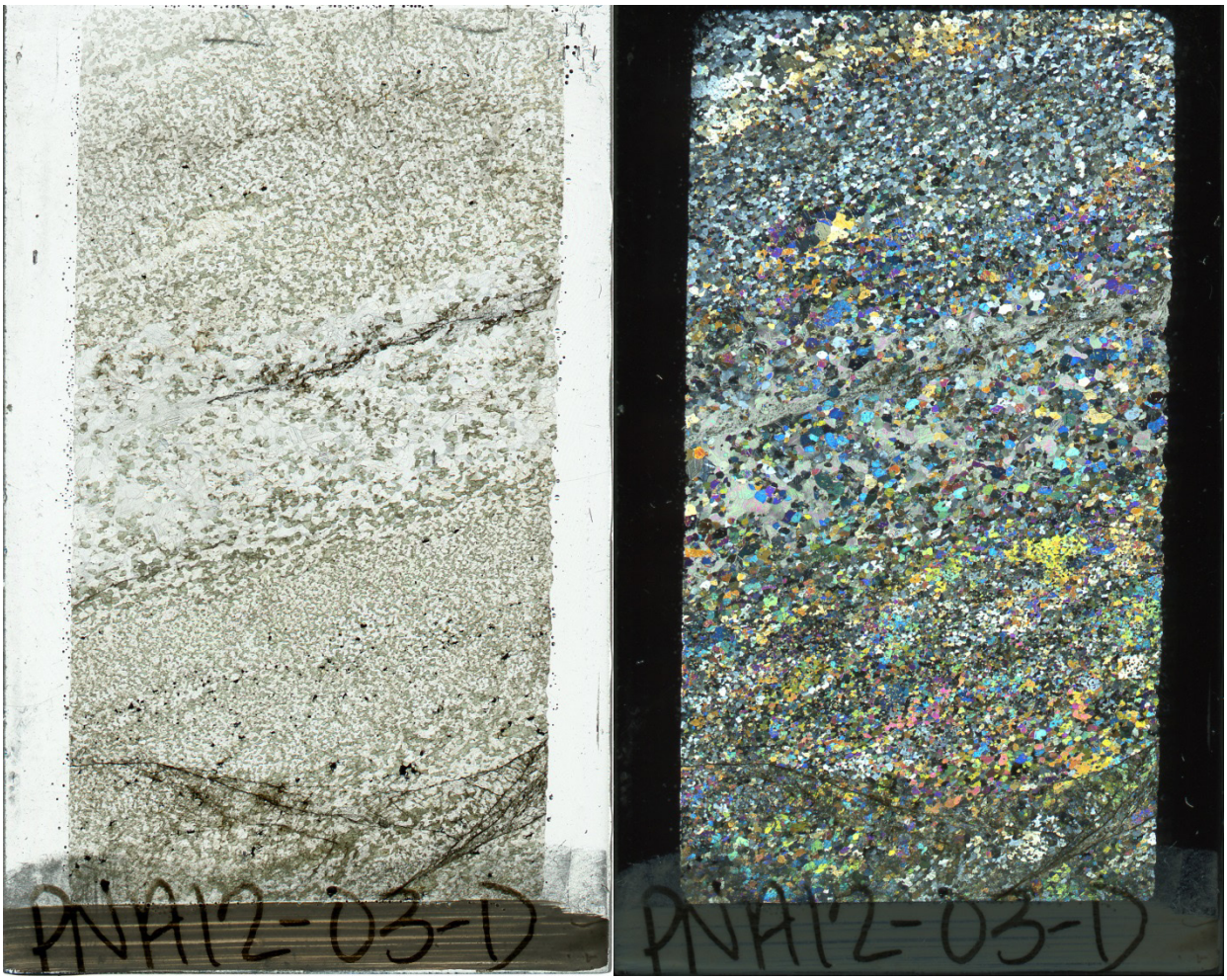

Mineralogy:

Quartz
Potassium Feldspar (Microcline)
Plagioclase
Calcite
Clinopyroxene (Diopside)
Titanite
Scapolite
Accessory: Tourmaline, Pyrrhotite, Pyrite, Chalcopyrite (Po>Py>Ccp)

Mineralogy verified by SEM.

Petrography:

Compositionally layered with granoblastic texture. Medium-grained with a coarser-grained band of carbonate. A weak fabric runs perpendicular to layering which is, in one part of the sample, marked by sericite (might be carbonate). Scapolite often encloses islands of diopside. Late fracturing is marked with dark, fine-grained gouge and sulfides.

Autoradiograph: Faint spots indicate radioactive grains.

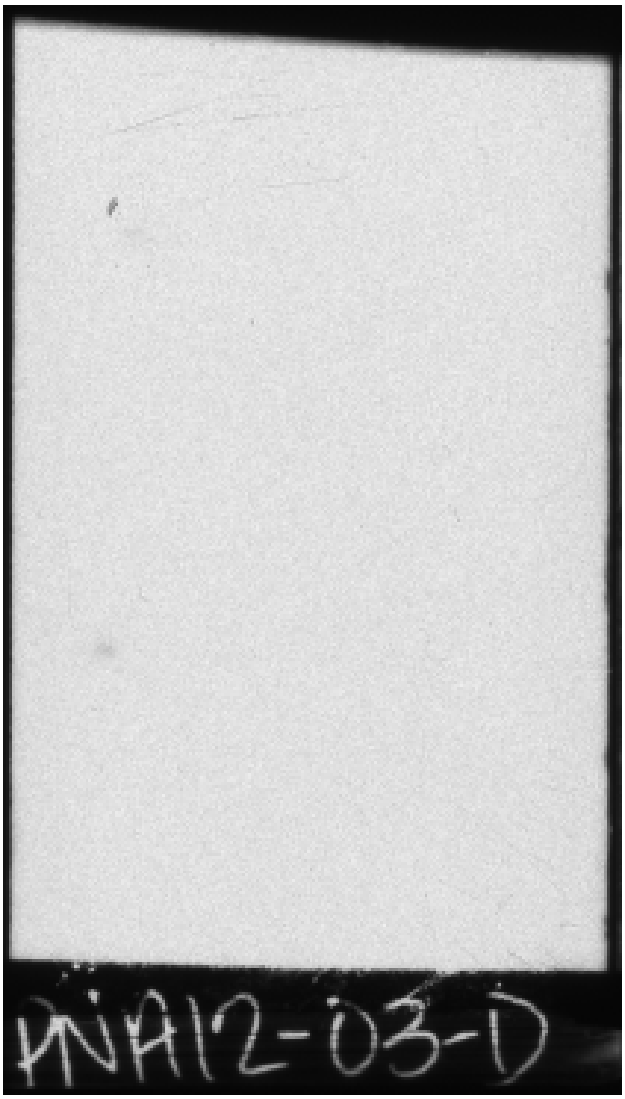

PNA12-03E : Mafic Gneiss

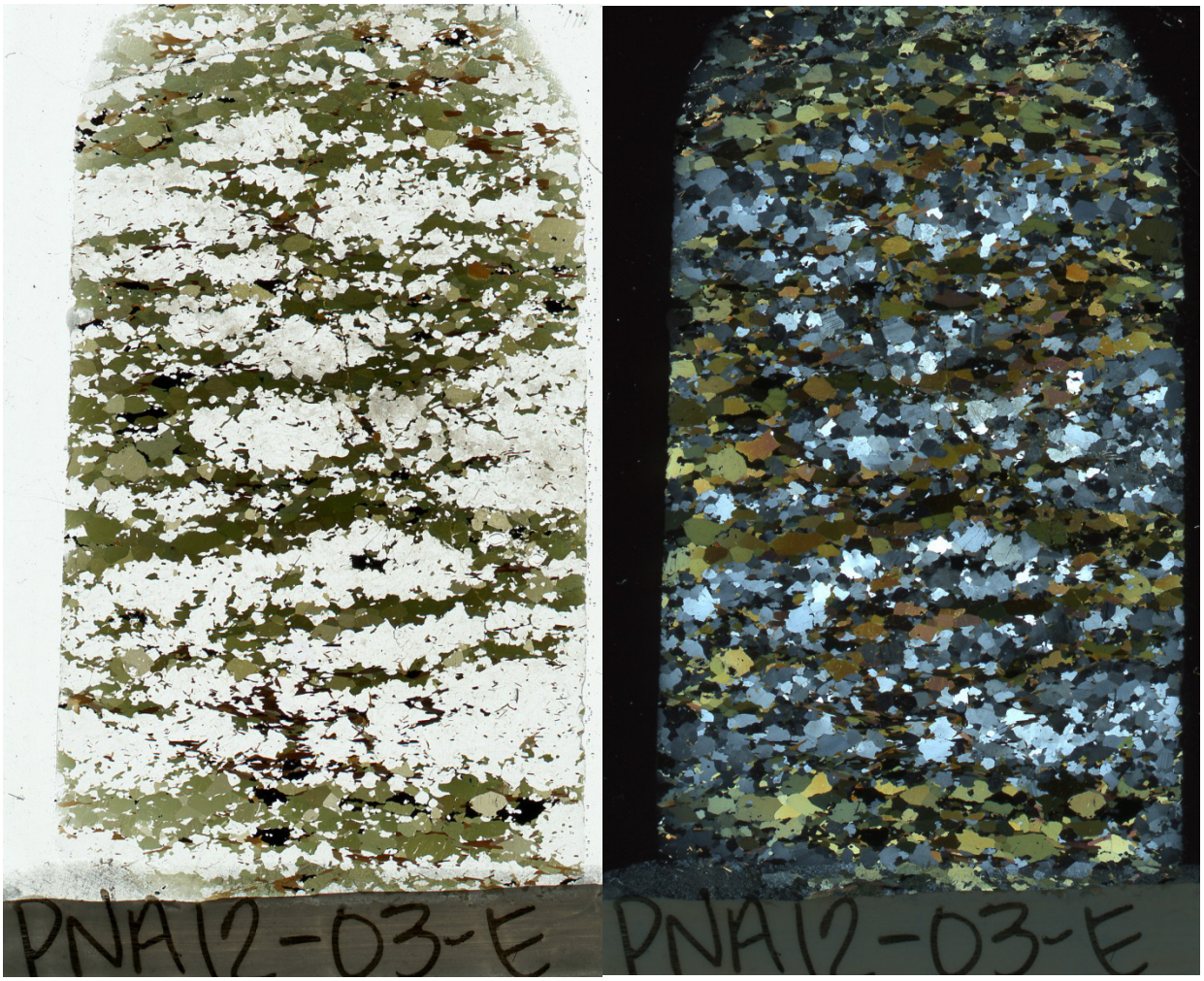

Mineralogy:

Quartz
Potassium Feldspar
Plagioclase
Ca-Amphibole (Hornblende, in places replaced by Hastingsite)
Accessory: Apatite, Magnetite, Pyrite, Pyrrhotite, Ilmenite

Mineralogy verified by SEM.

Petrography:

Decussate-textured amphibolite gneiss. Ca-amphibole (hornblende) in places is replaced by blue-green pleochroic more sodic amphibole (hastingsite) along cleavage plane. Pyrite: solid cores, rims are included, euhedral vuggy texture. Feldspar has rims of pyrite

Autoradiograph: No detectable radioactivity.

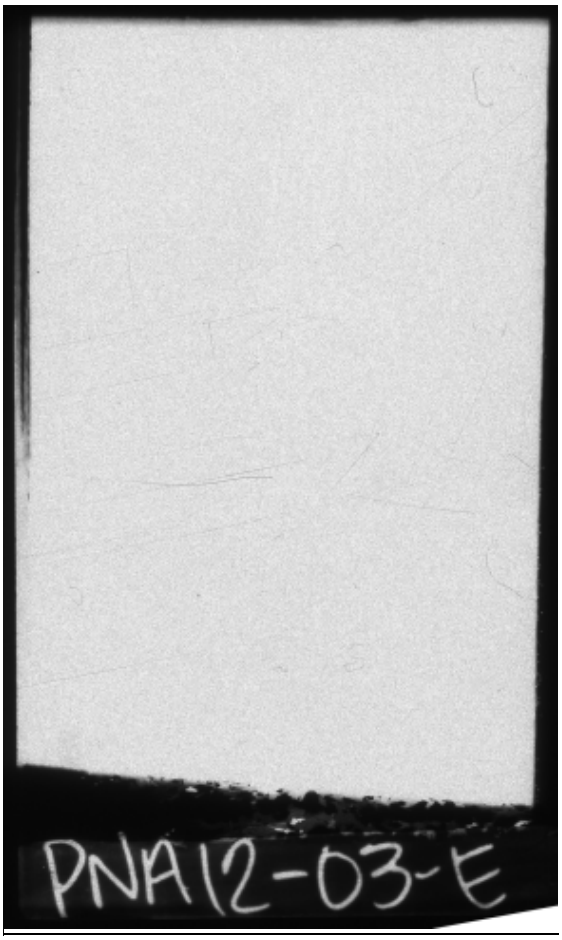

PNA12-06A: Mafic Gneiss

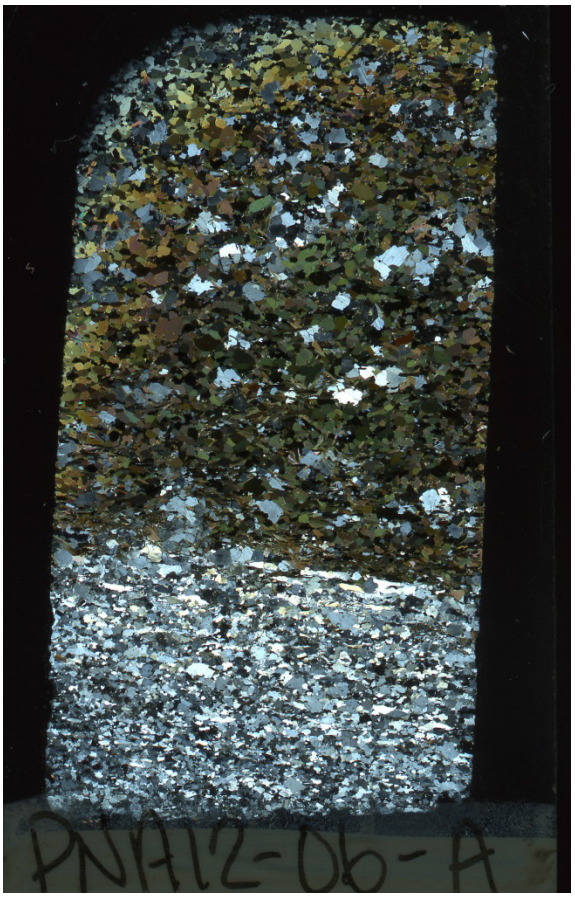

Mineralogy:

Quartz
Potassium Feldspar (Microcline)
Plagioclase
Ca-Amphibole (secondary Hastingsite)
Biotite
Garnet
Orthopyroxene
Accessory: Calcite, Apatite, Zircon, Fe-oxide, Pyrite, Unknown

Mineralogy verified by SEM.

Petrography:

Compositionally-layered garnet amphibole gneiss. Main amphibole is hornblendic, with change to blue-green hastingsite on some cleavage planes and rims. Equigranular with a moderate foliation marked by biotite, mainly seen in quartzo-feldspathic layer. Quartz shows undulose extinction and consertal texture with recrystallized grains at boundaries of larger grains. Small garnets are euhedral. Relic orthopyroxene occurs as rare inclusions in hornblende. One large broken zircon porphyroclast is present. There is abundant subhedral apatite and calcite. The main opaque mineral is Fe-oxide; pyrite has inclusions of an unidentified needle-shaped opaque.

Autoradiograph: No detectable radioactivity.

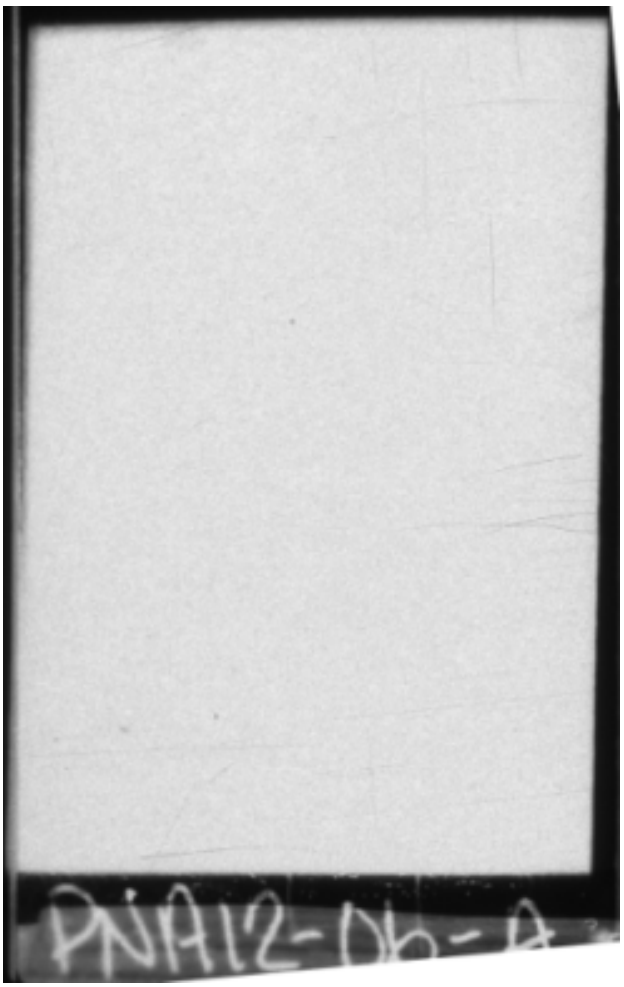

PNA12-06C: Calc-Silicate Gneiss

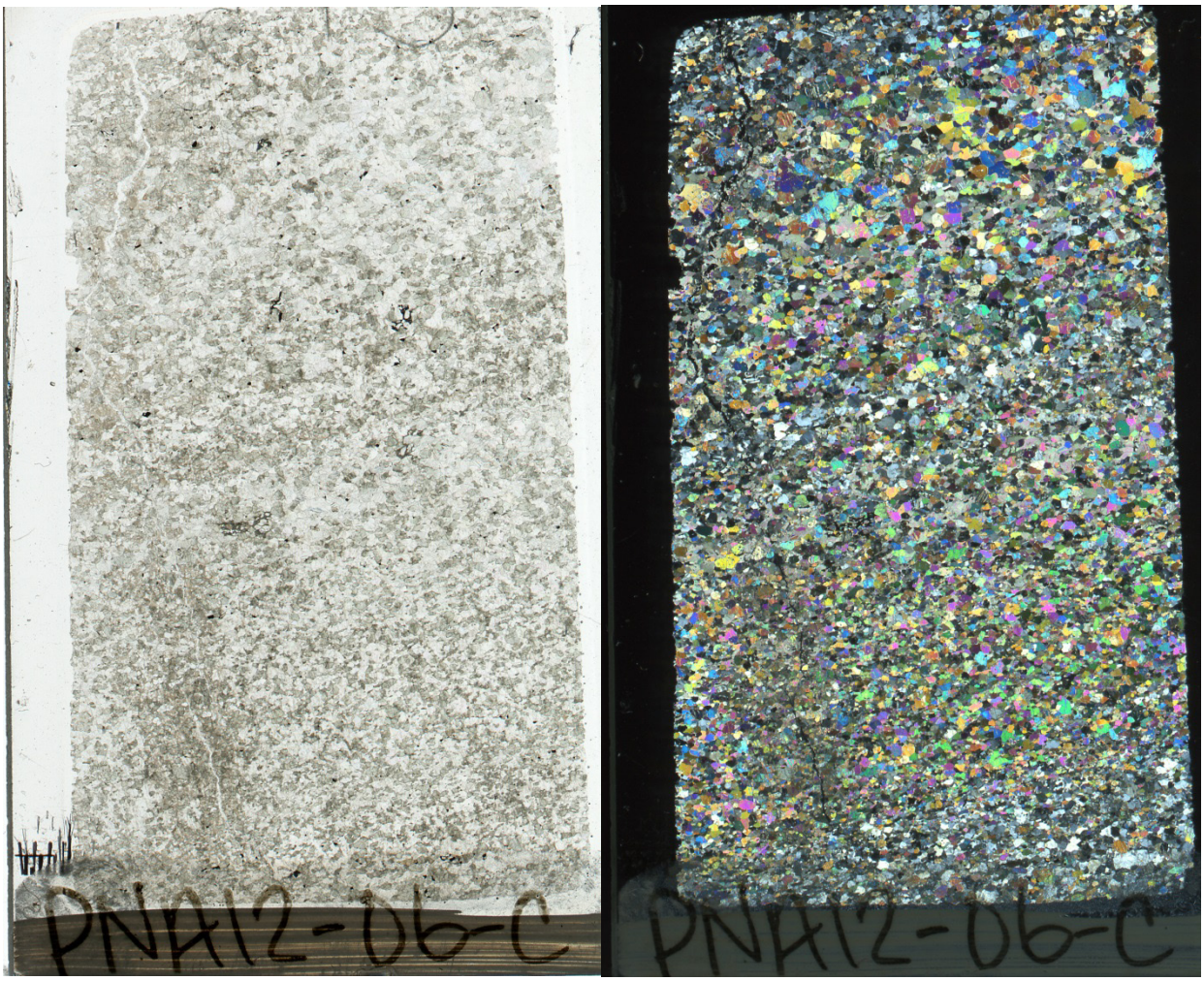

Mineralogy:
Quartz
Potassium feldspar
Plagioclase
Clinopyroxene (Diopside)
Calcite
Titanite
Scapolite
Accessory: Tourmaline, Graphite (?), Pyrrhotite, Pyrite
Mineralogy verified by SEM.

Petrography:

Granoblastic, anhedral texture. Scapolite alters to a fine-grained, brown, fibrous, birefringent mineral(s), largely in alteration halo next to fracture. Late quartz and tourmaline infill around grains. Vague suggestion of a fabric at high angle to compositional layering.

Autoradiograph: No detectable radioactivity.

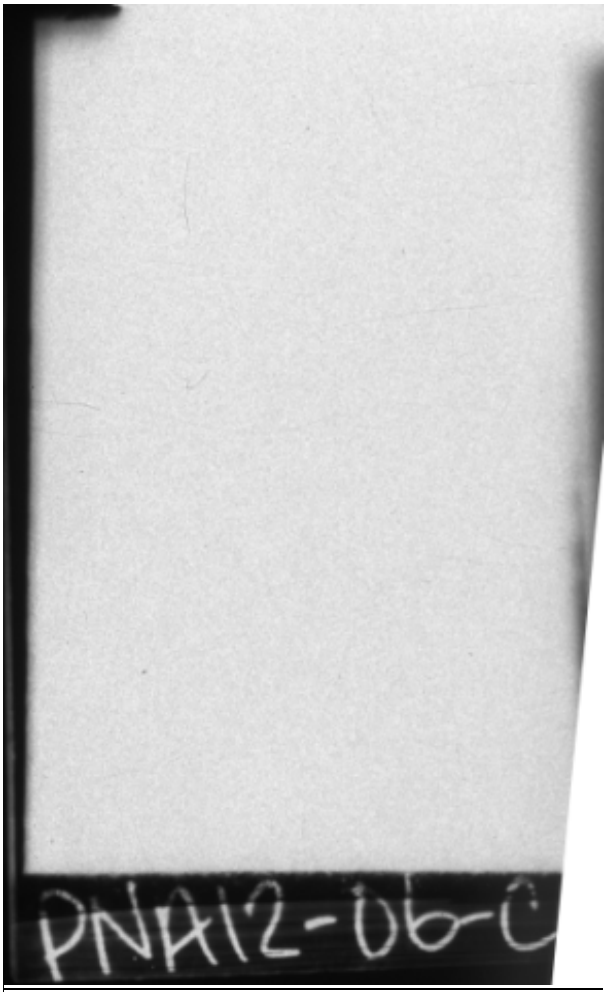

PNA12-10B: Calc-Silicate Gneiss

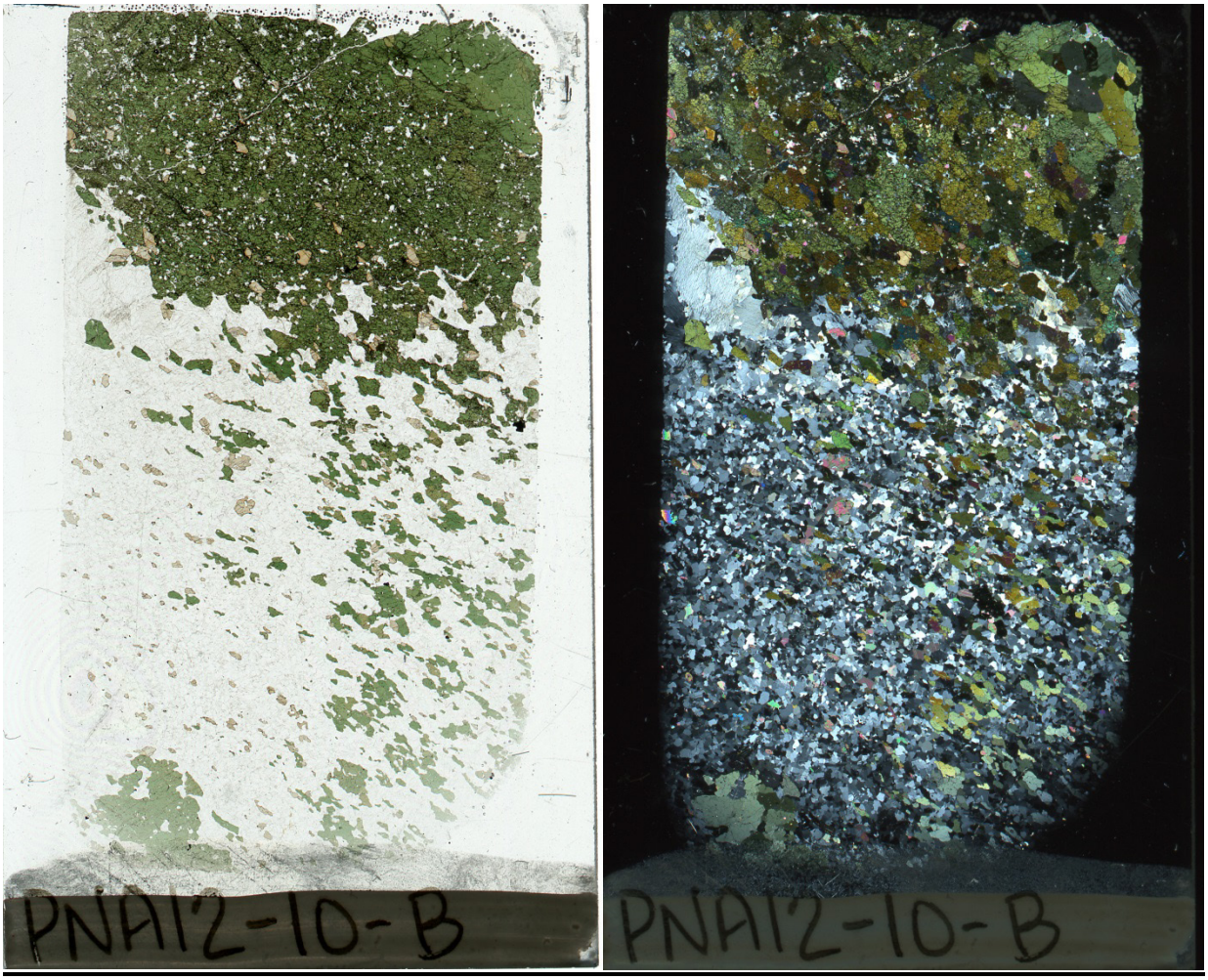

Mineralogy:

Quartz
Potassium Feldspar (Microcline, Microperthite)
Plagioclase
Clinopyroxene (Aegerine?)
Titanite
Calcite
Accessory: Magnetite, Hematite, Pyrite

Petrography:

Granoblastic texture with no oriented fabric. Large euhedral titanite wedges, showing parting. Minor quartz shows undulose extinction. Green clinopyroxene is shot through with fine-grained hematite and larger magnetite. Feldspar and calcite in matrix are anhedral.

Autoradiograph: Faint spots indicate radioactive grains.

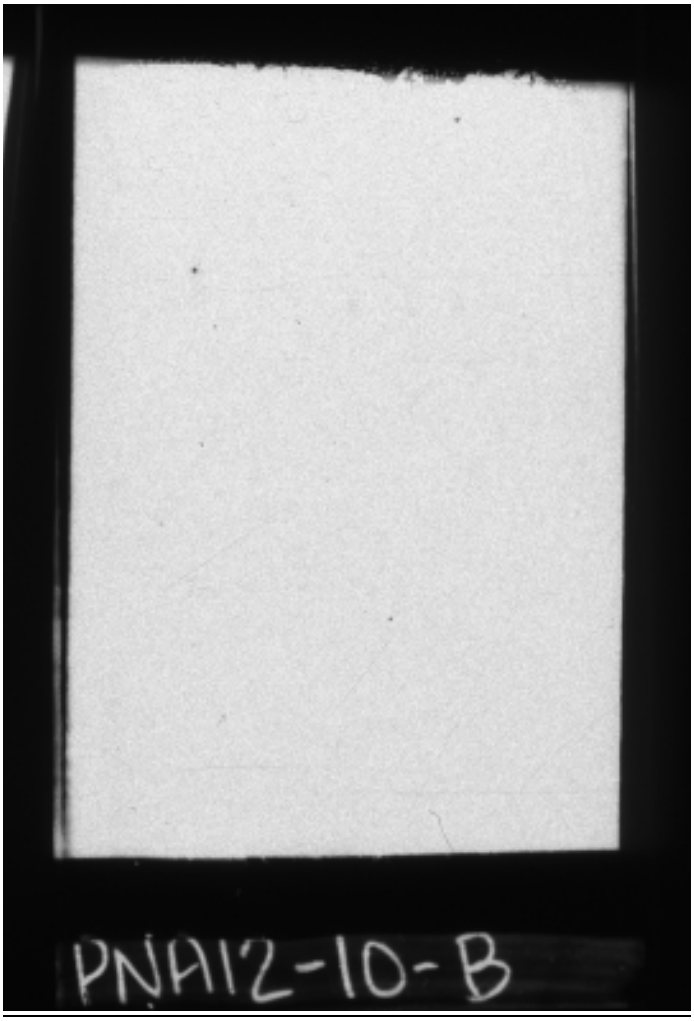

PNA12-10D: Mafic Gneiss

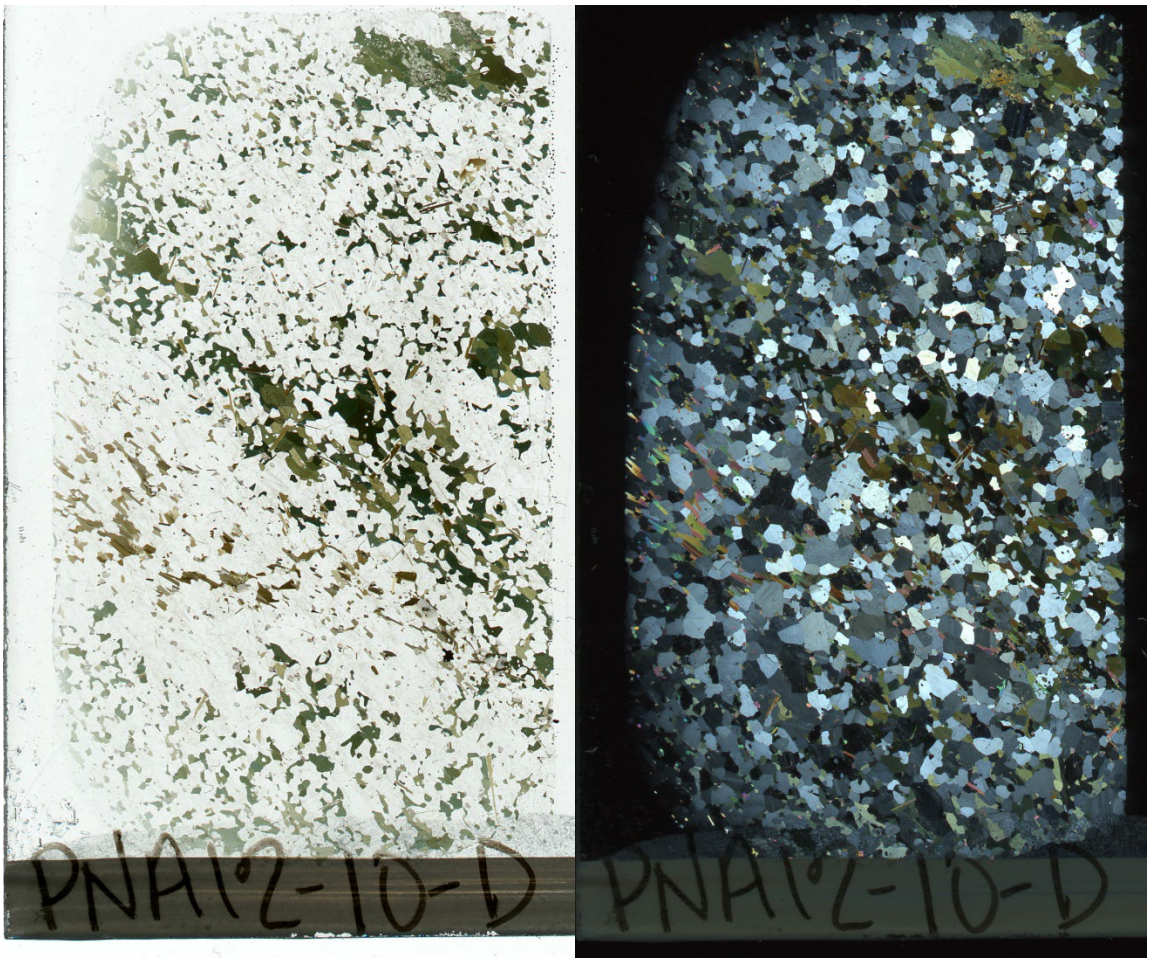

Mineralogy:

Quartz
Potassium Feldspar
Plagioclase
Ca-Amphibole
Clinopyroxene (Diopside)
Biotite
Accessory: Titanite, Calcite, Apatite, Zircon, Fe-oxide, Tourmaline

Petrography:

Layered, granoblastic to decussate textured. Mafic bands of amphibole (hornblende to arfedssonite), biotite and diopside, which are severely altered to a felted yellow/black mass. No obvious fabric.

Autoradiograph: No detectable radioactivity.

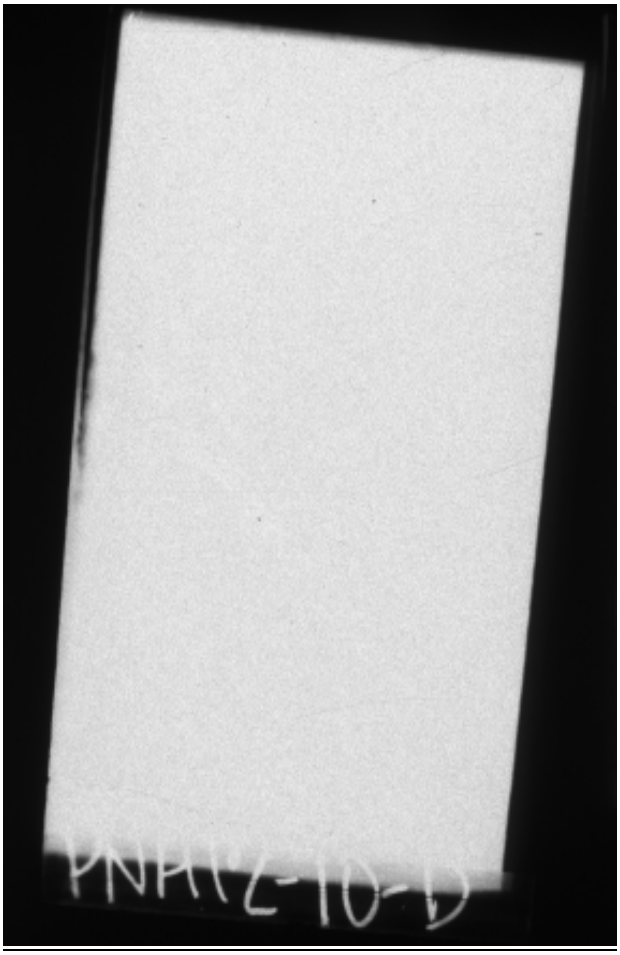

PNA12-12C: Calc-Silicate Gneiss

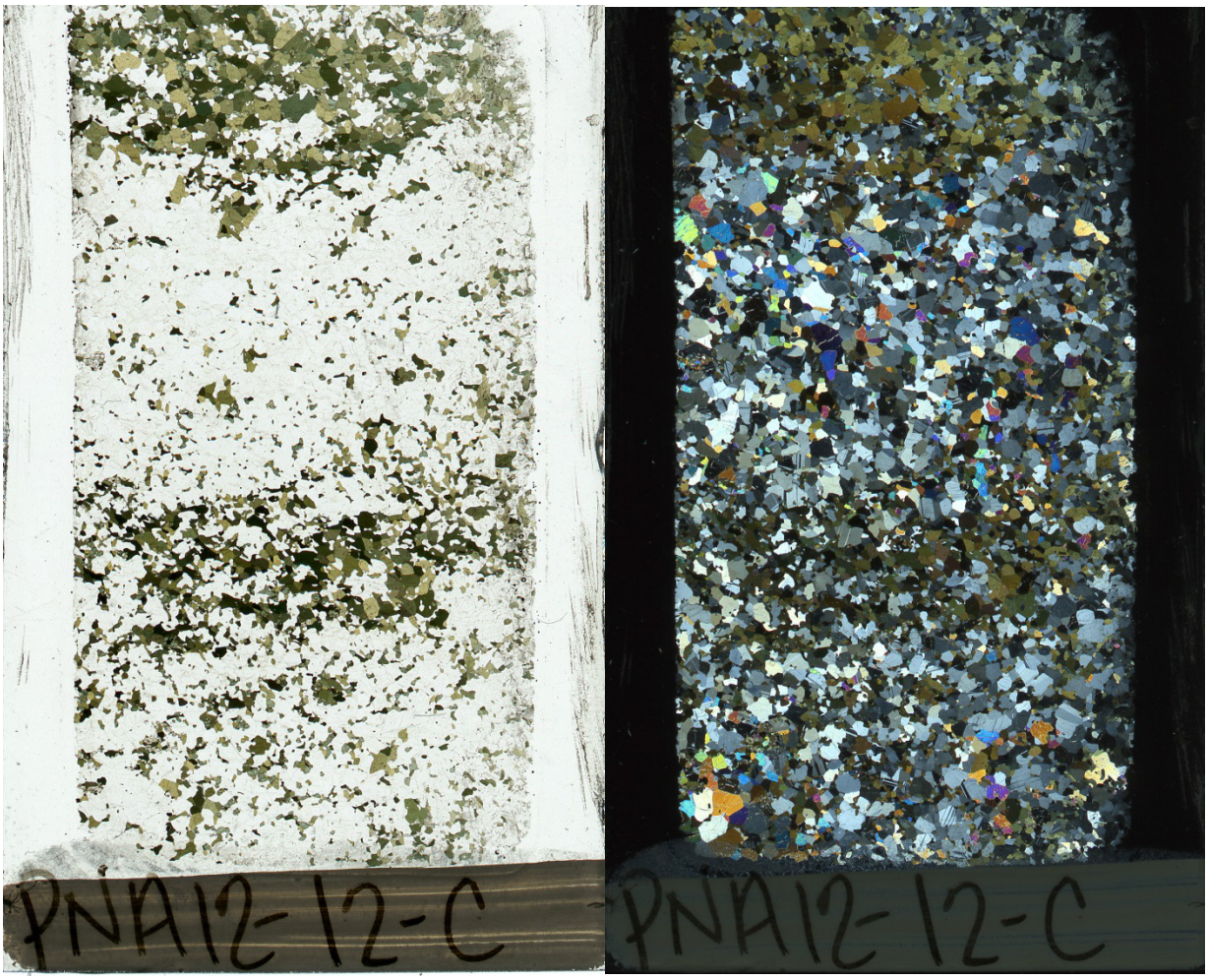

Mineralogy:

Ca-Amphibole
Clinopyroxene (Diopside)
Potassium Feldspar
Plagioclase
Scapolite
Titanite
Accessory: Apatite, Pyrite

Petrography:

Compositionally layered, medium-grained with granoblastic texture.

Autoradiograph: No detectable radioactivity.

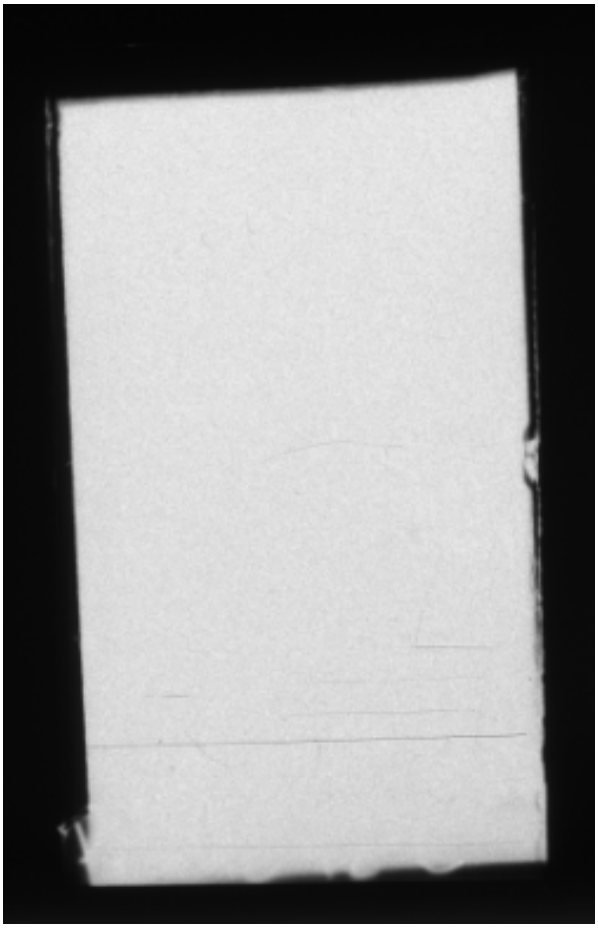

PNA12-12D: Layered Mafic Gneiss

Mineralogy:

Quartz
Potassium Feldspar (Microcline)
Plagioclase Feldspar
Ca-Amphibole
Accessory: Titanite, Calcite, Fe-oxide

Petrography:

Layered, medium-grained granoblastic quartz and feldspar with coarser bands of mafic minerals: blue-green pleochroic amphibole possibly altered pyroxene.

Autoradiograph: Faint spots indicate radioactive grains.

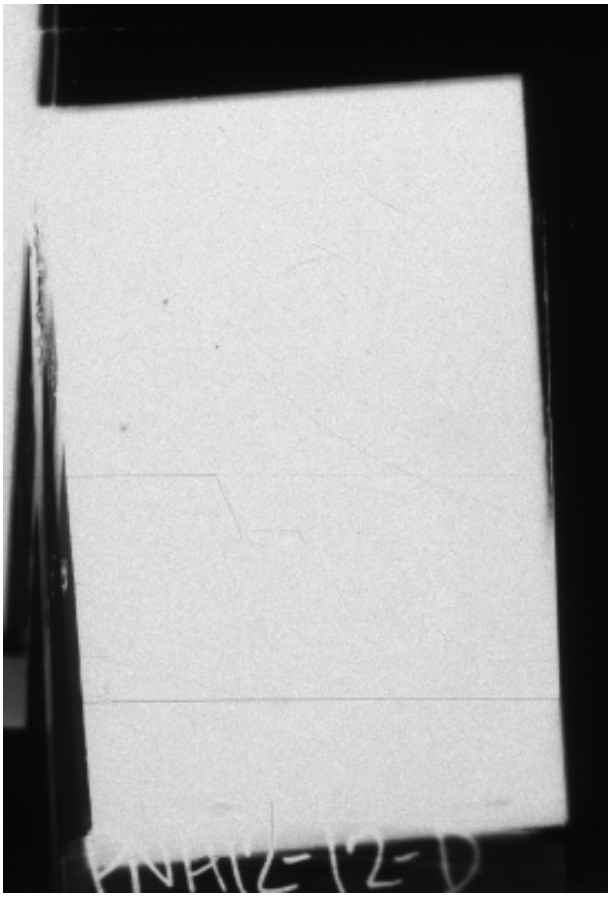

PNA12-12G: Calc-Silicate Gneiss

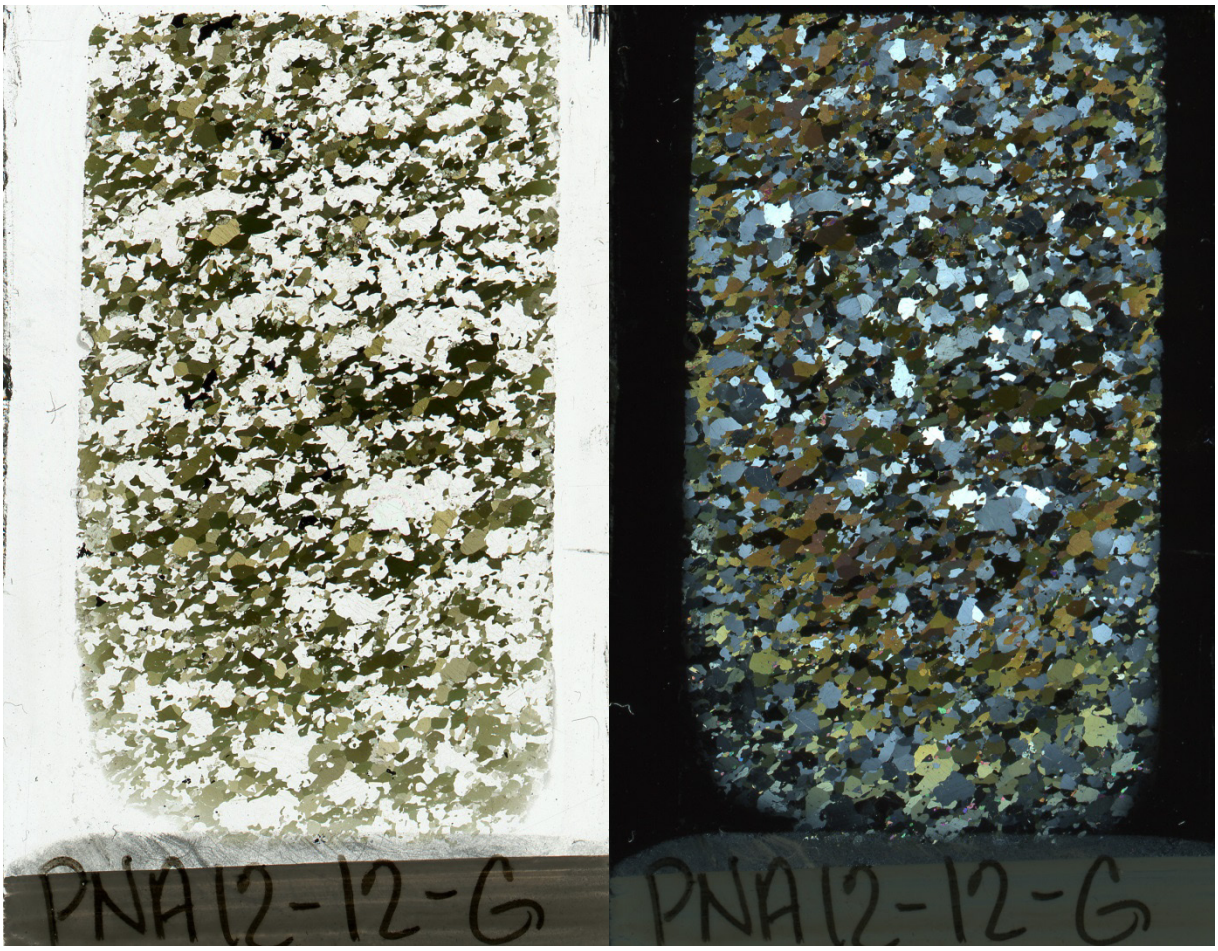

Mineralogy:

Quartz
Potassium Feldspar
Plagioclase
Ca-Amphibole
Clinopyroxene (Diopside)
Scapolite
Titanite
Biotite
Accessory: Apatite, Zircon, Magnetite, Pyrite

Petrography:

Medium-grained, granoblastic texture with a weak fabric.

Autoradiograph: No detectable radioactivity.

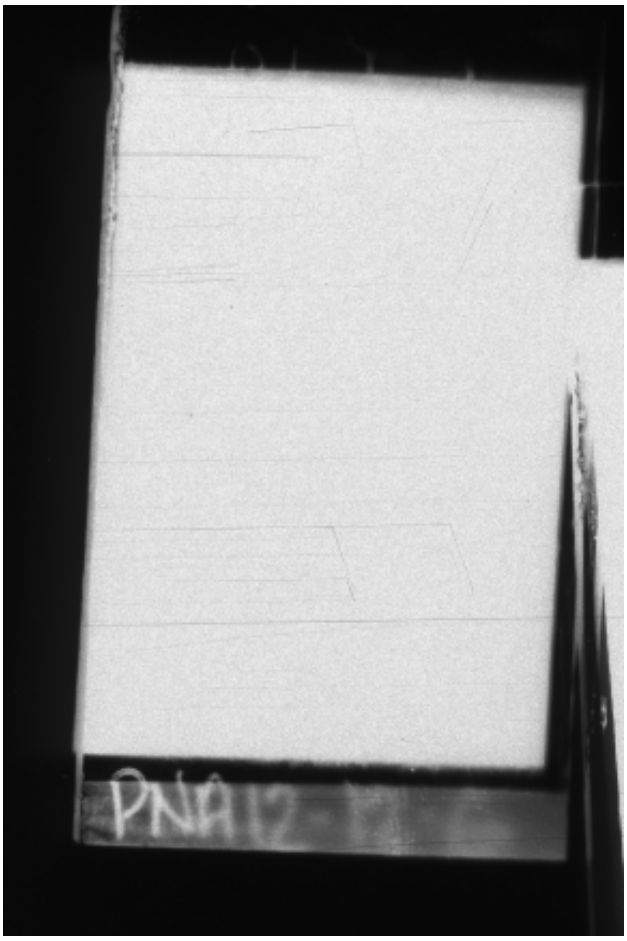

APPENDIX C

Geoenvironmental Ore Deposit Model

This Appendix presents a direct comparison between the thorium and rare earth element vein deposit geoenvironmental ore deposit model (Armbrustmacher *et al*.,1995) with the host rocks and granitic pegmatite-hosted U-Th-REE deposits of the Bancroft area. In addition, images showing the remediation efforts made by mining companies and the municipality are provided.

Geoenvironmental Ore Deposit Model for Bancroft

In the 1990s, the U.S. Geological Survey (U.S.G.S.) and others proposed the concept of geoenvironmental ore deposit modelling (Plumlee *et al*., 1994; Plumlee and Nash, 1995). Plumlee and Nash (1995) defined a geoenvironmental model as a compilation of geological, geochemical, hydrological and geophysical parameters related to the environmental behaviour of a particular ore deposit from pre-mining to mining and post-closure phases of development (Fig. C1). They built a viable classification for 32 diverse mineral deposits based on ore deposit models of Cox and Singer (1986). The approach of the U.S.G.S. provides the steps to develop a quantitative geoenvironmental model for any ore deposit type to plan for closure at the discovery stage. In order to facilitate this, explorationists must look at a prospective deposit with an environmental lens, determining solutions in advance for potential environmental issues and concerns. Kwong (1993, 2003) was a strong proponent of more coordination at all stages of the mining cycle to address environmental issues.

In the descriptions of these models, Plumlee and Nash (1995) provide a comprehensive list of geological controls regarding the environmental characteristics of mineral deposits. Mineralogy is a key component of these controls, as it influences the behaviour of the deposit during environmental interactions. Information on lithology, wall-rock alteration, ore and gangue mineralogy, texture, trace element composition, susceptibility to weathering and oxidation, and formation of secondary minerals allow predictions on how mineral phases will behave during weathering (*i.e*., climate conditions), mining, and mineral processing. The main objective of this part of the project was to define the mineralogical signature of the U-, Th- and REE-bearing veins associated with the granitic pegmatites in the Bancroft region.

The closest geoenvironmental ore deposit model for Bancroft is that of Armbrustmacher *et al*. (1995) who summarized the geological, environmental and geophysical parameters that inform a model for thorium and rare earth element vein deposits, based on Model 11d of Staatz (1992). Although the deposits and occurrences in Bancroft are uranium-rich, they do contain variable amounts of thorium and REE. A direct comparison between Bancroft and the Th-REE vein deposits is presented in Table C1.

Figure C1. Schematic diagram of a mineral exploration cycle, starting clockwise from the top. Modified after Mining 101 – Mine Development Cycle of the Mineral Resources Education Program of B.C. (https://www.mineralsed.ca/learning-resources/student-resources/earth-science/).

Based on this U.S.G.S. model, the thorium-vein deposits are considered low tonnage and high-grade whereas Bancroft deposits are low tonnage and variable grade in uranium. The host rocks are similar with respect to lithology, metamorphism and alteration; they both occur in intrusive complex terrains. The wall-rock alteration is due to metasomatism, and at Bancroft, according to Lentz (1991), is related to the formation of skarns. The ore tends to be structurally-controlled within veins and dykes and primary enrichment noted by Armbrustmacher *et al*. (1995) is U, Ba, Sr, Pb, Zn and Nb along with major amounts of Th, LREE, Fe-oxide, silica and S as sulphate. In contrast, Bancroft is enriched in U, Th, LREE, Mo and Mn within a large variety of ore minerals. Gangue mineralogy is comparable, with quartz, feldspars and other silicate and carbonate minerals. It is interesting to note that mineral characteristics are comparable, even to the mention of odiferous surfaces. Bancroft occurs in a bedrock area controlled by knobs and ridges whereas thorium-bearing veins tend to be in non-distinct topographic areas. With regard to hydrology, Armbrustmacher *et al.* (1995) indicated that there is no effect by these types of vein deposits. This would be the same observations for the Bancroft region. Finally, the processing methods have been limited to a few sites at Bancroft and consist of underground operations at three of four mines with on-site milling to produce a U_3O_8 concentrate along with some trenching and surface pits with abundant diamond drillhole exploration over several decades. Overall, the geological parameters identified by Armbrustmacher *et al*. (1995) are directly applicable to the Bancroft region.

Table C1. Summary of the geological factors that inform environmental effects at thorium-rare-earth element vein deposits (after Armbrustmacher *et al.,* 1995). Notes for Bancroft are based on this study and those listed in the references below.

Geologic Factors	**Thorium-REE Veins**	**Bancroft (Uranium, Thorium, REE)**
Deposit Size	~0.2 Mt Grades ThO_2 ~ 0.4 wt% [1] Low tonnage, high grade	1.36 Mt (1981) 0.11% U_3O_8 [2] Moderate tonnage, low grade
Host Rocks	Alkaline intrusive rocks Granitic rocks High-grade metamorphic rocks Fenitized carbonatite complexes Black shale	Granite pegmatite/granite gneiss Calc-silicate gneiss Quartzo-feldspathic gneiss Amphibolite gneiss Mafic gneiss Metapelite
Geological Terrane	Alkaline intrusive complexes Carbonatite complexes Stable, intracratonic areas	Intrusive complexes in a region of high-grade metamorphic and metasomatic rocks [2]
Wall-rock Alteration	Surrounded by several m-wide aureoles of metasomatically altered rock Alteration and fenitization caused by peralkaline fluids emanating from cooling alkaline silicate or carbonatite magmas	Hybridization/endoskarnification along pegmatite margins Marble/clinopyroxene-hosted exoskarns Fluorite/apatite/calcite veins [3]
Nature of Ore	Structurally-controlled	Disseminated in structurally-controlled pegmatite granite dykes [2,4]
Trace Element Geochemistry	Primary enrichments of uranium, barium, strontium, lead, zinc and niobium Major amounts of thorium, rare earth elements (e.g., LREE), ferric iron oxide, silica and sulphur as sulphate	Uranium, thorium, LREEs, molybdenum, manganese [5,6,7]
Ore Mineralogy	Thorite, thorianite, brockite, monazite, bastnäsite, parasite, synchysite ± sulphides (galena, sphalerite)	Uraninite, uranothorite, thorite, allanite, cyrtolite, pyrochlore, betafite, fergusonite, fluorite, apatite, pyrite, pyrrhotite, molybdenite, secondary uranium minerals, corundum, marble (building stone), sodalite [8]
Gangue mineralogy	Quartz, K-feldspar, barite, ferric iron oxide minerals + many carbonate minerals	Quartz, plagioclase feldspar, K-feldspar, amphibole, clinopyroxene, epidote, biotite, hematite, scapolite,

Geologic Factors	Thorium-REE Veins	Bancroft (Uranium, Thorium, REE)
	(carbonatite complexes) or other silicates and oxides	calcite, titanite ± tourmaline, zircon, garnet [8]
Mineral Characteristics	Quartz-barite veins + thorium-REE minerals, thorium-bearing veins, fine-grained, red and odoriferous fresh surfaces	In veins and pegmatites Irregular grains and aggregates Small to large well-developed crystals (suitable for mineral collecting) In deep red to purplish zones due to intense hematization Purple fluorite associated with uraninite produces a fetid odour when crushed [8]
Secondary Mineralogy	Localized carbonate mineral dissolution	Shattering of rock by radioactive minerals [4]; Fe- and Mn-(oxy)hydroxide precipitates on weathered surfaces, local sediments, and in areas where shallow groundwaters discharge at surface [10]
Physiography	No distinct topographic expressions	Bedrock-controlled knobs and ridges; glaciated terrain rounded topography and deposited till on stoss and lee side of bedrock hills [9]
Hydrology	Unaffected by Th-REE vein deposits	Unaffected by U-Th-REE vein deposits and pegmatites
Processing Methods	Small-scale exploitation Shallow surface pits, trenches	Underground operations for 3 (Bicroft, Canadian Dyno, Faraday) of 4 (Greyhawk-no mill) uranium mines with on-site milling to produce U_3O_8 concentrates; some trenching and surface pits, diamond drill holes

[1] Bliss (1992), as cited in Armbrustmacher *et al*. (1995); [2] Griffith (1986); [3] Lentz (1991); [4] Bullis (1965); [5] Robinson and Sabina (1955); [6] Robinson and Abbey (1957); [7] Robinson (1960); [8] Sabina (1986); [9] Barnett (1983); [10] Parsons *et al*. (2014)

Mine Safeguards

A variety of mitigations have been emplaced in the Bancroft area to secure the sites and reduce potential human injury (Fig. C2). The mitigations are physical and include sealing of portals to adits, bulldozing waste rock into manageable piles, fencing off mine hazards such as pits and shafts as well as placing concrete platforms over shafts. Where needed, the platforms have been vented to reduce the build-up of gases. At some sites the original drill hole casings were not removed and some of these continue to flow. This provided direct access to deep groundwaters for this overall study. Core samples were found discarded in piles near the sites, but most represent the country rock. Samples for this study were collected from these piles.

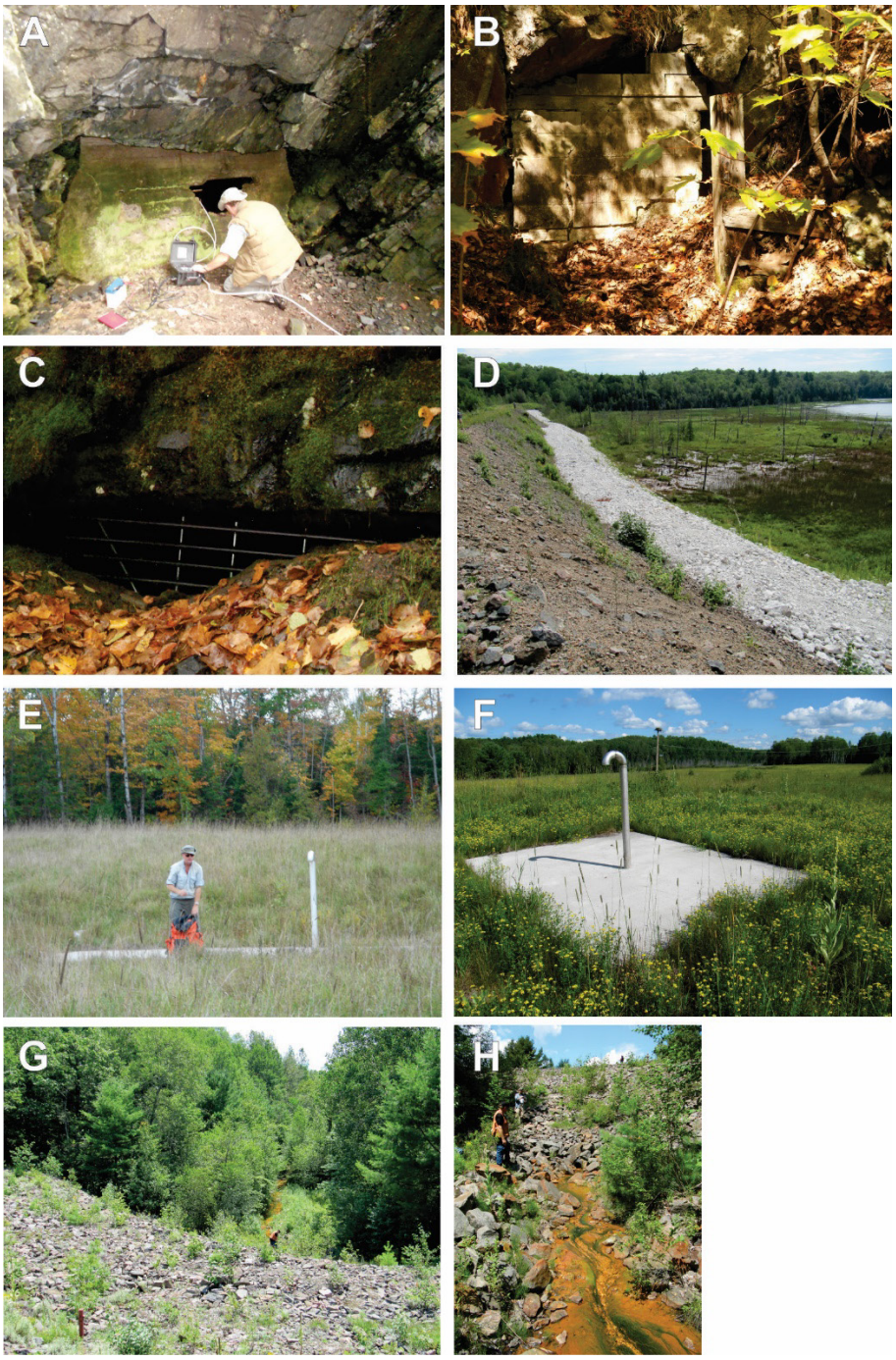

Figure C2. Safeguards emplaced for mine hazards in Bancroft area. A) partially sealed adit portal, Rare Earth Mine 2 (NRCan Photo 2025-016); B) secured adit portal, Halo Mine (NRCan Photo 2025-017); C) adit portal with metal barrier, Croft Mine (NRCan Photo 2025-018); D) rock toe berm to stabilize tailings dam, Dyno Mine (NRCan Photo 2025-019); E) AD in field standing on concrete pad over the Bicroft mine shaft (NRCan Photo 2025-020); F) concrete pad over Bicroft Mine shaft with ventilation pipe (F: Parsons *et al*., 2014; NRCan Photo 2025-021); G) rock berm built along tailings dam, Bicroft Mine(NRCan Photo 2025-022); H) Fe-oxyhydroxide precipitates from water draining Auger Lake tailings (neutral water) (NRCan Photo 2025-023). Photos A, B, C, E and G by J.B. Percival and D, F and H by M.B. Parsons.